Key
Black = Reviewer Comments, **Solid Blue = Responses**, *Italicized Blue = Modified Text*

We would like to thank the reviewers for taking the time to review our manuscript and for their thoughtful comments. Their feedback has helped us clarify and improve the manuscript. We have reproduced the reviewer comments in black text. For ease of review, our responses are given in blue text, while text that has been modified in the manuscript is quoted using blue italics. We would also like to point out that the numbering of the figures from the revised manuscript is used here in the responses.

Referee 1 Comments

Main comments

RC1.1

One thing to consider for good measure is iodine-based nucleation which has been observed in Arctic marine summers before. You should mention it in your introduction and then probably rule it out for your measurements.

The text has been updated in the introduction with:

Furthermore, iodine may be important for particle nucleation in the Arctic (Mahajan et al. 2010; Allan et al. 2015; Raso et al. 2017), although the processes leading to either nucleation or particle growth are not necessarily the same.

And in the Section 3.2 with:

While iodine may contribute to particle nucleation, the low resolution of the quadrupole AMS prevents quantification of iodine. Given the low signal at m/z 127 in this study during growth events, we believe that iodine is at most a minor contributor of mass to Aitken mode particles.

RC1.2

P3 paragraph 2

Why such a focus on GEOS-Chem? What about other models? Or just models in general?

As already discussed near the end of the in the introduction similar discrepancies have been observed in the GLOMAP model. We have focused on GEOS-Chem because to our knowledge there has been more recent work on particle nucleation in the Arctic, especially the Canadian Arctic, using this model.

RC1.3

Section 2.1

A map would be really useful here, showing where all the field sites are and preferably the orography as well

The Figure below has been added to the manuscript in the supporting information.

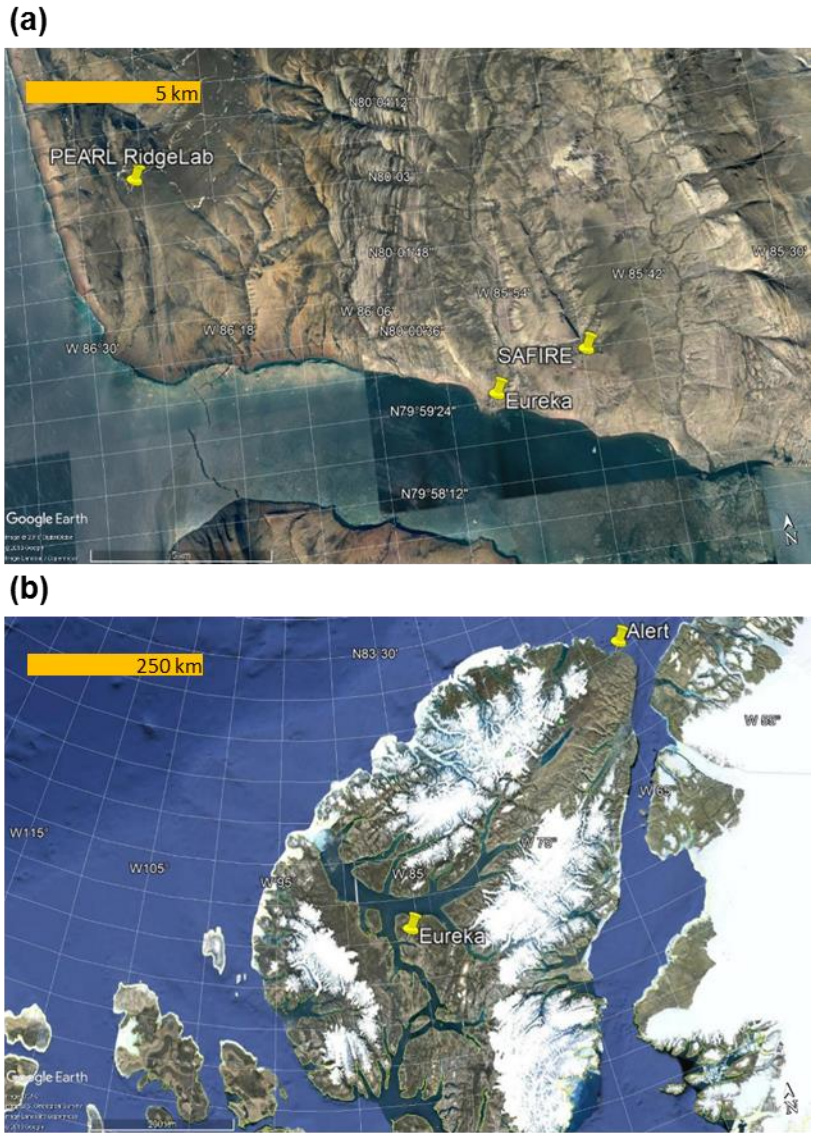

Figure S2. Local map of PEARL RidgeLab, SAFIRE and Eureka weather station (a) and zoomed-out map of Alert and Eureka (b).

RC1.4

P4 Paragraph 2

Could you move all the discussion of the tubing etc to the supplement? It's good to be thorough but this doesn't contribute to the science of the paper. I'm sure you'll agree it's also not the most interesting paragraph ever written...

This portion of the text has been moved to the supporting information.

RC1.5

P4 L23

Any idea why the difference in the OPC performance? How does that affect your AMS comparison?

It is difficult to provide a conclusive reason for the small difference in OPC performance between 2015 and 2016. A possible explanation is that the size range compared isn't exactly the same for the two instruments, 300 – 487 nm for the SMPS versus 300 – 500 nm for the OPC. Therefore, there may be some differences in the actual particle size distribution for 2015 compared to 2016 that leads to a larger difference between the two instruments in 2015. It should be noted that the 2015 data also corresponds to only a portion of the summer and starts on 26 July 2015, whereas the 2016 data includes the full summertime period beginning on 16 June 2016 until 26 September 2016.

Overall, the comparison against the AMS PM_1 is excellent with a linear regression analysis yielding a slope of 1.16 and a correlation coefficient of 0.89, which is well within published uncertainty for AMS measurements (Middlebrook et al. Aerosol Sci. Technol., 46, 258-271, 2012). Therefore, the difference in OPC performance is not large enough to have a significant impact on the AMS comparison.

RC1.6

P7 L25

This is written strangely, it sounds like you are saying you got the numbers from table 1 from the 3 papers you reference, which isn't the case. I think it would be better something like "Aerosol growth rates were calculated [say here very briefly how they are calculated and give the relevant reference(s)]. The initial growth rates from this study are included in Table 1." It would be useful to comment on the meaning of this average growth rate as well, since it takes a lot more mass to go from 100nm to 101 than to go from 10 to 11. Is the number skewed towards being more representative of growth at any particular part of the size distribution?

We have clarified this section of the text and the updated version is copied below.

Initial aerosol growth rates were calculated following previously published methods (Kulmala et al. 2004; Hussein et al. 2005; Salma et al. 2011). Briefly, the SMPS size distributions were fitted with a multi-mode log-normal distribution, and then a linear regression analysis was performed on the geometric mean of the Aitken mode as a function of time for particle diameters between 10 – 30 nm. The initial growth rates calculated for this study are given in Table 1.

The influence of the absolute particle size on the growth rate, as mentioned by the reviewer, is limited by calculating the growth rate for only the smallest particle sizes. We have added some discussion of this consideration in Section 3.1.2.

It should be noted that the size range used for calculating growth rates in our work (10 – 30 nm) is slightly different from that of Collins et al. (4 – 20 nm) and Nieminen et al. (10 – 25 nm), which may contribute to our relatively slower growth rates.

RC1.7

P8 L10 and Fig 6

Can you add on the inversion strength for non-nucleation events and see if there is an obvious difference? That would strengthen your hypothesis that it's the lack of inversion that's creating conditions conducive to nucleation at the measurement altitude

We have made several modifications to the text to address this comment and to add analysis and discussion of non-nucleation (or more precisely the non-growth) events. Specifically, the second paragraph of section 3.1.2 and Figure 7 (in the new text) have been updated. In addition, we have added Table S2 and Figures S5 and S6 to the supporting information. The new text, tables and figures are included directly below in this response.

Furthermore, we conducted a similar analysis for six periods when particle concentrations were low and for six periods with a persistent accumulation mode (summarized in Table S2 and Figures S5 and S6). Figure 7 shows that the average inversion temperature during the growth events (0.3 ± 0.7 ° C) was very similar to that during the selected periods with low particle concentration (0.3 ± 0.2 ° C), whereas the average inversion temperature during periods with a persistent accumulation mode and elevated particle concentrations was much higher (2.5 ± 1.2 ° C). The results shown in Figure 7 imply that growth events occur at the PEARL RidgeLab when the inversion is weak because, firstly, the low particle surface area and corresponding condensation sink in the marine boundary layer air allowed particle nucleation to occur, and secondly, the site was possibly influenced by more recent surface emissions that were less photochemically aged compared to air aloft. In contrast, when the inversion was strong, the aerosol and aerosol precursor species were more chemically aged due to slower transport into the free troposphere and thus the existing particles had already grown to

sizes corresponding to the accumulation mode. A few growth events were observed when the temperature inversion was larger, which may be due to the fact that the radiosondes were launched at the Eureka Weather Station located 11 km to the southwest of the PEARL RidgeLab. Thus, the temperature profile measured by a radiosonde may not be fully representative of that at the RidgeLab. Generally speaking, the observations reported here are consistent with previous work (Willis et al. 2016; Collins et al. 2017) suggesting that similar events measured in the Canadian Arctic are attributable to marine sources.

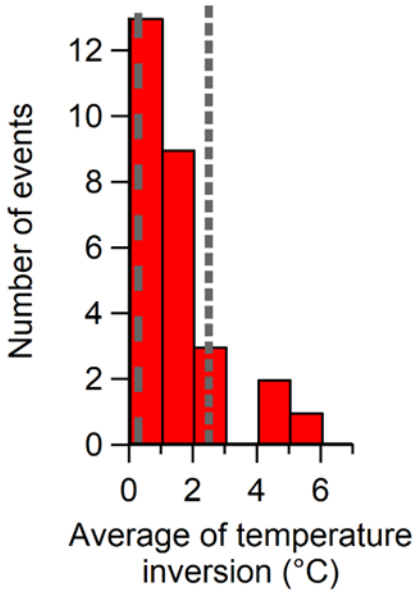

Figure 7. Histogram of the number of growth events near Eureka, binned by the average change in the temperature from 10 to 600 m above sea level. The average temperature change of each event is provided in Table S1, and was calculated from radiosonde measurements during 2015 and 2016, as shown in Figure 6. The dashed line indicates the average change in temperature during periods of low particle concentrations as shown in Table S2 and Figure S5 (0.3 ± 0.2 °C), and the dotted line indicates the average change in temperature during periods with a persistent accumulation mode as shown in Table S2 and Figure S6 (2.5 ± 1.2 °C). The values in parenthesis are the averages and their standard deviations.

Table S2. List of selected periods of low and high particle concentrations observed near Eureka during the summers of 2015 and 2016 . The periods of high concentrations do not exhibit particle growth and are therefore distinct from the growth events. The SMPS measurements for the periods of low and high concentrations are shown in Figure S5 and S6, respectively.

Non-Event (NE)	Time period (UTC)	
	Start	End
NEA (low)	2015-08-06 06:00	2015-08-07 02:00
NEB (low)	2015-08-24 11:00	2015-08-26 12:00
NEC (low)	2015-09-04 12:00	2015-09-05 18:00
NED (low)	2016-06-23 08:00	2016-06-24 15:00
NEE (low)	2016-06-30 12:00	2016-07-01 15:00
NEF (low)	2016-08-02 00:00	2016-08-02 12:00
NEG (high)	2015-08-10 07:00	2015-08-11 10:00
NEH (high)	2015-08-19 22:00	2015-08-24 10:00
NEI (high)	2015-08-29 07:00	2015-09-04 12:00
NEJ (high)	2016-07-13 19:00	2016-07-19 12:00
NEK (high)	2016-07-25 18:00	2016-07-26 03:00
NEL (high)	2016-07-30 00:00	2016-08-02 00:00

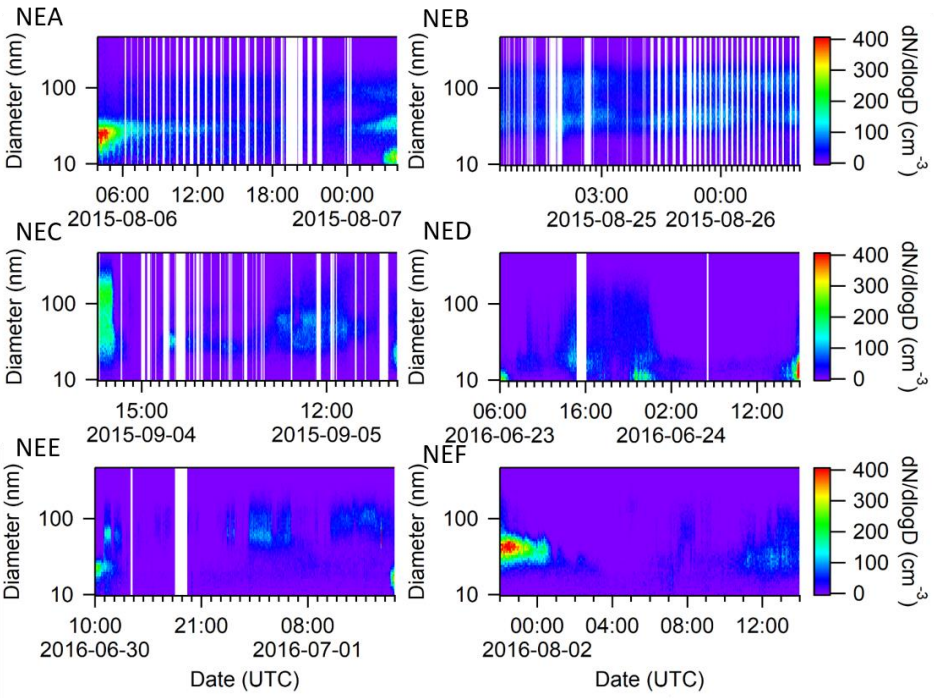

Figure S5. SMPS measurements of selected periods with low particle concentrations observed near Eureka during the summers of 2015 and 2016 as summarized in Table S2. Note that the figures display an additional 2 hours before and after the analyzed period. The sizes are mobility diameters measured by an SMPS, which are equal to the physical diameters under the assumption that the particles are spherical and contain no voids.

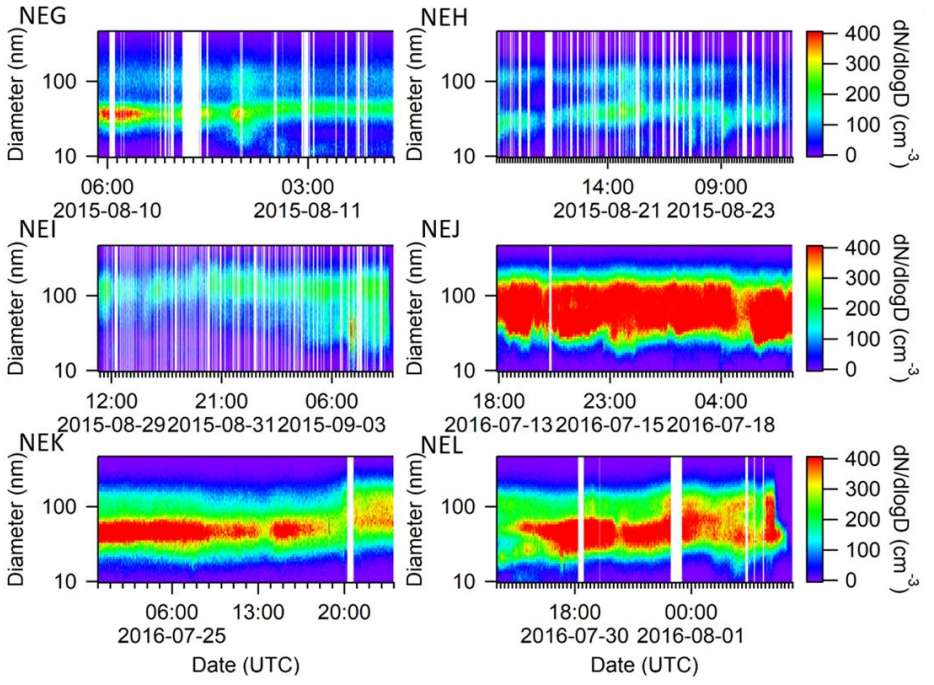

Figure S6. SMPS measurements of selected periods with high particle concentrations and without growth observed near Eureka during the summers of 2015 and 2016 as summarized in Table S2. Note that the figures display an additional 2 hours before and after the analyzed period. The sizes are mobility diameters measured by an SMPS, which are equal to the physical diameters under the assumption that the particles are spherical and contain no voids.

RC1.8

P10 L19

I'm not sure I agree there's a clear trend- there's a slight trend if you take some pretty big averages but mostly there's just random noise. The average data points are not very far apart either. How does that compare to what you expect in this environment? I think adding some literature values to Fig 8 would be useful to add some context.

The first panel, panel (a), does show a distinct change in the f_{44}:f_{43} graph during GE3. The trend is not as large compared to typical presentations of the f_{44}:f_{43} space, because of the greater limits in our figure and relatively smaller changes in f_{44} and f_{43}. The trend is less clear for the other event, GE6, and we have adjusted the text in the manuscript to more clearly explain this point. To our knowledge, only one other paper has reported growth events in this space and over these timescales. In that sub-tropical urban location, both the f_{44} and f_{43} were found to decrease as growth events evolved (Salimi et al. Atmospheric Chemistry and Physics, 15, 13475-13485, 2015). This contrasting behavior is interesting and may be attributable to fact that this previous work was performed in a location where other sources of particles besides nucleation (e.g. primary combustion particles) may have been contributing to the measured f_{44} and f_{43}. In general, the f_{44}:f_{43} values observed are consistent with values of oxygenated organic aerosols (a proxy for SOA) as measured at continental and marine locations (Ng et al. Atmospheric Chemistry and Physics, 10, 4625-4641, 2010; Choi et al. Atmospheric Environment, 171, 165-172, 2017). The text in Section 3.2 now reads:

For GE 3, there was a clear trend during the evolution of the growth event wherein both f_{44} and f_{43} increase, which is consistent with an increase in the relative concentration of carboxylic acids and non-acid oxygenates in the organic aerosol. For GE 6, a change in organic composition is not apparent. The f_{44} may have increased, but the trend with time is more ambiguous than for GE 3. In comparison, the size-resolved composition measurements shown in Figure 8, show smaller particles have a higher fraction of m/z 43 and larger particles formed later during the growth events have a higher fraction of m/z 44 suggesting that aerosol growth led to an increase in the amount of oxidation due to, in part, the production of carboxylic acids. However, we emphasize that our results are for a very limited data set and further analysis of SOA composition during additional growth events using f_{44} and f_{43} would be necessary to confirm our observations.

RC1.9

P11 L6

Could you put the NASA worldview images in the supplement?

The Figure below has been added to the manuscript in the supporting information.

(a)

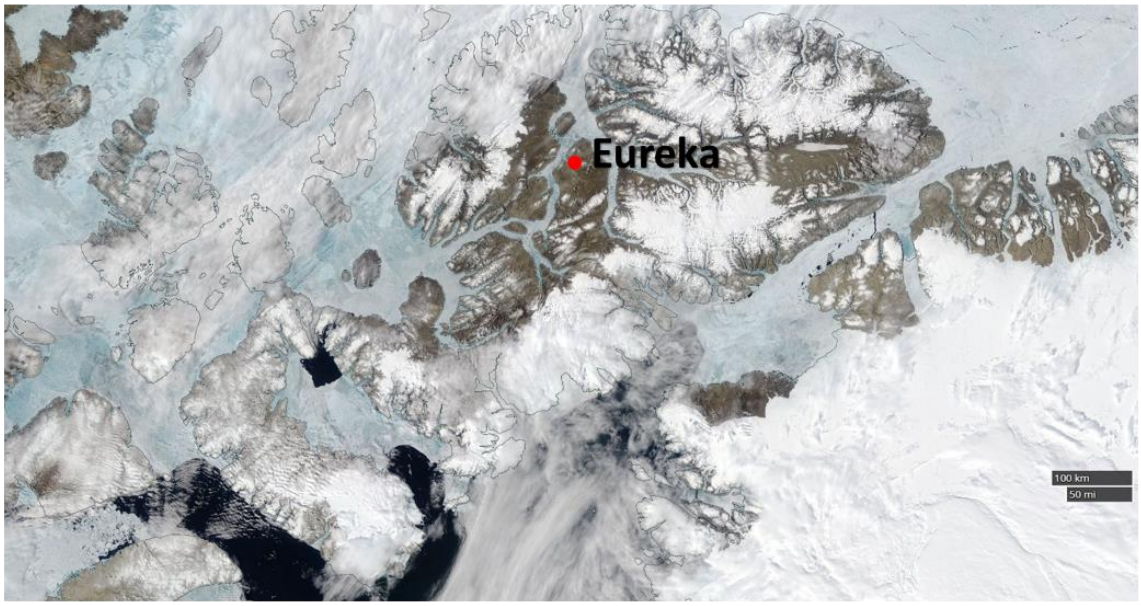

(b)

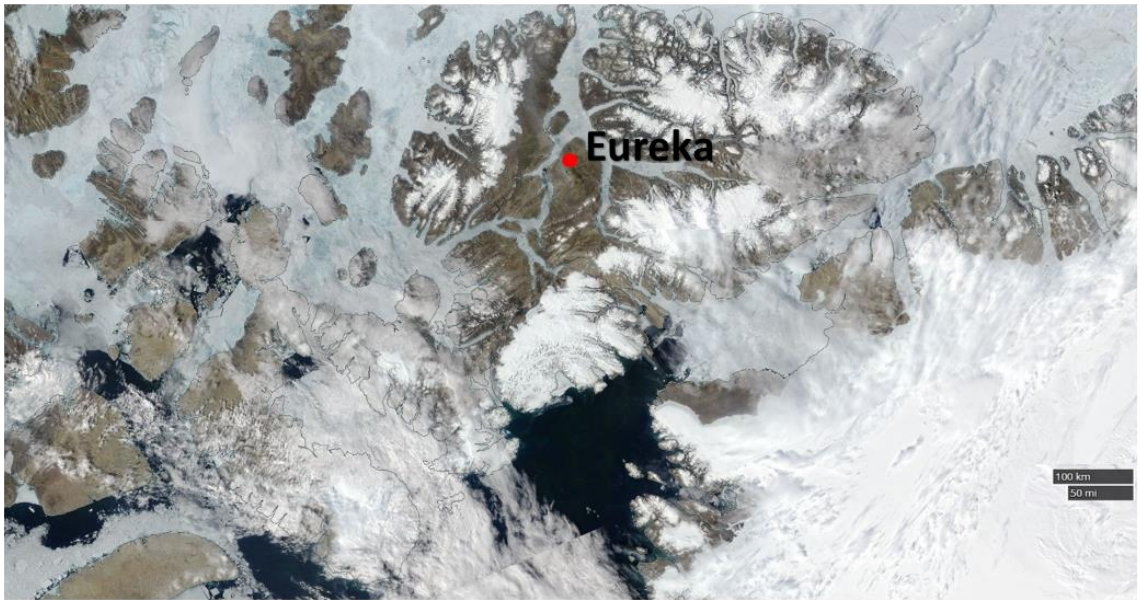

Figure S9. Image of the ice coverage around Eureka during 25 June 2016 (a) and during 7 July 2016 (b) given by NASA Worldview.

RC1.10

Finally, I think it would be useful to discuss the implications for of your findings for CCN concentrations in the Arctic.

This is an excellent suggestion and the following text has now been added to the conclusion section.

Previous work in the summer time Arctic found that particles smaller than 50 nm could be contributing to cloud droplet activation (Leaitch et al. 2016). The growth of small particles to diameters larger than 60 nm observed in our study could therefore make them an important contributor to CCN, ultimately impacting the radiation balance and hydrologic cycle.

Technical/stylistic corrections

RC1.11

I found the tenses very confusing throughout. Take for example the abstract. You say "Measurements...were taken during…2015 and 2016". You then switch to the present (incorrectly in my view) and say "These events are observed beginning in June…marine sources are the primary cause." It's not like you took data from 2 decades and can really talk in general terms about events that you expect to happen every summer. You have data from 2 years, so it's appropriate to refer to your measurements and things that you observed in the past. Then you talk about what the graphs show in the present. Other examples of incorrect tense are P2L16, P3L24, P4L18, but there are many more. Please be consistent and refer to things that happened in the past, in the past tense.

The manuscript has been revised to make the tenses consistent. In the interest of clarity, we did not highlight every change that was made to address this comment.

RC1.12

P7 L23

Preceding not proceeding

The text has been corrected.

RC1.13

Figure 5 parts b,d,f,h,j

I think there are too many lines on one graph, it's very difficult to make sense of. I think split these in two and consider using a more colorblind-friendly colorscheme.

The figure in question has been changed in the manuscript. In particular, we have split the old Figure 5 into two new figures (Figures 5 and 6 in the revised manuscript). We have also added patterned lines to the graphs of the temperature profiles. In total, we think these changes make the data and graphs easier to read.

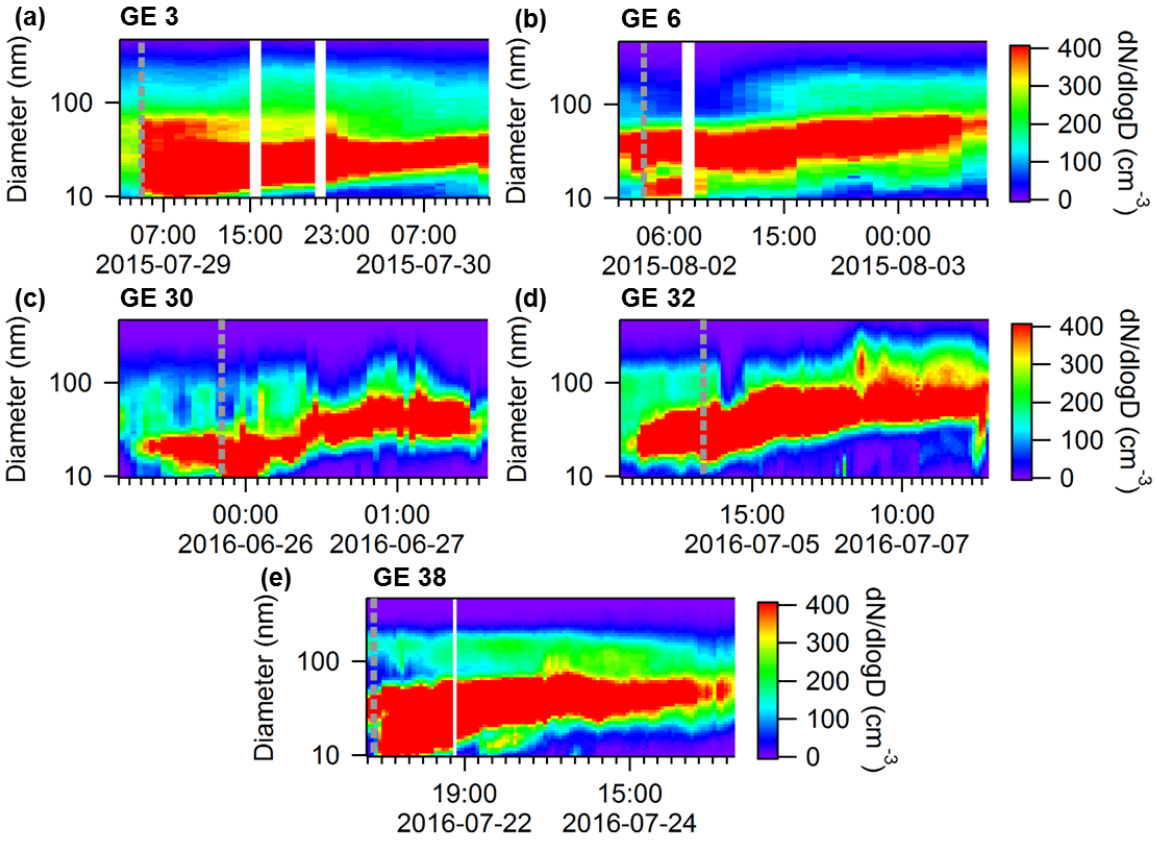

Figure 5. Five selected growth events near Eureka during the summers of 2015 and 2016. The grey dashed line indicates the start of each growth event. The sizes are mobility diameters measured by an SMPS, which are equal to the physical diameters under the assumption that the particles are spherical and contain no voids.

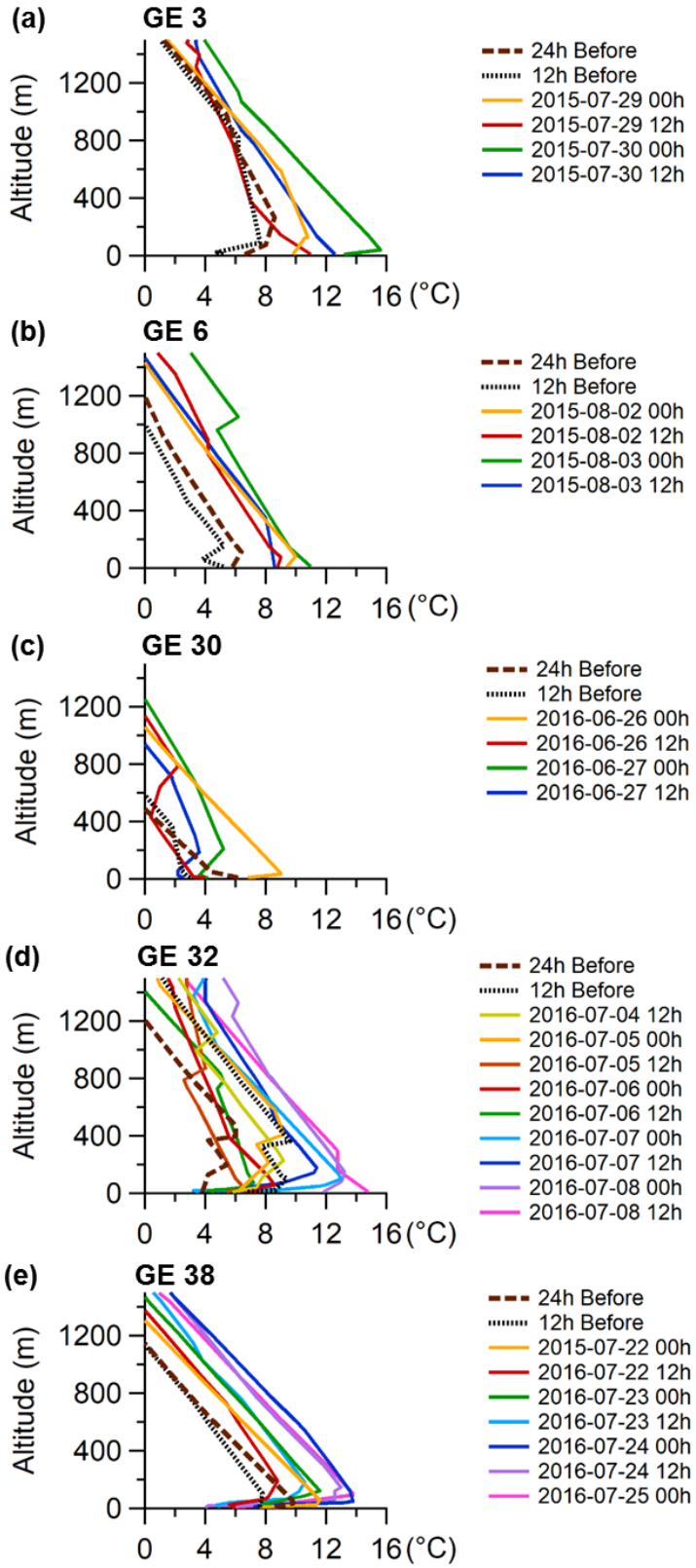

Figure 6. Vertical temperature profiles every 12 h during the 5 selected growth events that are shown in the previous figure. Data includes 24 h and 12 h prior to the start of the growth event.

RC1.14

Figure 7

Why are parts e and f plotted as m/z 43 44 and not f43 44? You do that with the mass fraction of OA vs SO4, I think it would be useful for the organic markers

The Figure below has been added to the manuscript in the supporting information.

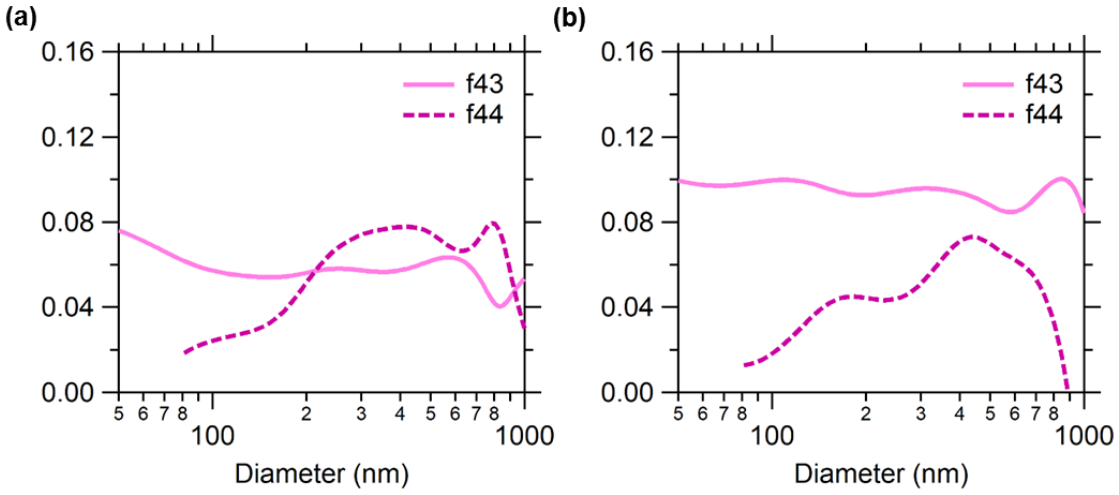

Figure S12. Organic aerosol fraction measured at m/z 43 and m/z 44 during GE 3 (a) and GE 6 (b) near Eureka.

RC1.15

Figure S5

Could you normalise the y axis so that the heights are also the f's ie f44, f43 etc.

The figure has been updated as shown below.

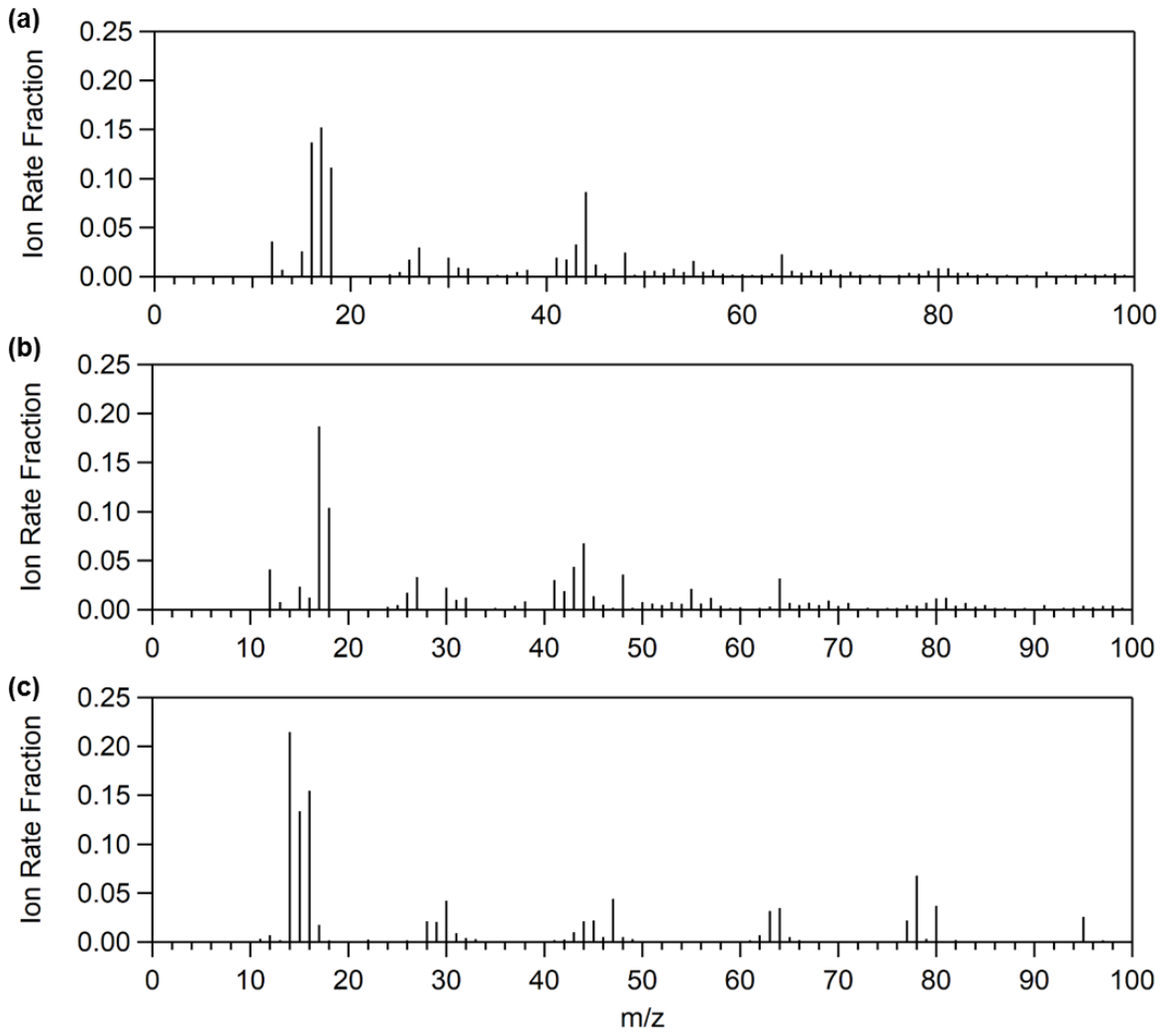

Figure S11. AMS average ambient aerosol mass spectrum of GE 3 (a) and GE 6 (b) compared with the mass spectrum of MSA (c). The Ion Rate Fraction is the normalized Ion Rate (in Hz).

Referee 2 Comments

RC2.1

The authors reference the NASA MODIS imagery quite a bit in the text, yet they provide no images in the text or SI; since the influence of open water is key to the results of this work, I highly recommend adding representative images as a figure in the main text.

We kindly refer the reviewer to our response to comment RC1.9.

Major Comments

RC2.2

Page 1, Lines 23-24, Page 9, Lines 32-33, Page 11, Lines 31-32

Please define the size range measured, rather than just "smaller than 100 nm". It appears from Fig 7 that 60-100 nm is the size range measured. Please state as such to avoid misleading the reader since much of this paper focuses on <50 nm particles. Since organics are expected to primarily responsible for aerosol growth, one would expect that the mass of 60-100 nm would be dominated by organics.

In all the different places specified by the reviewer the text has been changed to "*between 50 and 80 nm*", **when before it was written** "*smaller than 100 nm*" **or** "*less than 100 nm*". **Please note that we have used a slightly different diameter range than suggested by the reviewer because we have converted the vacuum aerodynamic diameters to physical diameters.**

RC2.3

Introduction

It would be useful to add a brief summary of previous Arctic growth event papers to give greater context for the reader.

The second and third paragraphs of the introduction have been restructured and additional references included to provide better context. The update text is quoted directly below.

In tropical marine locations, new particle formation tends to occur in the upper part of the troposphere, usually at the outflow of clouds, and these particles are entrained to the surface through mixing, which contributes to relatively stable aerosol size distributions (Hoppel et al. 1986; Clarke et al. 2006). In contrast, modelling studies of the Arctic summer show that persistent cloud and drizzle causes wet deposition and results in low condensation sinks at the surface (Browse et al. 2014; Croft et al. 2016a). These same studies show that these conditions can favour particle nucleation followed by growth between drizzle events. This is supported by surface observations of aerosol size distributions in the Arctic at Alert and Ny-Ålesund that show an annual cycle during which summertime surface aerosols exhibit much smaller particle diameter than wintertime aerosols (Tunved et al. 2013; Croft et al. 2016a). Additional surface observations have suggested that new particle formation could be the source of these small particles, with dimethyl sulphide (DMS) emitted from the ocean being a key gaseous precursor of less volatile species, such as sulphuric acid and methanesulphonic acid, that contributes to aerosol mass (Chang et al. 2011; Leaitch et al. 2013).

Sulphuric acid has long been known to contribute to new particle formation and growth events (Twomey 1977; Charlson et al. 1992; Napari et al. 2002; Lohmann and Feichter 2005; Kirkby et al. 2011; Almeida et al. 2013; Croft et al. 2016b). More recent work has shown that in coastal Arctic environments, ammonia from sea-bird colonies can contribute to new particle formation (Croft et al. 2016b). In addition, organic compounds, especially those with lower volatilities, have also been found to contribute secondary aerosol mass to particle growth and nucleate new particles in forested and anthropogenically influenced regions (Allen et al. 2000; Zhang et al. 2009; Pierce et al. 2012; Riipinen et al. 2012) as well as in laboratory studies (Kirkby et al. 2016; Trostl et al. 2016). Box models have inferred the contribution of non-sulphur species (i.e. organic compounds) to aerosol growth in Greenland (Ziemba et al. 2010) and in tropical marine cloud outflow (Clarke et al. 1998). Burkart et al. (2017) provided indirect evidence that organic compounds contribute to aerosol growth in high-latitude marine environments using both microphysical modeling of a particle growth event as well as cloud condensation nuclei (CCN) hygroscopicity measurements. In a comparison of ship-borne observations in the Canadian Arctic in 2014 and 2016, Collins et al. (2017) found that increased activity in marine microbial communities along with greater solar radiation and lower sea ice concentrations contributed to new particle formation and growth. Recent work by Mungall et al. (2017) in the Canadian Arctic also suggests that a photo-mediated marine source of oxygenated volatile organic compounds could produce precursor vapors for new particle formation or growth. Furthermore, iodine may be important for particle nucleation in the Arctic (Mahajan et al. 2010; Allan et al. 2015; Raso et al. 2017), although the processes leading to either nucleation or particle growth are not necessarily the same.

RC2.4

SMPS, OPC, & AMS size comparisons

It is not clear whether the diameters have been adjusted (between mobility, optical, vacuum aerodynamic) for comparisons between these instruments. This is necessary. See DeCarlo et al 2004 (AS&T). Please also label mobility diameter appropriately throughout (e.g. Fig. 1, 3, 5).

Following DeCarlo et al. AS&T 2004, if it is assumed that the particles are spherical and contain no voids, then their mobility diameter will be equal to their physical (or geometric) diameter. The assumed particle shape and morphology are reasonable given the evidence that the largest portion of the particles mass is due to secondary formation (either secondary organic aerosols or sulphate).

To address this point we have modified the text in Section 2.1.

Following the work of DeCarlo et al. (2004), the mobility diameter measured by the SMPS was assumed to be equal to the physical diameter, which would be valid if the sampled particles are spherical and contain no voids. This is a reasonable assumption given the secondary origin of the observed particles.

We have also added the following sentence to the figure captions for those figures containing SMPS data. We prefer to not write "mobility diameter" directly on the figure axes as that would create a lot of visual clutter.

The sizes are mobility diameters measured by an SMPS, which are equal to the physical diameters under the assumption that the particles were spherical and contained no voids.

The vacuum aerodynamic particle diameter measured by the AMS is now adjusted to be mobility diameter and thus is now equal to the physical diameter, under the assumptions given above. We have added the following text to the manuscript in Section 2.2 to explain the adjustment.

Vacuum aerodynamic diameters measured by the AMS were converted to physical diameter under the assumption that the particles were spherical, contained no voids, and had a density of 1.25 g cm^{-3} (DeCarlo et al. 2004). This density is typical for ambient organic aerosol (Middlebrook et al. 2012), and was selected for this study since the analysis was focused on the particle composition during the predominantly organic aerosol growth events.

Lastly, the OPC diameter should be equal to physical diameter insofar as the Mie scattering curve of the calibration particles is similar to that of the actual ambient aerosol. In this case, polystyrene latex spheres were used by the manufacturer for calibration. While the Mie Scattering curve for ambient aerosol may vary from that of the PSLs, any variation will be small and likely within specified instrument size accuracy of ±10%, insofar as the ambient particles are spherical and predominately organic (and therefore have an index of refraction similar to PSLs). These assumptions seem reasonable for this study. The following text was added to Section 2.1.

It was further assumed that the OPC diameter was equal to the physical diameter, given that the Mie scattering curve of the ambient aerosols was likely within 10% of that of the calibration particles composed of polystyrene latex spheres.

RC2.5

Page 6, Line 8

Provide the exact number of events identified. Please also define how these events were identified, and how they were differentiated from local emissions.

The text in the Section 3.1.1 has been updated with:

Figure 1 shows the aerosol size distributions measured at the PEARL RidgeLab and at Alert for 16 June to 26 September 2016. Particle growth events were evident at both sites. In total, 34 events with elevated concentrations of small particles (< 20 nm diameter) were observed at the PEARL RidgeLab during this period, 22 of which were followed by growth lasting between 2 to 6 days. It is important to note that the local anthropogenic emissions should be completely negligible due to the extremely remote position of the site. The electricity for the PEARL RidgeLab is generated by a small power plant located 11 km from the site and there is no indication from the measurements that the site is significantly influenced by emissions from the power plant or the Eureka Weather Station.

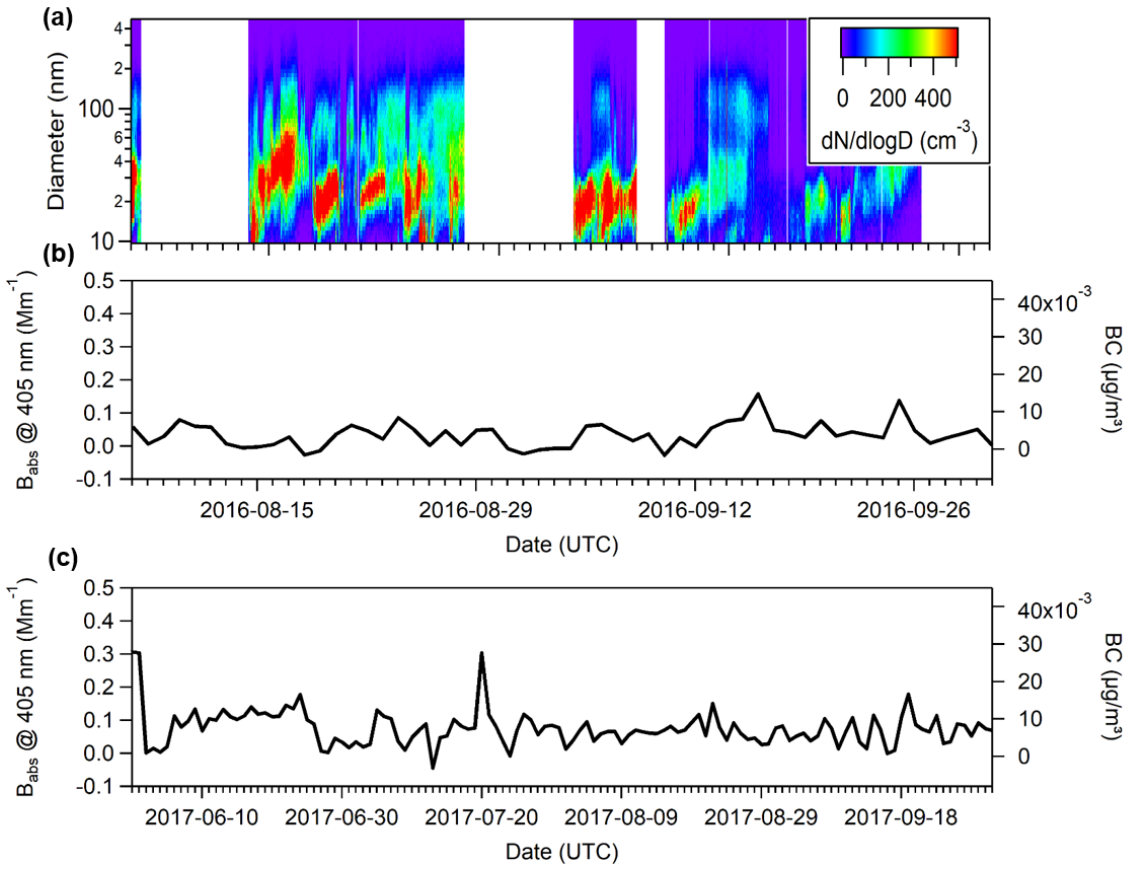

To confirm that local emissions did not influence the site and the observed growth events, the figure above shows the SMPS data during August and September 2016 (a), when a PAX (Photoacoustic Extinctiometer) was installed at the PEARL RidgeLab. The PAX measures the aerosol light scattering and absorption, as well as the concentration of black carbon (BC). The PAX measurements for this period (b) show that growth events occurred in the absence of BC during the end of the summer 2016. Furthermore, during the summer of 2017 (c), the concentration of BC was extremely low and consistent with background arctic conditions (Law and Stohl, Science, 315, 1537-1540, 2007). From these observations, it is possible to conclude that there was no significant contribution from local emissions given the very low concentrations of BC at the PEARL RidgeLab.

RC2.6

Page 6, Lines 31-32

This references circulation patterns in a paper that is over 10 years old. What was the meteorology during the observations presented herein? Was the meteorology similar between the two summers? Were there ever periods when a growth event was observed at one location and not the other? IF so, could differences in circulation or weather (e.g. precipitation) explain this?

We agree that the reference may not accurately describe circulation patterns during our study period, and thus it has been deleted. Available observations of temperature, RH and wind speed at the PEARL RidgeLab and Alert for the relevant periods in 2015 and 2016 are shown below. They are surprisingly similar, suggesting that the meteorology experienced at both sites was similar. Nevertheless, growth events were sometimes observed at one site but not the other. For some of these single site growth events, it is possible that differences in meteorology, especially RH, could be the cause of the discrepancy. However, it is not consistently different, with some single site growth events occurring when the RH is the same and some simultaneous growth events occurring when the RH is different. As such, we do not believe we can attribute specific differences in weather to the observed differences in growth events. This is consistent with sites at lower latitudes where identical meteorological conditions do not always lead to nucleation and growth events (e.g. Jeong et al. Atmospheric Chemistry and Physics, 10, 7979-7995, 2010.)

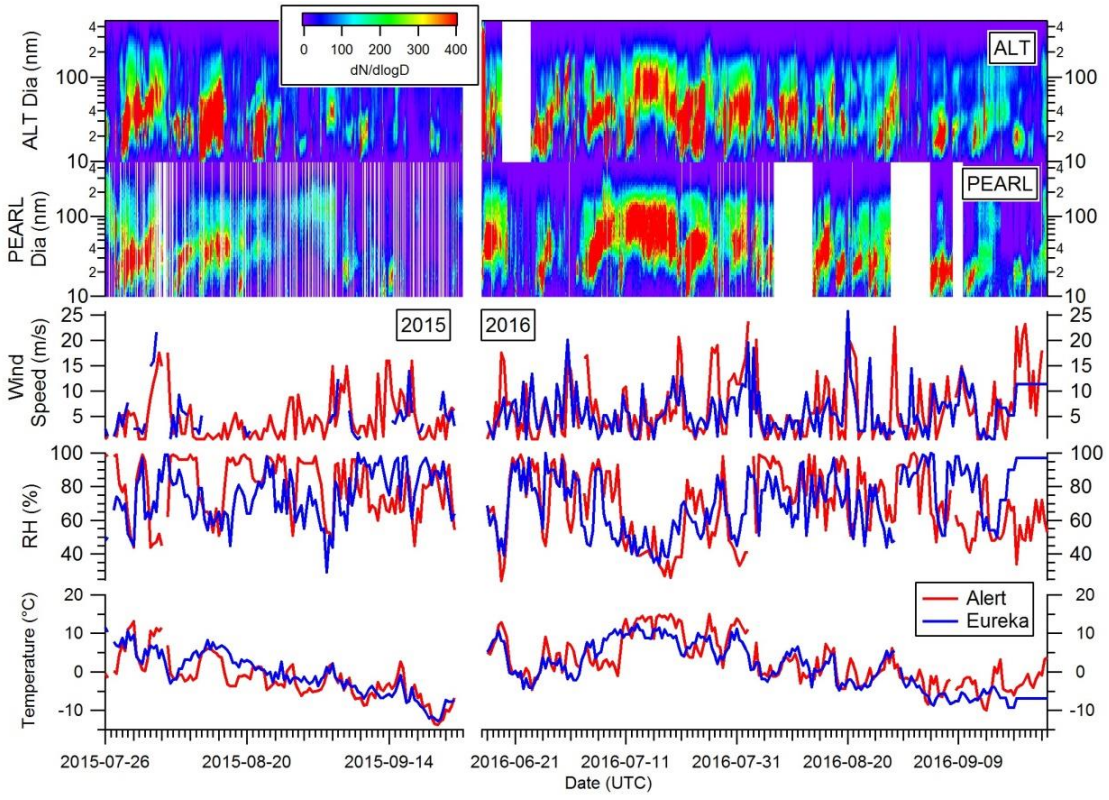

RC2.7

Page 7, 2nd paragraph

Please test for statistical significance to bolster these arguments.

This paragraph has been shortened so that the arguments are more precise. (See the copied text below.)

In order to evaluate the influence of the appearance of small particles and growth events on the particle number concentrations at the two sites, the total concentration and the concentration of particles with a size between 10 to 100 nm, measured by the SMPS are summarized in Figure 4 for 27 Jul – 9 Sep 2015 and 2016. The particle concentrations are similar at both sites and for both periods. The one exception is that the 90th percentile was higher for Alert in 2015, which was driven by two events with especially elevated particle concentrations. Coinciding events were observed at Eureka, but the particles concentrations were much lower. The reason for the elevated concentrations at Alert but not at Eureka is unknown. It is important to note that for 2016, the mean is approximately 50 – 100 particles cm-³ higher than the results shown in Figure 4 if data from 16 Jun – 26 Sep 2016 are analyzed instead. This can be explained by the fact that the total duration of growth events was longer in June and July compared to events occurring in August and September.

For reference, the mean and the standard deviation for the particle concentrations at each site and for 2015 and 2016 are given below, which further illustrates the similarity in the frequency distribution of the particle number concentration. The data in the table is for particle diameters between 10 – 487 nm, and very similar results are obtained when limiting the size range to 10 – 100 nm.

	Mean ± Standard Deviation (particles/cm^3)
Alert 2015	**204 ± 290**
Alert 2016	**168 ± 125**
Eureka 2015	**145 ± 170**
Eureka 2016	**200 ± 127**

RC2.8

Page 7, Line 21

This sentence mentions 28 events, but the previous page (line 8) references 40 events. Please explain or fix this discrepancy.

The text has been clarified regarding the number of events. The text on page 6 now reads as follows.

Figure 1 shows the aerosol size distributions measured at the PEARL RidgeLab and at Alert for 16 June to 26 September 2016. Particle growth events were evident at both sites. In total, 34 events with elevated concentrations of small particles (< 20 nm diameter) were observed at the PEARL RidgeLab during this period, 22 of which were followed by growth lasting between 2 to 6 days.

In Section 3.1.2, the new text is as follows.

To further analyze the growth events and periods with elevated concentrations of ultrafine particles, two different sets of case studies were selected comprising 5 (Table 1) and 28 events (Table S1). The latter represents all the growth events observed during the measurement period (22 events during 2016 and 6 events during the shorter 2015 period), and the smaller set of 5 was used to calculate growth rates. This subset was chosen because they were distinct, without overlap with preceding or subsequent growth events and exhibited relatively smooth growth curves.

In total, 28 growth events were observed during the entire study period, with 22 of those events occurring in 2016. The number of 40 given in the previous version of the manuscript was an estimated value and incorrect.

RC2.9

Page 8, Line 21

Provide the growth rates observed by Nieminen et al in parentheses here for easy comparison. Please also clarify that by "all the events", I believe you mean "all five events"?

The text has been updated with:

Previous studies have characterized aerosol growth rates in remote regions including the Arctic. In particular, Collins et al. (2017) reported growth rates ranging from 0.2 – 15.3 nm h^{-1} during two research cruises conducted in the Canadian Arctic and calculated a corresponding average growth rate of 4.3 ± 4.1 nm h^{-1}. Similarly, Nieminen et al. (2018) reported for Alert and Mt Zeppelin, Norway, that the average growth rates, between June and August, were 1.1 and 1.2 nm h^{-1}, respectively for the years 2012-2014 and 2005-2013. In our study, growth rates ranged from 0.1 – 1.0 nm h^{-1} for the aerosols at the PEARL RidgeLab and at Alert, with an average rate of 0.5 ± 0.3 nm hr^{-1} (Table 1). These values are consistent with those reported in Collins et al. and in Nieminen et al. It should be noted that the size range used for calculating growth rates in our work (10 – 30 nm) is slightly different from that of Collins et al. (4 – 20 nm) and Nieminen et al. (10 – 25 nm), which may contribute to our relatively slower growth rates. Lastly, the growth rates are similar for all 5 events analyzed in Table 1, which suggests that the atmospheric processes (e.g. the condensation of semi-volatile or low volatility vapors to the particle surfaces as discussed below) and conditions governing the growth events are similar for all the events in this study.

RC2.10

Page 8, Line 31

Comment on sea ice vs open water in the area at this time.

We now include NASA Worldview images in Figure S13, where open waters south of Ellesemere Island can be seen starting on 25 June 2016 and near Eureka Sound starting on 7 July 2016.

RC2.11

Section 3.2

Does m/z 79 (MSA tracer) vs size show a pattern?

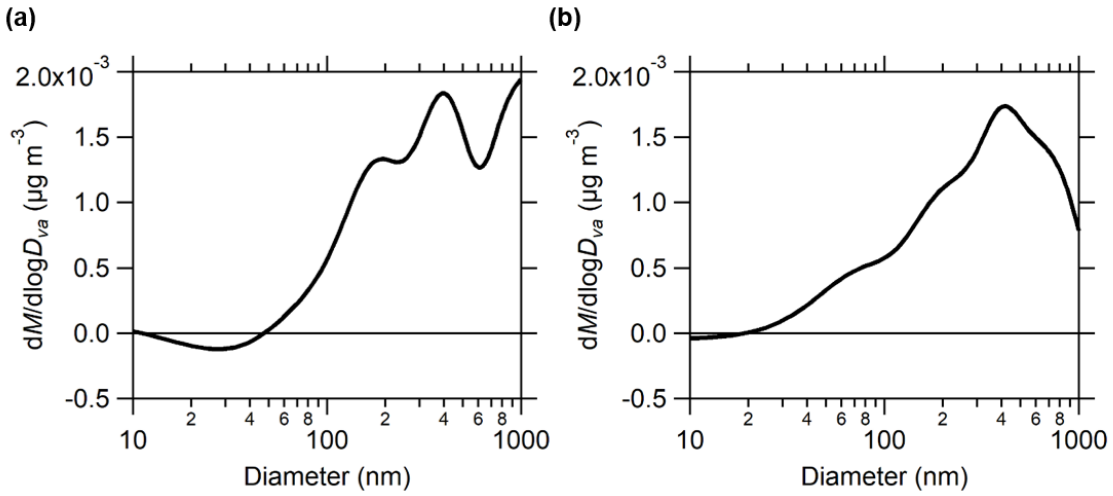

The figure above shows the m/z 79 size distribution for GE 3 (a) and GE 6 (b). The m/z 79 size distribution does not resemble the m/z 43 or the m/z 44 distribution. It is also different from the total organic size distribution. Since we do not have high mass resolution, it is possible there are other organic fragments contributing to m/z 79. Nevertheless, MSA does not appear to be an important contributor to the total mass, because if that were the case the m/z 79 distribution and the total organic distribution would be similar. The following text has been added to this section:

The size distribution of m/z 79 also peaks at larger sizes, suggesting that any MSA present would be in the accumulation mode

RC2.12

Figure 4

What time resolution was used to make this plot (was averaging done?)? Since this paper focuses on ultrafine particles, it would also be useful to add a section to this plot with the same categories, but only showing the <100 nm particle concentration binned.

The figure has been updated to:

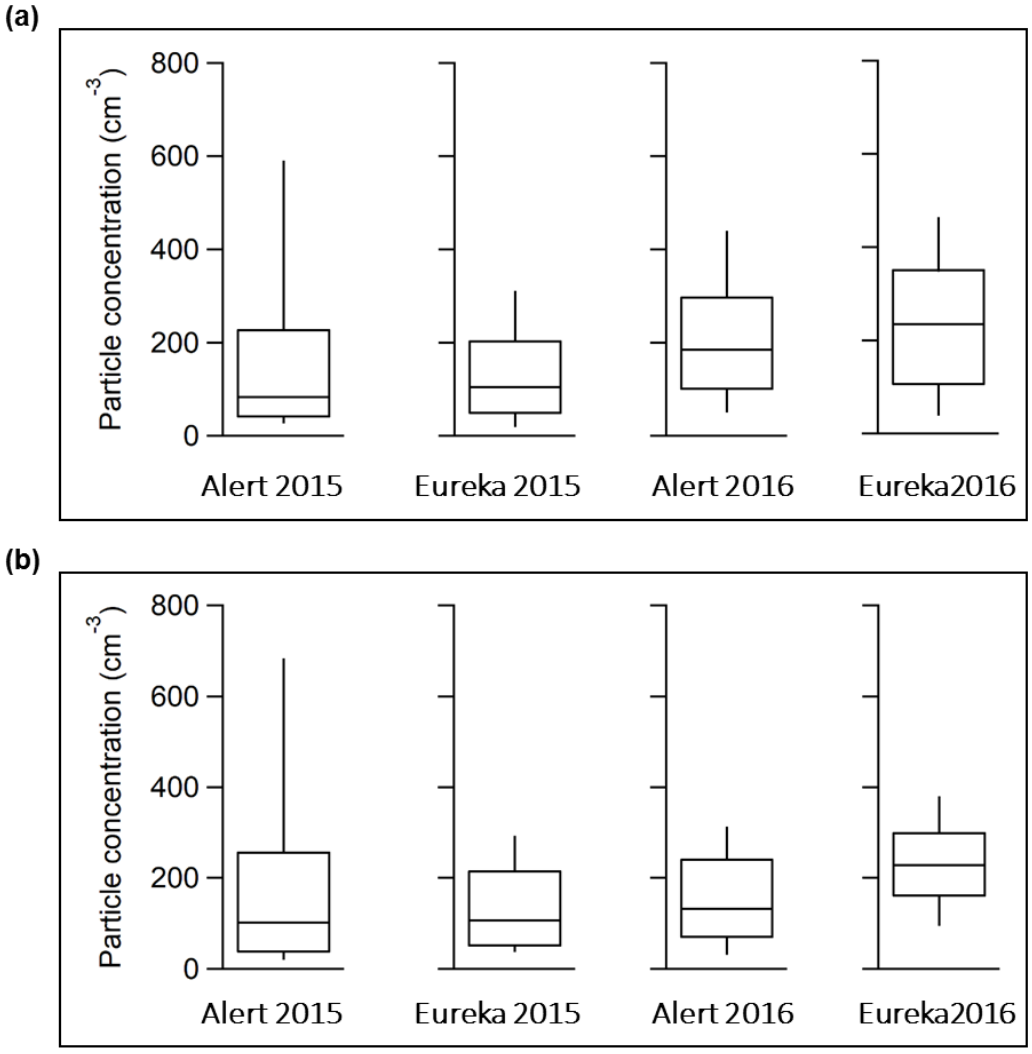

Figure 4. Box and whiskers plots of hourly particle number concentrations for diameters between **(a)** 10 – 487 nm, and **(b)** 10-100 nm measured during 27 Jul to 9 Sep 2015 and 2016 in Alert and at the PEARL RidgeLab near Eureka. The plots indicate the 10^{th}, 25^{th}, 50^{th}, 75^{th} and 90^{th} percentiles.

RC2.13

Figure S1

Please add a note, with references, that this doesn't include the instrument inlet efficiencies so that the reader is not confused.

The figure caption has been updated to read as follows.

Figure S1. Inlet particle transmission efficiency for the AMS (a) and SMPS (b) at the PEARL RigdeLab. Note that the curves do not include the instrument transmission efficiencies for the AMS (Jayne et al. Aerosol Sci. Technol. 2000, 33, 49-70) or for the SMPS (Wiedensohler et al. Atmos. Meas. Tech. 2012, 5, 657-685).

Minor Comments

RC2.14

Page 1, Line 20

Fix typo.

We have replaced "growths" with "growth"

RC2.15

Page 1, Lines 25-26

Define 'larger particles' here for the reader not familiar with the AMS size range. Similarly, please define "m/z 44" here in terms that the non-AMS reader will understand.

We have updated the text as indicated below. The term "m/z 44" has been deleted from this section of the abstract as well.

The oxidation of the organics also changed with particle size, with the fraction of organic acids increasing with diameter from 80 to 400 nm.

RC2.16

Page 2, Line 12

It would seem appropriate to cite an older paper by Leck here.

Reference is now made to the following paper.

Leck and Bigg, Source and evolution of the marine aerosol—A new perspective, Geophysical Research Letters, 32, L19803, 2005.

RC2.17

Page 2, Line 15 & 25

Add references.

A reference has been added to Line 15 of the previous version (Croft et al. Processes controlling the annual cycle of Arctic aerosol number and size distributions, Atmospheric Chemistry and Physics, 16, 3665-3682, 2016) and the text and references have been re-organized to read as follows.

In contrast, modelling studies of the Arctic summer show that persistent cloud and drizzle causes wet deposition and results in low condensation sinks at the surface (Browse et al. 2014; Croft et al. 2016a). These same studies show that these conditions can favour particle nucleation followed by growth between drizzle events.

RC2.18

Page 3, Line 4

Fix sentence phrasing – "which is photo-mediated" doesn't describe the Canadian Arctic.

The sentence has been re-worded. The updated text is copied below for the reviewer's convenience.

Recent work by Mungall et al. (2017) in the Canadian Arctic also suggests that a photo-mediated marine source of oxygenated volatile organic compounds could produce precursor vapors for new particle formation or growth.

RC2.19

Section 2.1 & 2.2

Please provide tubing diameter in metric, rather than English, units. Also, inner diameters would be more useful than outer diameters.

The text has been updated with:

At the PEARL RidgeLab, the instruments sampled year-round through a common aerosol inlet, made of 6 m of stainless steel tubing with a 25.4 mm outer diameter (OD) and an inner diameter (ID) of 22 mm, sampling 2 m above the roof of the laboratory with a total flow rate of 11 L/min, as previously described by Kuhn et al. (2010). The SMPS flow passed first through 0.5 m of 25.4 mm OD and 22 mm ID stainless steel tubing

connected to the common aerosol inlet; this flow then entered a 9.53 mm OD stainless steel tube with a length of 0.45 m and finally passed through a 6.35 mm OD and 4.72 mm ID copper tube that was 1.05 m long. For the OPC, the flow passed from the common aerosol inlet into a 12.7 mm OD copper tube with an ID of 9.40 mm and a length of 0.8 m, and then into a 6.35 mm OD copper tube with an ID of 4.72 mm and a length of 0.58 m, which was connected to the OPC by 6.35 mm OD conductive rubber tubing with an ID of 3.18 mm and a length of 0.04 m. Particle transmission efficiency to the SMPS has been calculated and the resulting transmission curve is shown in Figure S1 (von der Weiden et al. 2009). From the common aerosol inlet, the AMS flow passed first through 0.5 m of 25.4 mm OD and 22 mm ID stainless steel tubing and then through a 9.53 mm OD stainless steel tube with a length of 0.45 m before entering the AMS.

And following the recommendation given in comment RC1.4, this portion of the text is now in the supporting information.

RC2.20

Page 3, Lines 25-28

Provide sampling inlet information, as was done for the Eureka sampling.

We have updated the text to reference the appropriate articles that contain the sampling inlet information.

Details of the aerosol sampling inlet at Alert are described in the previous work of Leaitch et al. (2013) and Leaitch et al. (2018).

RC2.21

Section 2.2 and Page 9, Line 11

Provide the size range of the AMS.

The text has been updated with:

In Section 2.2:

Both hourly bulk and size-resolved concentrations were measured by switching between mass spectrometry (MS) mode and particle time-of-flight (PToF) mode, which provides quantitative measurements in the range of 50 to 1000 nm (aerodynamic diameters).

And the Section 3.2:

AMS measurements of aerosol chemical composition and mass concentration for the summer of 2015 are shown in Figures 3a and 3b, where the PM_1 mass concentrations include the four dominant types of non-refractory aerosol.

RC2.22

Page 5, Line 21

Please clarify what is meant by “in a straight line”. Upwind?

We agree with the reviewer that the term “in a straight line” is unnecessary and thus confusing. It has been deleted. Simply stated, the distance between the PEARL RidgeLab and the ECCC Weather Station is 11 km.

RC2.23

Page 7, Line 11

Please clarify “this year”.

The text has been updated in Section 3.1.1 with:

The one exception is that the 90th percentile was higher for Alert in 2015, which was driven by two events with especially elevated particle concentrations. Coinciding events were observed at Eureka, but the particles concentrations were much lower. The reason for the elevated concentrations at Alert but not at Eureka is unknown.

RC2.24

Page 7, Line 22-23

Is this the case for all 23 other events? Please clarify.

The text has been updated with a new sentence in the Section 3.1.2:

To further analyze the growth events and periods with elevated concentrations of ultrafine particles, two different sets of case studies were selected comprising five (Table 1) or 28 events (Table S1). The latter represents all the growth events observed during the measurement period (22 events during 2016 and 6 events during the shorter 2015 period), and the smaller set of 5 was used to calculate growth rates. This subset of events was chosen because they were distinct, without overlap with proceeding or subsequent growth events and exhibited relatively smooth growth curves. The remaining 23 growth events were sometimes interrupted, presumably due to changes in air mass origin, or consisted of several events overlapping each other. All of the 5 growth events presented in Table 1 represent complete and smooth growth events that were suitable for calculating growth rate.

RC2.25

Page 7, Line 26

Are these references misplaced? The data shown in Table 1 is original to this work.

We kindly refer the reviewer to our response to comment RC1.6 for which we have reorganized the references and added a short description of the method for calculating the growth rate.

RC2.26

Page 9, Lines 7-8

Please clarify – did only one growth event (of the 5?) have a similar growth rate and back trajectory? Did other growth events, for which growth rates weren't calculated, have similar back trajectories? This would be useful to know.

We have added back-trajectories for additional growth events in Figure S7, and the text in Section 3.1.3 has been updated accordingly.

To understand the influence of the air mass history on the occurrence of the growth events, back-trajectories were calculated using FLEXPART (Figure S7) for Eureka and Alert. (The particle size distributions for the analyzed events for Eureka and Alert are shown in Figures 5 and S8, respectively). This calculation permits the precise evaluation of the spatial distribution of the potential emissions sensitivity at the beginning of each growth event. In general, these calculations show that the aerosols measured at the PEARL RidgeLab are mostly influenced by source regions located in the Canadian Arctic Archipelago, in Baffin Bay and to the north of Ellesmere Island. These results mostly coincide with the research reported by Collins et al. (2017), in which they observed high concentrations of ultrafine particles in these regions. Furthermore, the analyzed growth events generally have similar air mass histories for both the PEARL RidgeLab and Alert for a given event. The exception is GE 30 at the PEARL RidgeLab, which began on 25 June 2016, was more influenced by areas near and further north of Alert with a small contribution from the Nares Strait region. Interestingly, NASA Worldview images (https://worldview.earthdata.nasa.gov/) show that on 25 June 2016 (Figure S13) and for several preceding days, while the ocean in these regions was mostly covered in sea-ice, the potential emissions sensitivity was still influenced by large areas of open water. In conclusion, growth events can occur within air masses with different back-trajectories, as also reported by Collins et al. (2017), although the potential emissions sensitivities for the five growth events shown in Figure S7 have a substantial amount of overlap.

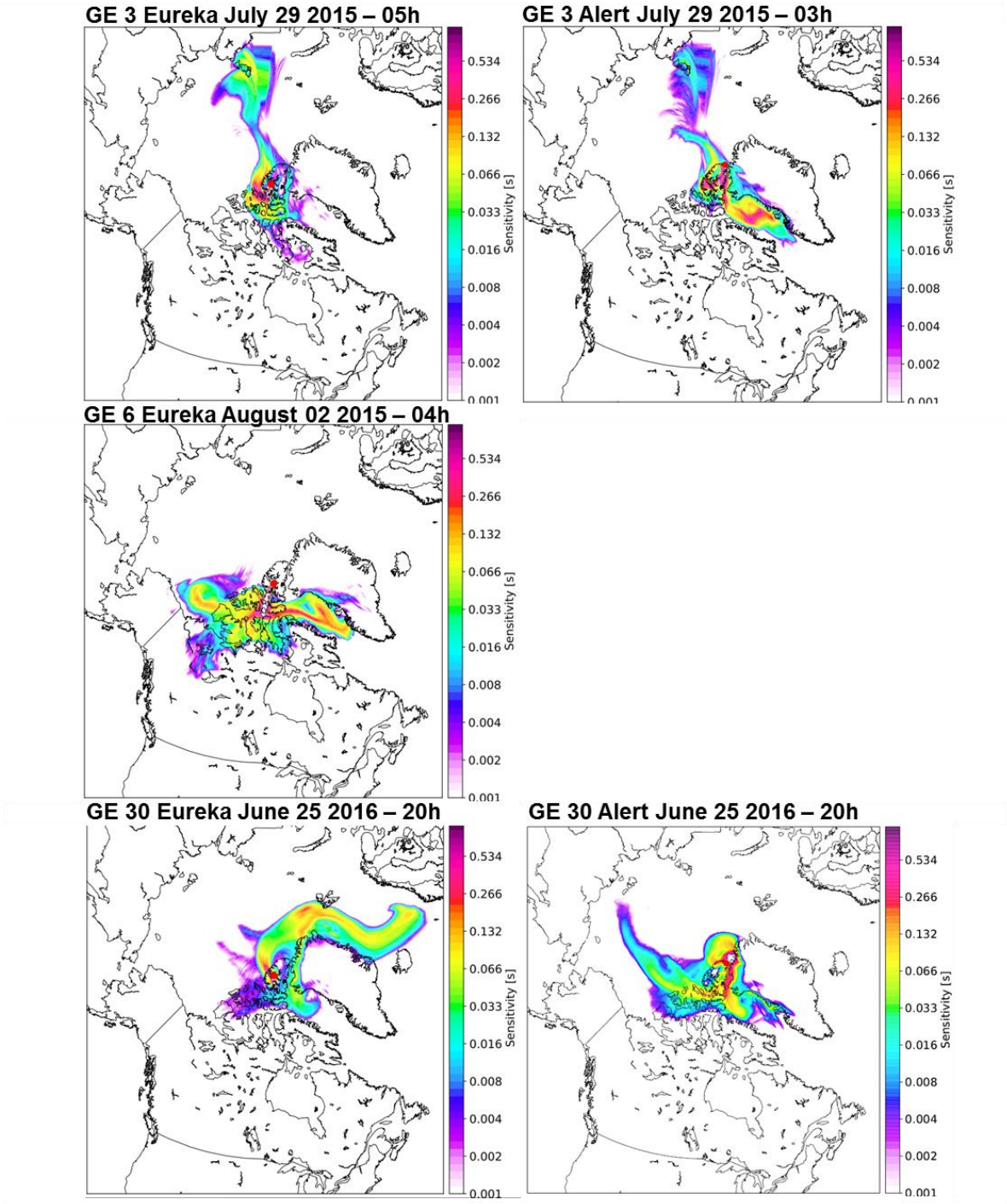

Figure S7. Evaluation of the air mass history during the five selected growth events summarized in Table 1 and shown in Figure 5 of the main text. The back-trajectory and potential emissions sensitivity were calculated using FLEXPART. The left column corresponds to air masses arriving at Eureka and the right column corresponds to those arriving at Alert.

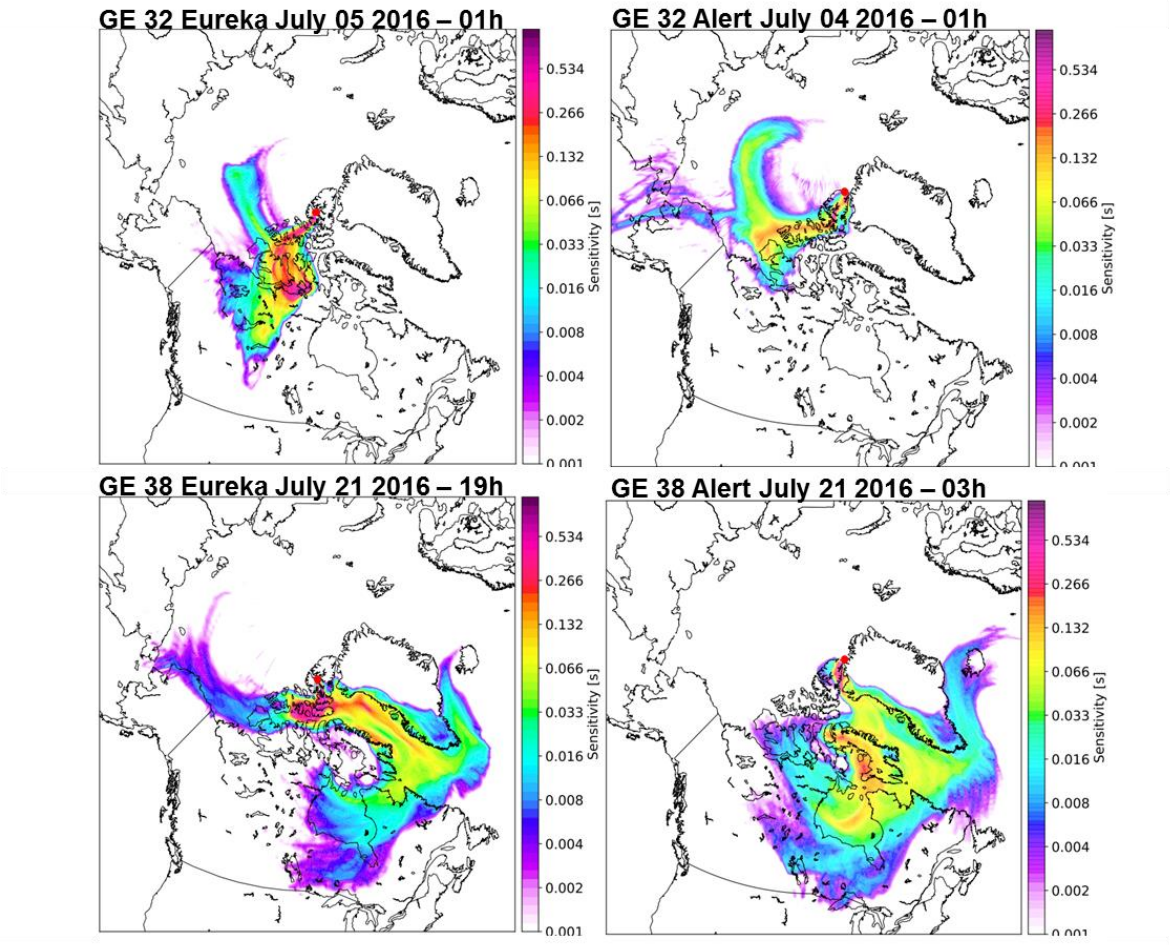

Figure S7. Evaluation of the air mass history during the five selected growth events summarized in Table 1 and shown in Figure 5 of the main text. The back-trajectory and potential emissions sensitivity were calculated using FLEXPART. The left column corresponds to air masses arriving at Eureka and the right column corresponds to those arriving at Alert (continued).

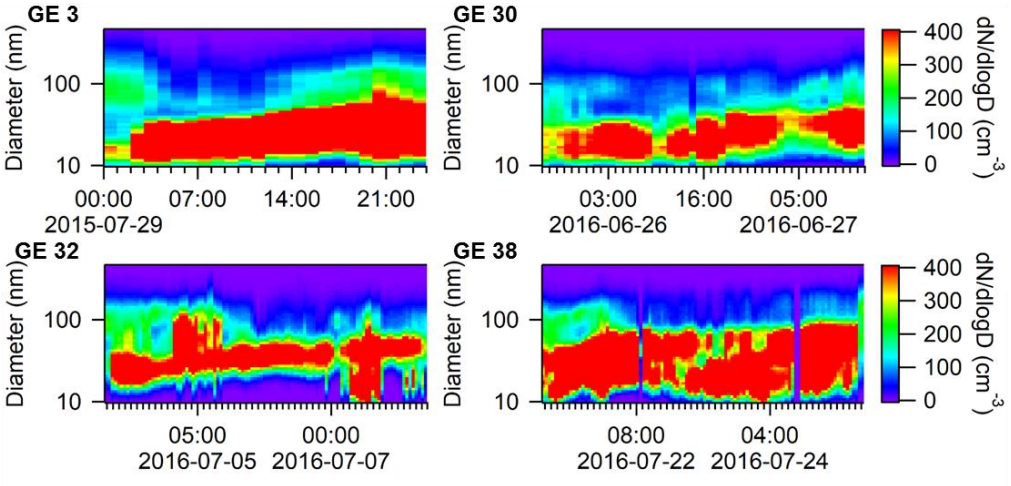

Figure S8. SMPS measurements of 4 growth events at Alert during the summers of 2015 and 2016 corresponding to the periods summarized in Table 1. The sizes are mobility diameters measured by an SMPS, which are equal to the physical diameters under the assumption that the particles were spherical and contained no voids.

RC2.27

Page 9, Line 13

By “later in the year”, do you mean “later in the summer”?

The text has been updated with:

In contrast, later in the summer (approximately 30 August 2015 to 5 September 2015) there is a period of larger particles when the mass concentration of sulphate is higher than the organic component.

RC2.28

Page 10, Line 10-11

This sentence is not related to this paragraph.

This sentence : “*Overall, the size-resolved measurements indicate that for the two growth events analyzed here, which occurred during summer 2015, the mass of the growing particles is predominately organic matter.*” **has been removed from the article.**

RC2.29

Page 12, Line 1

Please clarify the exact size range measured in this previous work.

The text has been updated with:

This result is in contrast to previous indirect measurements of aerosol composition using a volatility tandem differential mobility analyzer system installed near Ny-Ålesund, Svalbard (Giamarelou et al. 2016), which suggested that 12 nm particles were predominately ammonium sulphate, although it was not possible in that study to conclusively distinguish ammonium sulphate from organics with similar volatility.

RC2.30

Figure 2b

Are these daily averages? This needs to be clarified.

The caption has been updated with:

Note that the data in the scatter plot correspond to daily averages of particles with diameters between 20 and 70 nm.

RC2.31

Figure 6

Please state the years included in this plot.

The caption has been updated with:

The average temperature change of each event is provided in Table S1, and was calculated from radiosonde measurements during 2015 and 2016, as shown in Figure 6.

RC2.32

Figure 7a-d

These plots are missing legends, which impacts interpretation of the figure.

We updated the figure to include the legend.

RC2.33

Figure S2

Please note the averaging used for this plot. Were the diameters adjusted?

Hourly averages were used for this plot, and this averaging interval is now indicated in the figure caption. The equivalence of the SMPS and OPC diameters is discussed above in our response to comment RC2.4, and we kindly refer the reviewer to that response.

Referee 3 Comments

Major comments

RC3.1

Influence of meteorology on measurements performed at PEARL:

In the paper is said that "growth events (and presumably nucleation) are more commonly observed when the inversion is weaker or not present" however only vertical profiles during event days are analysed. The authors should look at vertical profiles during non-

event days and compare them with those presented in the paper. For example it would be useful to plot the histogram shown in fig. 6 both for event and non-event days and check if the difference is significant or not.

We kindly refer the reviewer to our response to comment RC1.7.

RC3.2

Moreover, for certain days, it seems like growth is happening with a relatively strong temperature inversion. I would suggest to check the diurnal profile of water vapour mixing ratio (I assume this to be measured at PEARL), this should show an increase if the airmass is coming from the boundary layer compared with the free troposphere. In case no evidences for boundary layer air contribution are found it would be interesting to check if the particle chemical composition during the growth is different from other events.

Based on the reviewer's suggestion, we compared observations at the surface, as measured at the Eureka weather station, and at the PEARL RidgeLab. The figure below illustrates the water vapour mixing ratio at the two heights. Only data from 2016 are included because observations were missing from the PEARL RidgeLab for most of August 2015, when growth events were observed. The first box-and-whiskers plot represents all times when data were available between June and September 2016 inclusive, and the second (GE) represents values when the growth events were occurring in 2016. (Note that the whiskers represent the farthest point that is less than or equal to the interquartile difference multiplied by a factor of 1.5.) Based on the lack of a difference in the water vapour mixing ratio, it appears that the air is fairly well-mixed between the surface and the PEARL RidgeLab. In addition, box-and-whiskers plots are given for periods when a growth event was not observed and either low concentrations of aerosols were present (NE low) or a persistent accumulation mode was present (NE High). These selected "non-events" are summarized in Table S2 of the supporting information. The NE low plot is similar to the All and GE plots, but the NE High plot has surprisingly a negative median indicating that the airmass at the PEARL RidgeLab had a higher water vapour mixing ratio compared to the Eureka weather station. Overall, these results suggest that the PEARL RidgeLab is generally influenced by the surface throughout the summer, including during growth events. There were however periods of elevated concentrations of relatively large particles that were not growing (as shown in Figure S6), and the water vapour observations during these periods would be consistent with an airmass at the PEARL RidgeLab that is more influenced by regions warmer than the surface at Eureka. We note lastly that the NE High periods also tended to exhibit a more pronounced inversion as described in our response to comment to RC1.7.

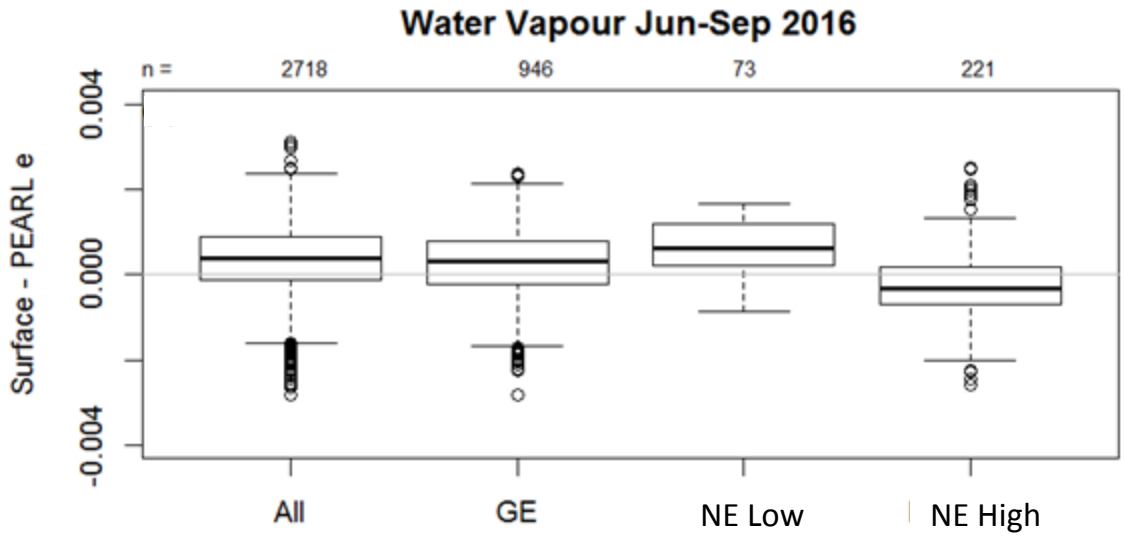

RC3.3

Methanesulfonic acid contribution:

Mass spectra for 2 aerosol growth events are compared with lab measurements of MSA particles to prove that there are organics contributing to the growth besides MSA. The relative differences and the small correlation between ambient and lab spectra provides a qualitative argument in favour of this hypothesis but the authors should try to quantify the contribution of MSA to the total organic mass. I'm aware of the fact that, due to the low resolution of a Q-AMS, this could be tricky but there are previous studies [1] reporting MSA concentration with the same instrument (the same paper is also cited by Tremblay et al.), so with the available data it should be possible to calculate at least an upper bound on the organic mass fraction attributable to MSA.

We have addressed this comment by adding the following text to the manuscript in section 3.2.

To further verify these findings, the AMS fragmentation table was also modified to separately quantify MSA following Phinney et al. (2006), but the concentration of MSA was generally at or below the detection limit (0.021 $\mu g/m^3$ as determined by multiplying by 3 the standard deviation when the AMS was sampling through a filter). Based on this detection limit, the MSA concentration was 5% or less of the total organic and sulfate mass concentration during the two measured growth events, GE3 and GE6.

RC3.4

Size resolved aerosol chemical composition:

In figure 7, the authors show chemical composition down to 10 nm, whereas the sizing calibration is done until 80 nm. This extrapolation is beyond AMS capabilities (it would be incredibly good if an AMS could really measure 10 nm particles) and needs to be corrected, a non-AMS user could easily be fooled by these figures.

It is true that the calibration is only performed to a vacuum aerodynamic diameter of 80 nm. However, the AMS transmission curve allows qualitative detection of particles with sizes down to approximately 30 nm vacuum aerodynamic diameter (Jayne et al. *Aerosol. Sci. Technol.* 2000, *33*, 49-70). Furthermore, it is also useful to display the size distribution trace to 10 nm in order to verify that the AMS PToF baseline is correctly located near zero. Nevertheless, we agree with the reviewer that particle size calibration must be extrapolated below 80 nm, which means that the AMS size distribution data should not be interpreted in a quantitative manner below this diameter. We have therefore added the following sentence to Section 2.2 of the manuscript.

Importantly, it should be noted that the extrapolation of the aerodynamic diameter calibration below 80 nm is not well constrained, so particle size data below this diameter should be considered qualitative rather than quantitative.

RC3.5

Aerosol composition during growth events:

The high organic-to-sulfate ratio reported in this paper for particles below 100 nm is surprising, in particular considering the marine sources, unfortunately the authors provide only a snapshot for 2 events while a more complete analysis should be performed to support their findings.

We agree with the reviewer that, ideally, a much longer measurement campaign would be carried out to characterize the aerosol chemistry. Unfortunately, it has continued to be logistically challenging and very expensive to conduct AMS measurement in this region, so there is no additional data available before or after the period shown in the article. To reflect this, we have updated the conclusions and text to emphasize that the conclusions are drawn from a limited data set. On the other hand, there is now an emerging body of literature, including this study, which supports the conclusion that secondary organics are an important contributor to aerosol growth in the Arctic.

The text has been updated in several different sections in response to this comment:

Abstract:

It was found that particles with diameters between 50 and 80 nm during these growth events were predominately organic with only a small sulphate contribution.

Introduction:

The mass spectrometry measurements indicate that these ultrafine particles (<100 nm) were predominately organic during the observed growth events. This work builds on other studies that have indirectly characterized the organic content of Aitken mode aerosols in the Arctic (Burkart et al. 2017) and have measured oxidised volatile organic compounds in the Arctic atmosphere (Mungall et al. 2017).

Conclusion:

Moreover, in this study AMS measurements showed that particles between 50 and 80 nm in diameter during two observed growth events were predominately organic.

RC3.6

The first thing that is not clear from figure 7 is why sulfate is present only in the larger particles, is this due to a second mode of aerosols that have a different history? The authors should comment on this. There are no indications about the period considered for the calculation of the size resolved chemical composition: is this an average over the whole growth event or a selection of a defined period?

The size resolved chemical composition was calculated by averaging over the whole growth event using the times indicated in Table 1 of the manuscript. This averaging is now mentioned in the Figure 8 caption.

We agree with the reviewer that the most likely explanation for the relatively high concentration of sulfate in the larger particles is the presence of a second aerosol mode with a different history. We have added a sentence to the text in Section 3.2 to address this point.

Between 80 and 1000 nm, the measured aerosol composition changes depending on the particle size and the larger aerosol particles contain a greater fraction of sulphate. The higher concentration of sulphate in the larger particles is most likely explained by the presence of a distinct accumulation mode having a history and source different from the Aitken mode aerosols.

RC3.7

I would appreciate if the authors could show the size resolved chemical composition at 2/3 different stages of the event, this could tell a little bit more about the mechanisms beyond the growth.

The figure below shows the unnormalized organic and sulphate aerosol concentration for GE3 and GE6 for the first half (a and b) and the second half (c and d) of each event. We can see clearly the organic size distribution is shifting to larger sizes from the beginning to the end of the growth event. The unnormalized data has not been mathematically normalized to the bulk measured AMS concentration. In this case normalizing is not necessary because only particle sizes are compared. (The AMS diameter has been adjusted to match the SMPS diameter.)

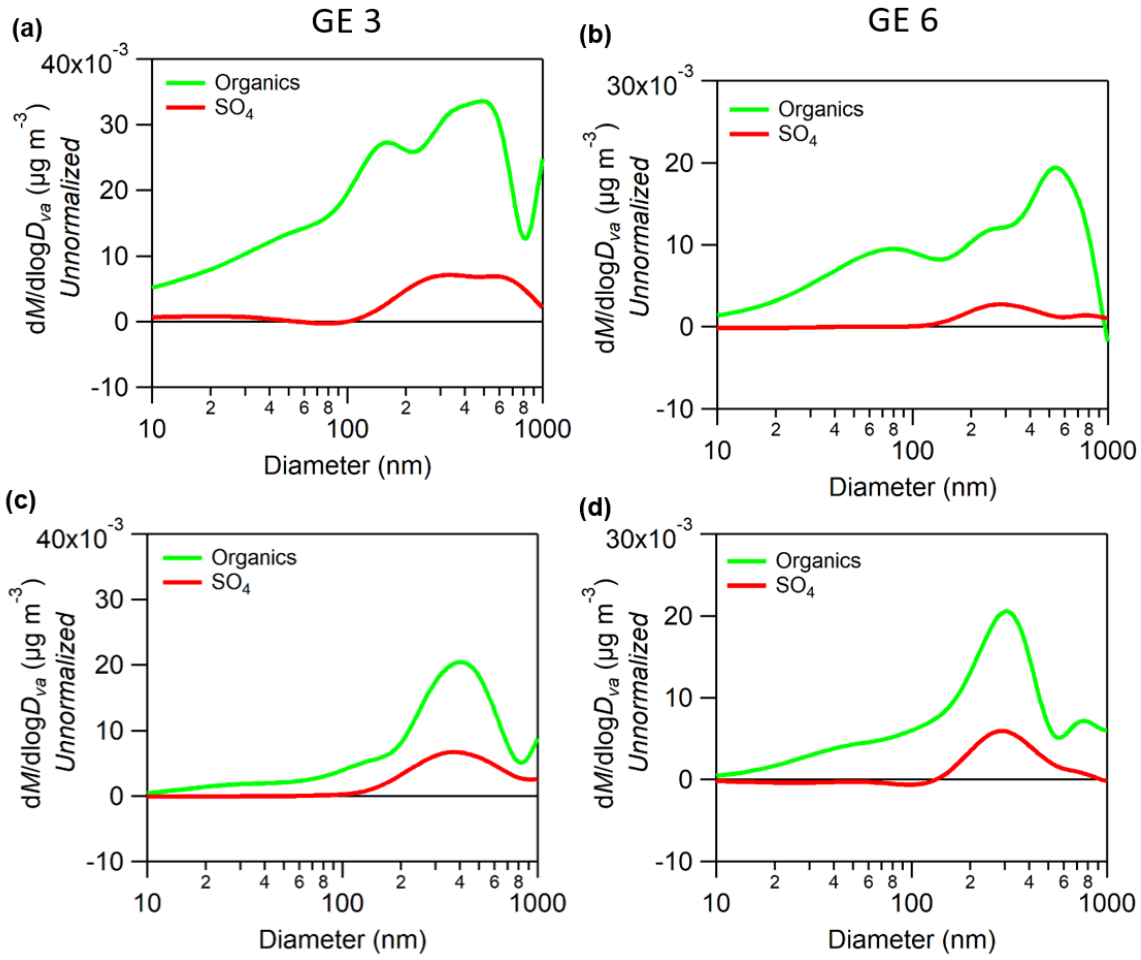

RC3.8

Moreover, it would be really useful if the authors could plot the total organic and sulfate time series concentration during the growth event. If the growth is mostly due to organics then I would expect to see an increase of organic concentration whereas sulfate should stay more or less constant.

As seen in the figure below, the sulphate mass shows a much smaller increase compared to the organic mass at the beginning of the two growth events. At the end of GE 3, other processes begin to affect the aerosol size distribution, which results in a small overall loss in total aerosol mass (0.06 µg/m^3). However, the expected

increase in aerosol mass during GE 6 based on the SMPS data (0.12 – 0.36 µg/m^3) is reflected in the time series of the organic concentration. This figure has been added to the manuscript in the supporting information.

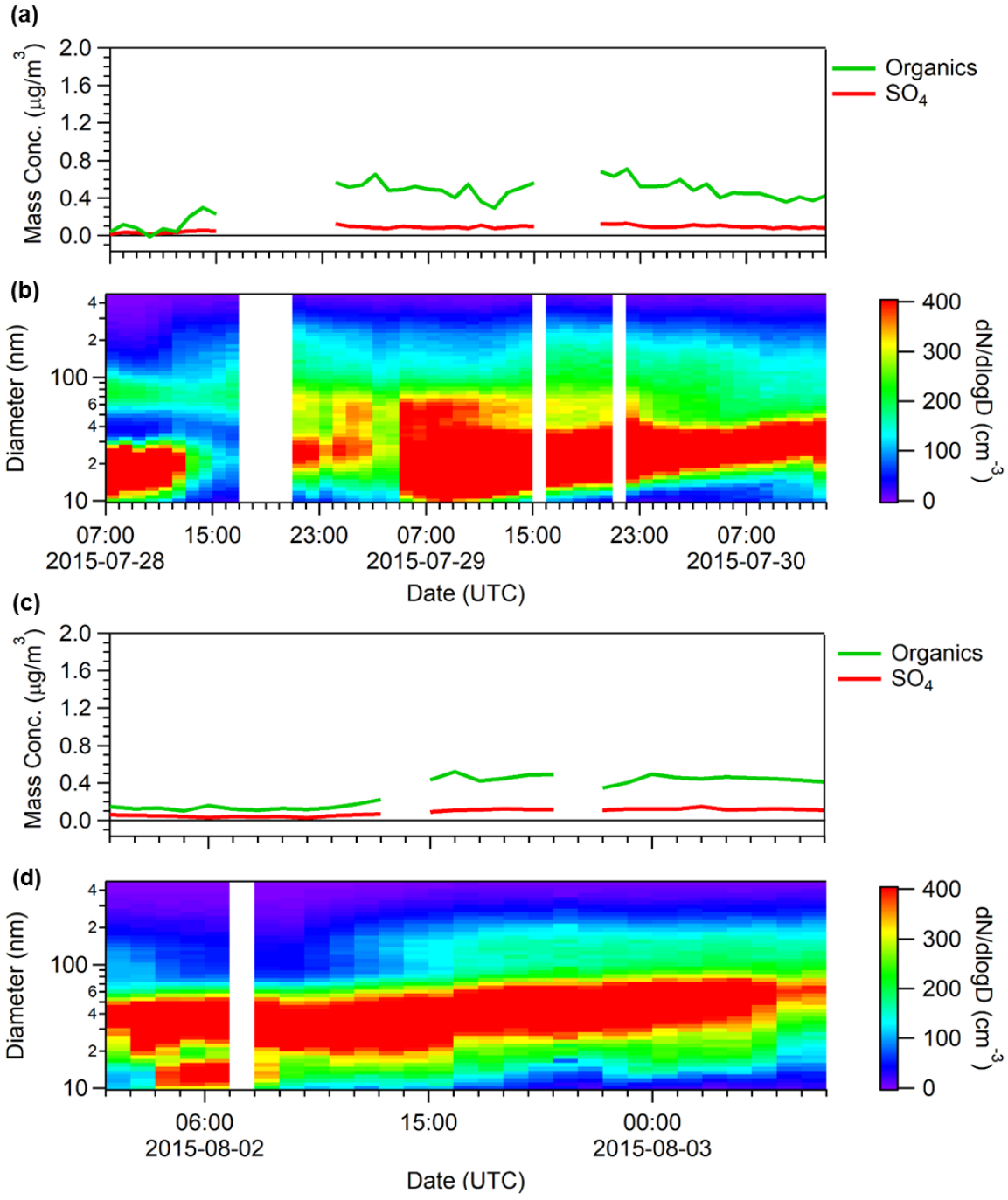

Figure S10. Aerosol mass spectrometry measurements of aerosol composition taken at the PEARL RidgeLab near Eureka showing only the organic and sulphate (SO_4) composition for GE3 **(a)** and GE6 **(c)** and the corresponding SMPS data for GE3 **(b)** and GE6 **(d)**. The sizes are mobility diameters measured by an SMPS, which are equal to the physical diameters under the assumption that the particles were spherical and contained no voids.

RC3.9

In addition, uncertainties on aerosol composition should be estimated and added to figure 7.

The uncertainties are now described in the caption of the figure. We don't show the uncertainties in the figures because the overlapping error bars reduce the clarity of the figure.

RC3.10

Finally, the authors conclude saying that "particles smaller than 100 nm in diameter are predominately organic with the organic-to-sulphate ratio increasing for smaller particle sizes", this is a general conclusion but is based on the analysis of only 2 events that does not provide any statistical basis for such kind of conclusion. For this reason the authors should look at the size resolved organic-to-sulfate ratio for all the events to check whether this statement is verified or not.

We kindly refer the reviewer to our response to comment RC3.5.

RC3.11

It would be useful also to compare the size resolved chemical composition with non event days.

We agree that this would be extremely useful. Unfortunately, it was not possible to do such a comparison because the mass concentrations are too low.

Minor comments

RC3.12

The authors often speak of particle nucleation, I would avoid using this terminology in the paper because there are no measurement for particles below 10 nm. For this reason there are no proof that nucleation is really happening at the measuring sites (in particular considering the small growth rates reported in this paper).

We agree and the necessary changes have made throughout the manuscript.

RC3.13

I would suggest to add a couple of sentences about iodine nucleation in the introduction. This has been proven to be a very effective mechanism in certain coastal regions [2] and a recent paper in the Arctic also showed evidence of this [3]. Later in the manuscript (chapter 3.2) the authors should also mention whether they see or not any evidence for iodine particles in their spectra.

We kindly refer the reviewer to our response to comment RC1.1.

RC3.14

In chapter 3.1.2 growth rates for 5 selected events are reported. However, there is no mention to the method used to estimate the growth, nor to the size range considered for the calculation. The authors should add this information to the manuscript that is really important in particular when comparing with results from other studies.

We kindly refer the reviewer to our response to comment RC1.6.

RC3.15

In chapter 3.2 a detailed analysis of fragments m/z 43 and 44 is provided, I wonder whether the authors can exclude any contamination from combustion or other sources (e.g. the generator) on fragment m/z 43.

We kindly refer the reviewer to our response to comment RC2.5.

RC3.16

Moreover, I agree with referee #1 in saying that figure 8 doesn't show any clear trend and the authors should reconsider their conclusions here.

We kindly refer the reviewer to our response to comment RC1.8.

RC3.17

Figure 3 shows a nice agreement between the PM1 as measured by the AMS and SMPS+OPC, however the authors should mention which density values were used to calculate the total mass for this comparison.

The average density as a function of time was calculated from the AMS composition measurements and used to calculate the total mass for the comparison. For the entire AMS measurement period the average density was 1.31 g/cm^3. The following has been added to Section 2.2: *Applying the density calculated from the AMS data to the particle size distribution, a linear regression…*

RC3.18

Figure 4 reports the total particle number concentration at the 2 measurement sites, I would suggest to add a second box and whisker plot showing only the concentration of Aitken mode particles.

We kindly refer the reviewer to our response to comment RC2.12.

NOTE: Modified text is highlighted in yellow (PLH)

Characterization of aerosol growth events over Ellesmere Island during summers of 2015 and 2016

Samantha Tremblay[1], Jean-Christophe Picard [1], Jill O. Bachelder[1], Erik Lutsch[2], Kimberly Strong[2], Pierre Fogal[2], W. Richard Leaitch[3], Sangeeta Sharma[3], Felicia Kolonjari[3], Christopher J. Cox[4], Rachel Y.-W. Chang[5], Patrick L. Hayes[1]

[1]Department of Chemistry, Université de Montréal, Montréal, Québec, Canada
[2]Department of Physics, University of Toronto, Toronto, Ontario, Canada
[3]Climate Research Division, Environment and Climate Change Canada, Toronto, Ontario, Canada
[4]Cooperative Institute for Research in Environmental Sciences (CIRES), Boulder, CO, USA and NOAA Physical Sciences Division, Boulder, CO, USA
[5]Department of Physics and Atmospheric Science, Dalhousie University, Halifax, Nova Scotia, Canada

Correspondence to: Patrick L. Hayes (patrick.hayes@umontreal.ca), Rachel Chang (rachel.chang@dal.ca)

Abstract. The occurrence of frequent aerosol nucleation and growth events in the Arctic during summertime may impact the region's climate through increasing the number of cloud condensation nuclei in the Arctic atmosphere. Measurements of aerosol size distributions and aerosol composition were taken during the summers of 2015 and 2016 at Eureka and Alert on Ellesmere Island in Nunavut, Canada. These results provide a better understanding of the frequency and spatial extent of elevated Aitken mode aerosol concentrations as well as of the composition and sources of aerosol mass during particle growth. Frequent appearance of small particles followed by growth occurred throughout the summer. These particle growth events were observed beginning in June with the melting of the sea ice rather than with polar sunrise, which strongly suggests that influence from the marine boundary layer was the primary cause of the events. Correlated particle growth events at the two sites, separated by 480 km, indicate conditions existing over large scales play a key role in determining the timing and the characteristics of the events.

In addition, aerosol mass spectrometry measurements were used to analyze the size-resolved chemical composition of aerosols during two selected growth events. It was found that particles with diameters between 50 and 80 nm during these growth events were predominately organic with only a small sulphate contribution. The oxidation of the organics also changed with particle size, with the fraction of organic acids increasing with diameter from 80 to 400 nm.

The growth events at Eureka were observed most often when the temperature inversion between the sea and the measurement site (at 610 m ASL) was non-existent or weak, presumably creating conditions with low aerosol condensation sink and allowing fresh marine emissions to be mixed upward to the observatory's altitude. While the nature of the gaseous precursors responsible for the growth events are still poorly understood, oxidation of dimethyl sulphide alone to produce particle phase sulphate or methanesulphonic acid was inconsistent with the measured aerosol composition, suggesting the importance of other gas phase organic compounds condensing for particle growth.

1 Introduction

Surface aerosol concentrations in the Arctic are characterized by a distinct seasonal cycle, with high mass loadings in the winter followed by very low mass loadings in the summer (Sharma et al. 2004; Quinn et al. 2007; Engvall et al. 2008; Sharma et al. 2013; Tunved et al. 2013; Croft et al. 2016a; Nguyen et al. 2016). This cycle is caused by different transport patterns and by changes in wet deposition, with wintertime air influenced by pollution originating from continental regions at lower latitudes such as Europe, Siberia and even South Asia (Stohl 2006). In contrast, during summertime, air masses originating from lower latitudes experience greater wet deposition during transport northwards, resulting in very few particles arriving to the north. Consequently, local sources dominate the surface aerosol. In wintertime, Arctic air near the surface spends about one week continuously above 80°N, whereas in summertime the air near the surface spends about two weeks continuously above 80°N (Stohl 2006), also increasing the relative importance of aerosols originating in the Arctic. The nature and sources of aerosols of Arctic origin during summertime are still poorly understood, although marine and snow or ice-related sources have been suggested in the past (e.g. Leck and Bigg 2005b; Fu et al. 2013; Willis et al. 2016). As the Arctic continues to warm and summer sea-ice coverage decreases, contributions from marine sources will likely increase while snow or ice-related sources will decrease. In addition, increased shipping and industrial activities during the Arctic summer in the future could completely shift the relative importance of natural and anthropogenic aerosol sources (Croft et al. 2016a).

In tropical marine locations, new particle formation tends to occur in the upper part of the troposphere, usually at the outflow of clouds, and these particles are entrained to the surface through mixing, which contributes to relatively stable aerosol size distributions (Hoppel et al. 1986; Clarke et al. 2006). In contrast, modelling studies of the Arctic summer show that persistent cloud and drizzle causes wet deposition and results in low condensation sinks at the surface (Browse et al. 2014; Croft et al. 2016a). These same studies show that these conditions can favour particle nucleation followed by growth between drizzle events. This is supported by surface observations of aerosol size distributions in the Arctic at Alert and Ny-Ålesund that show an annual cycle during which summertime surface aerosols exhibit much smaller particle diameter than wintertime aerosols (Tunved et al. 2013; Croft et al. 2016a). Additional surface observations have suggested that new particle formation could be the source of these small particles, with dimethyl sulphide (DMS) emitted from the ocean being a key gaseous precursor of less volatile species, such as sulphuric acid and methanesulphonic acid, that contributes to aerosol mass (Chang et al. 2011; Leaitch et al. 2013).

Sulphuric acid has long been known to contribute to new particle formation and growth events (Twomey 1977; Charlson et al. 1992; Napari et al. 2002; Lohmann and Feichter 2005; Kirkby et al. 2011; Almeida et al. 2013; Croft et al. 2016b). More recent work has shown that in coastal Arctic environments, ammonia from sea-bird colonies can contribute to new particle formation (Croft et al. 2016b). In addition, organic compounds, especially those with lower volatilities, have also been found to contribute secondary aerosol mass to particle growth and nucleate new particles in forested and anthropogenically influenced regions (Allen et al. 2000; Zhang et al. 2009; Pierce et al. 2012; Riipinen et al. 2012) as well as

in laboratory studies (Kirkby et al. 2016; Trostl et al. 2016). Box models have inferred the contribution of non-sulphur species (i.e. organic compounds) to aerosol growth in Greenland (Ziemba et al. 2010) and in tropical marine cloud outflow (Clarke et al. 1998). Burkart et al. (2017) provided indirect evidence that organic compounds contribute to aerosol growth in high-latitude marine environments using both microphysical modeling of a particle growth event as well as cloud condensation nuclei (CCN) hygroscopicity measurements. In a comparison of ship-borne observations in the Canadian Arctic in 2014 and 2016, Collins et al. (2017) found that increased activity in marine microbial communities along with greater solar radiation and lower sea ice concentrations contributed to new particle formation and growth. Recent work by Mungall et al. (2017) in the Canadian Arctic also suggests that a photo-mediated marine source of oxygenated volatile organic compounds could produce precursor vapors for new particle formation or growth. Furthermore, iodine may be important for particle nucleation in the Arctic (Mahajan et al. 2010; Allan et al. 2015; Raso et al. 2017), although the processes leading to either nucleation or particle growth are not necessarily the same.

The GEOS-Chem chemical transport model has been used to model particle formation and size distributions in the Arctic (Bey et al. 2001; Wild and Prather 2006; Croft et al. 2016a; Croft et al. 2016b; Christian et al. 2017). Recent work using GEOS-Chem with the size-resolved aerosol microphysics package TOMAS (Croft et al. 2016a; Croft et al. 2016b) analyzed size distributions of aerosols measured in the Arctic, and showed that GEOS-Chem-TOMAS underestimates Aitken mode particle sizes during the summertime. It was also shown that new particle formation can be driven by neutralization reactions, where missing ammonia emissions can be accounted for by seabird colonies. However, this work acknowledged poor constraints on marine primary aerosol and secondary organic aerosol precursors. These results demonstrate the difficulties that the GEOS-Chem model has in predicting particle size distributions for the Aitken mode during summertime, which is presumably due to missing processes contributing to particle growth (e.g. the condensation of semi-volatile or low-volatility vapors). Similar discrepancies are also observed in the chemical transport model GLOMAP (Global Model of Aerosol Processes) (Korhonen et al. 2008; Browse et al. 2014), with a low bias observed for either Aitken or Accumulation mode aerosols.

In this study we present direct measurements of size-resolved aerosol chemical composition using mass spectrometry to better understand the processes contributing to aerosol growth during the summertime in the Canadian High Arctic. These measurements, as well as those of aerosol number size distribution, were conducted at Eureka, Nunavut on Ellesmere Island in the Canadian Arctic Archipelago. For comparison, aerosol size distributions measured at Alert, which is located further north on Ellesmere Island, are also reported. Numerous concomitant events in which small particles appear and then grow are observed at both sites throughout the summer, resulting in large variations in the number concentration of particles with diameters smaller than 100 nm. The mass spectrometry measurements indicate that these ultrafine particles (<100 nm) were predominately organic during the observed growth events. This work builds on other studies that have indirectly characterized the organic content of Aitken mode aerosols in the Arctic (Burkart et al. 2017) and have measured oxidized volatile organic compounds in the Arctic atmosphere (Mungall et al. 2017). Taken together, these results provide

important evidence that the condensation of lower volatility organic vapors on particle surfaces leads to frequent particle growth events observed at two sites on Ellesmere Island (e.g. approximately 20 events during summer 2016 at Eureka).

2 Experimental

2.1 Field Site Information and Aerosol Sizing Instrumentation

The primary measurement site for surface aerosols was the Polar Environment Atmospheric Research Laboratory (PEARL) (Fogal et al. 2013) located on Ellesmere Island in Nunavut, Canada (80.05° N, 86.42° W). The PEARL Ridge Laboratory (RidgeLab) is located 610 m above sea level and 11 km northeast of the Environment and Climate Change Canada (ECCC) Eureka Weather Station, located at sea level. Radiosondes are launched twice a day from the Weather Station at 00:00 UTC and 12:00 UTC and are used in this work to evaluate the vertical temperature profile and presence of temperature inversions between sea level and the altitude of the RidgeLab. Solar radiation data were measured by a pyranometer (Kipp & Zonen CM 21) at the Surface and Atmospheric Flux, Irradiance and Radiation Extension (SAFIRE) site, situated near Eureka Weather Station at 85 meters above sea level (79.98° N, 85.93° W). A map showing the PEARL RidgeLab, Eureka weather station and SAFIRE is provided in Figure S2.

A scanning mobility particle sizer (SMPS, TSI 3034) measured the aerosol size distribution for diameters between 10 and 487 nm in 54 channels, while an optical particle counter (OPC, Met One GT-526S) measured the aerosol size distribution at diameters between 0.3 and 10 µm in six channels. Both instruments were connected to a common inlet, which is described in greater detail in the SI. Following the work of DeCarlo et al. (2004), the mobility diameter measured by the SMPS was assumed to be equal to the physical diameter, which would be valid if the sampled particles were spherical and contained no voids. This is a reasonable assumption given the secondary origin of the observed particles. It was further assumed that the OPC diameter was equal to the physical diameter, given that the Mie scattering curve of the ambient aerosols was likely within 10% of that of the calibration particles composed of polystyrene latex spheres.

Measurements from these instruments are reported for a period starting in July 2015 through September 2016, and thus consist of one full 2016 summer season and the full summer month of August 2015. (Wintertime measurements were taken too, but are not presented in this article.) Both the OPC and SMPS data were recorded every three minutes, and then averaged hourly for analysis and comparison to other data sets. Agreement between the SMPS and OPC was evaluated by comparing the particle number concentration between 300 – 487 nm measured by the SMPS against the concentration measured by the OPC for approximately the same range of particle diameters (300 – 500 nm). The results are shown in Figure S3 and the agreement is generally satisfactory (slope = 1.3 and 0.96, R^2 = 0.96 and 0.97, for 2015 and 2016 respectively).

The aerosol size distributions measured at the PEARL RidgeLab were compared against those measured at Alert, Nunavut located 480 km to the northeast (Figure S2), where the surface measurements were conducted at the Dr. Neil Trivett Global Atmosphere Watch Observatory (82.5° N, 62.3° W), 210 m above sea level. At this site, particle size distributions

between 10 and 487 nm were measured using a SMPS (TSI 3034) (Leaitch et al. 2013). Details of the aerosol sampling inlet at Alert are described in the previous work of Leaitch et al. (2013) and Leaitch et al. (2018).

2.2 Aerosol Mass Spectrometer

Between 26 July and 8 September 2015, a quadrupole aerosol mass spectrometer (AMS, Aerodyne Research Inc.) measured the chemical composition of submicron non-refractory aerosol particles at the PEARL RidgeLab (Canagaratna et al. 2007). Both hourly bulk and size-resolved concentrations were measured by switching between mass spectrometry (MS) mode and particle time-of-flight (PToF) mode, which provides quantitative measurements in the range of 50 to 1000 nm (aerodynamic diameters). All data were analyzed using standard AMS software (AMS Analysis Toolkit v1.43) with Igor Pro v6.3.7.2 (WaveMetrics). The instrument was calibrated multiple times during the measurement period with 300 nm diameter ammonium nitrate particles to determine the ionization efficiency. The aerodynamic diameter was calibrated using polystyrene latex spheres at 80, 125, 240 and 300 nm. Importantly, it should be noted that the extrapolation of the aerodynamic diameter calibration below 80 nm is not well constrained, so particle size data below this diameter should be considered qualitative rather than quantitative. Filtered air was sampled every day to establish the air beam corrections. Aerosol mass measured by the AMS was corrected for the instrumental collection efficiency using the method of Middlebrook et al. (2012). The collection efficiency (CE) varied between 0.45 and 0.86 with the increases in CE corresponding to periods when aerosol sulfur was present in its acidic forms (sulphuric acid and ammonium bisulphate) rather than as ammonium sulphate. Vacuum aerodynamic diameters measured by the AMS were converted to physical diameter under the assumption that the particles were spherical, contained no voids, and had a density of 1.25 g cm^{-3} (DeCarlo et al. 2004). This density is typical for ambient organic aerosol (Middlebrook et al. 2012) and was selected for this study since the analysis was focused on the particle composition during the predominantly organic aerosol growth events.

To evaluate the accuracy of the AMS measurements, they were compared to the mass concentration of particles having a diameter of less than 1 µm (PM_1) from the combined SMPS and OPC measurements. Applying the density calculated from the AMS data to the particle size distribution, a linear regression analysis of the AMS PM_1 mass concentration versus that calculated from the combined SMPS and OPC measurements resulted in a correlation coefficient of 0.89 and a slope of 1.16. These values confirm that the collection efficiency algorithm from Middlebrook et al. (2012) was reasonable.

2.3 Meteorological Data

Radiosondes (Vaisala RS92-SGP) launched from sea level at the Eureka Weather Station provided different meteorological parameters for altitudes both below and above the PEARL RidgeLab. The radiosondes are launched every 12 h by ECCC meteorological technicians, and the reported data were obtained from the University of Wyoming, Department of Atmospheric Sciences' Upper Air Data Website (http://weather.uwyo.edu/upperair/sounding.html). While the resulting measurements provide a means to evaluate the vertical temperature profile, and thus whether the PEARL RidgeLab at 610 m

was located within or above the inversion layer, caution must be taken in interpreting the results due to a number of considerations: (1) the ECCC Weather Station is located approximately 11 km from the PEARL RidgeLab, (2) the complex terrain in the region, and (3) the radiosondes do not necessarily fly straight up and can meander significantly after launch because of the wind direction. Therefore, the radiosonde measurements do not necessarily reflect the vertical temperature profile near the PEARL RidgeLab.

2.4 Back-Trajectory Analysis

Air mass histories were computed using the FLEXible PARTicle (FLEXPART (Stohl et al. 2005)) Lagrangian-dispersion model. The tracer particles are inert and non-interacting and are released from the position of the PEARL RidgeLab at an altitude of 610 m above sea level. Backward dispersion runs were initialized by releasing an ensemble of 6000 air-tracer particles over a 6 hour period around the times corresponding to the beginning of the growth events listed in Table 1. FLEXPART was run in backward mode for 6 days driven by meteorological data from the National Centers for Environmental Prediction (NCEP) Climate Forecast System (CFS V2) 6 hourly product (Saha et al. 2014) to calculate the spatially resolved potential emissions sensitivity, which is proportional to the residence time of a tracer above a given grid cell. Potential emissions sensitivity represents the amount of time that an air mass is influenced by emissions within a given grid cell during the duration of the FLEXPART run. In this study, the potential emissions sensitivity is time-integrated over a period of 6 days before the particle release time.

3. Results and Discussion

3.1 Summertime Aerosol Size Distributions

3.1.1 Observations at Eureka and Alert

Figure 1 shows the aerosol size distributions measured at the PEARL RidgeLab and at Alert for 16 June to 26 September 2016. Particle growth events were evident at both sites. In total, 34 events with elevated concentrations of small particles (< 20 nm diameter) were observed at the PEARL RidgeLab during this period, 22 of which were followed by growth lasting between 2 to 6 days. It is important to note that the local anthropogenic emissions should be completely negligible due to the extremely remote position of the site. The electricity for the PEARL RidgeLab is generated by a small power plant located 11 km from the site and there is no indication from the measurements that the site is significantly influenced by emissions from the power plant or the Eureka Weather Station. The sudden appearance of Aitken mode particles is consistent with previous field observations performed in the Canadian Arctic during research flights and cruises (Chang et al. 2011; Leaitch et al. 2013; Willis et al. 2016; Collins et al. 2017). While the sources of these particles remains poorly understood, this previous work suggested that the formation and growth of ultrafine particles may be due to marine biological activity and the oxidation of DMS and volatile organic compounds (VOCs). The sustained particle growth observed at the PEARL RidgeLab and at Alert, as well as in the previously published work cited above suggests that there is

a significant atmospheric reservoir of chemical compounds with volatilities that are low enough to partition to a condensed phase and could thus also be contributing to the nucleation process. Nevertheless, it is not possible to rule out primary marine emissions as a source of particles that provide the necessary surface area for condensing gases (Leck and Bigg 2005a). During certain events that exhibit the appearance of Aitken mode particles and subsequent growth, there are also signs of successive events that merge into the growth events from previous days, consistent with other observations in the Arctic (Collins et al. 2017).

Despite being almost 500 km apart, the particle growth events occurred at similar times at both the PEARL RidgeLab and Alert (Figure 1). While simultaneous nucleation events at sites as far apart as 350 km have been observed in continental regions where SO_2 concentrations are high (Jeong et al. 2010; Crippa and Pryor 2013), to our knowledge this work is the first time such a correlation of specific events has been observed in the Arctic, although monthly averages have been previously compared (Freud et al. 2017). It is also important to note substantial topographic barriers exist between the two stations that are located on opposite sides of the Arctic Cordillera, which hinders direct passage of air masses between the two sites (see discussion of back-trajectories in Section 3.1.3). The particle number concentrations measured at the two sites for diameters between 10 and 487 nm are similar (Figure 2a), and the number concentration of particles between 20 and 70 nm at the two sites shows a moderate correlation with a correlation coefficient of 0.61 (Figure 2b). These results confirm that the growth events have a tendency to occur at similar times at both sites, demonstrating that conditions can exist in the Arctic that are favourable for aerosol growth over distances of at least 500 km.

Similar to Figure 1, the aerosol size distributions at the PEARL RidgeLab and Alert were measured for a portion of summer 2015 (26 July to 26 September 2015) as shown in the bottom panels of Figure 3. Again there is a clear correlation of Aitken mode particles and their subsequent growth at the two sites, leading to the conclusion that the similarities in the growth events at the two sites are not specific to 2016.

In order to evaluate the influence of the appearance of small particles and growth events on the particle number concentrations at the two sites, the total concentration and the concentration of particles with a size between 10 to 100 nm, measured by the SMPS are summarized in Figure 4 for 27 Jul – 9 Sep 2015 and 2016. The particle concentrations are similar at both sites and for both periods. The one exception is that the 90th percentile was higher for Alert in 2015, which was driven by two events with especially elevated particle concentrations. Coinciding events were observed at Eureka, but the particles concentrations were much lower. The reason for the elevated concentrations at Alert but not at Eureka is unknown. It is important to note that for 2016, the median is approximately 50 – 100 particles cm^{-3} higher than the results shown in Figure 4 if data from 16 Jun – 26 Sep 2016 are analyzed instead. This can be explained by the fact that the total duration of growth events was longer in June and July compared to events occurring in August and September.

3.1.2 Case Studies of Aerosol Growth Events

To further analyze the growth events and periods with elevated concentrations of ultrafine particles, two different sets of case studies were selected comprising 5 (Table 1) and 28 events (Table S1). The latter represents all the growth

events observed during the measurement period (22 events during 2016 and 6 events during the shorter 2015 period), and the smaller set of 5 was used to calculate growth rates. This subset of events was chosen because they were distinct, without overlap with preceding or subsequent growth events and exhibited relatively smooth growth curves. The remaining 23 growth events were sometimes interrupted, presumably due to changes in air mass origin, or consisted of several events overlapping each other. All of the 5 growth events presented in Table 1 represent complete and smooth growth events that were suitable for calculating growth rate. For the smaller set of case studies near Eureka, the measured particle size distributions are shown in Figure 5, along with the temperature profiles measured using radiosondes launched from the Eureka Weather Station (Figure 6). Initial aerosol growth rates were calculated following previously published methods (Kulmala et al. 2004; Hussein et al. 2005; Salma et al. 2011). Briefly, the SMPS size distributions were fitted with a multi-mode log-normal distribution, and then a linear regression analysis was performed on the geometric mean of the Aitken mode as a function of time for particle diameters between 10 – 30 nm. The initial growth rates calculated for this study are given in Table 1. Looking more closely at the meteorology of the five growth events, one can evaluate the optimal conditions that favor the presence of the growth events at the PEARL RidgeLab. In particular, the absence of an inversion below the PEARL RidgeLab would correspond to air masses measured at the site that are more influenced by local, less photochemically aged and possibly marine sources. In contrast, if the sources of aerosol mass during growth are the sea or the land surface and within the stable stratification, then these influences are expected to be less important when an inversion is present below the PEARL RidgeLab. Figure 6 demonstrates that while temperature inversions that terminate with a maximum below 600 m (the altitude of the PEARL RidgeLab) do sometimes exist before or at the beginning of a growth event, the presence of such inversions is infrequent and often weak (less than 2°C). These inversion conditions will thus result in air masses measured by the instruments at PEARL that are directly influenced by local emissions near or below the PEARL RidgeLab.

To more systematically analyze all the growth events for the summers of 2015 and 2016 at the PEARL RidgeLab, a histogram of the number of events binned by the average inversion temperature (i.e. the temperature at the top of the inversion minus that at the bottom) during each event is plotted in Figure 7. (All the growth events used in creating Figure 7 are summarized in Table S1 and the particle size distributions are shown in Figure S4.) There was a clear tendency for particle growth events (and presumably nucleation) to occur when the inversion was weak or absent. Furthermore, we conducted a similar analysis for six periods when particle concentrations were low and for six periods with a persistent accumulation mode (summarized in Table S2 and Figures S5 and S6). Figure 7 shows that the average inversion temperature during the growth events (0.3 ± 0.7°C) was very similar to that during the selected periods with low particle concentration (0.3 ± 0.2°C), whereas the average inversion temperature during periods with a persistent accumulation mode and elevated particle concentrations was much higher (2.5 ± 1.2°C). The results shown in Figure 7 imply that growth events occur at the PEARL RidgeLab when the inversion is weak because, firstly, the low particle surface area and corresponding condensation sink in the marine boundary layer air allowed particle nucleation to occur, and secondly, the site was possibly influenced by

more recent surface emissions that were less photochemically aged compared to air aloft. In contrast, when the inversion was strong, the aerosol and aerosol precursor species were more chemically aged due to slower transport into the free troposphere and thus the existing particles had already grown to sizes corresponding to the accumulation mode. A few growth events were observed when the temperature inversion was larger, which may be due to the fact that the radiosondes were launched at the Eureka Weather Station located 11 km to the southwest of the PEARL RidgeLab. Thus, the temperature profile measured by a radiosonde may not be fully representative of that at the RidgeLab. Generally speaking, the observations reported here are consistent with previous work (Willis et al. 2016; Collins et al. 2017) suggesting that similar events measured in the Canadian Arctic are attributable to marine sources.

Previous studies have characterized aerosol growth rates in remote regions including the Arctic. In particular, Collins et al. (2017) reported growth rates ranging from 0.2 – 15.3 nm h^{-1} during two research cruises conducted in the Canadian Arctic and calculated a corresponding average growth rate of 4.3 ± 4.1 nm h^{-1}. Similarly, Nieminen et al. (2018) reported for Alert and Mt Zeppelin, Norway, that the average growth rates, between June and August, were 1.1 and 1.2 nm h^{-1}, respectively for the years 2012 – 2014 and 2005 – 2013. In our study, growth rates ranged from 0.1 – 1.0 nm h^{-1} for the aerosols at the PEARL RidgeLab and at Alert, with an average rate of 0.5 ± 0.3 nm hr^{-1} (Table 1). These values are consistent with those reported in Collins et al. and in Nieminen et al. It should be noted that the size range used for calculating growth rates in our work (10 – 30 nm) is slightly different from that of Collins et al. (4 – 20 nm) and Nieminen et al. (10 – 25 nm), which may contribute to our relatively slower growth rates. Lastly, the growth rates are similar for all 5 events analyzed in Table 1, which suggests that the atmospheric processes (e.g. the condensation of semi-volatile or low volatility vapors to the particle surfaces as discussed below) and conditions governing the growth events are similar for all the events in this study.

3.1.3 Back-Trajectory Analysis

To understand the influence of the air mass history on the occurrence of the growth events, back-trajectories were calculated using FLEXPART (Figure S7) for Eureka and Alert. (The particle size distributions for the analyzed events for Eureka and Alert are shown in Figures 5 and S8, respectively.) This calculation permits the precise evaluation of the spatial distribution of the potential emissions sensitivity at the beginning of each growth event. In general, these calculations show that the aerosols measured at the PEARL RidgeLab are mostly influenced by source regions located in the Canadian Arctic Archipelago, in Baffin Bay and to the north of Ellesmere Island. These results mostly coincide with the research reported by Collins et al. (2017), in which they observed high concentrations of ultrafine particles in these regions. Furthermore, the analyzed growth events generally have similar air mass histories for both the PEARL RidgeLab and Alert for a given event. The exception is GE 30 at the PEARL RidgeLab, which began on 25 June 2016, was more influenced by areas near and further north of Alert with a small contribution from the Nares Strait region. Interestingly, NASA Worldview images (https://worldview.earthdata.nasa.gov/) show that on 25 June 2016 (Figure S9) and for several preceding days, while the ocean in these regions was mostly covered in sea-ice, the potential emissions sensitivity was still influenced by large areas of

open water. In conclusion, growth events can occur within air masses with different back-trajectories, as also reported by Collins et al. (2017), although the potential emissions sensitivities for the five growth events shown in Figure S7 have a substantial amount of overlap.

3.2 Aerosol Bulk and Size Resolved Chemical Composition

AMS measurements of aerosol chemical composition and mass concentration for the summer of 2015 are shown in Figures 3a and 3b, where the PM_1 mass concentrations include the four dominant types of non-refractory aerosol. During two major growth events in July and August (GE 3 and GE 6), it can be seen that the aerosol organic fraction represented a large majority of the aerosol mass (Figure S10). In contrast, later in the summer (approximately 30 August 2015 to 5 September 2015) there is a period of larger particles when the mass concentration of sulphate is higher than the organic component. While iodine may contribute to particle nucleation, the low resolution of the quadrupole AMS prevents quantification of iodine. Given the low signal at m/z 127 in this study during growth events, we believe that iodine is at most a minor contributor of mass to Aitken mode particles.

While sulphate is a key contributor to nucleation at lower latitudes and is an oxidation product of dimethyl sulphide (DMS) from marine emissions, relatively little sulphate is observed during growth events. At the same time, the observation of relatively high bulk organic aerosol concentrations during Arctic summer is consistent with previous analyses of organic aerosol functional groups in samples collected at Alert (Leaitch et al. 2018). Since the bodies of water in the vicinity of Eureka were relatively open and not covered in sea ice during this period, the water may have been a source of precursors to the observed aerosol mass, which would be consistent with the correlation of the occurrence of growth events and the breakdown of the temperature inversion below the altitude of the PEARL RidgeLab. It is possible that methanesulphonic acid (MSA), an atmospheric oxidation product of DMS, could be contributing to the overall organic mass (Park et al. 2017). However, the mass spectra for GE 3 and GE 6 are very different from the MSA spectrum measured in the laboratory (Figure S11) (Phinney et al. 2006). In particular, the relative intensity of m/z 79 is much lower in the ambient spectra. Furthermore, in the MSA spectrum the sulphate fragments at m/z 48 and 64 are much greater than the organic fragments at m/z 43 and 44 whereas these organic fragments had greater intensity in the ambient spectra. Lastly, the correlation coefficient for the two average ambient mass spectra (R = 0.84) is much higher than the correlation coefficient between each ambient spectrum and the spectrum measured for MSA (R = 0.60 and 0.48 for GE 3 and GE 6 versus MSA, respectively). When taken together, these differences between the ambient and MSA mass spectra indicate that other organics were contributing to the aerosol mass besides MSA. The size distribution of m/z 79 also peaks at larger sizes, suggesting that any MSA present would be in the accumulation mode. To further verify these findings, the AMS fragmentation table was also modified to separately quantify MSA following Phinney et al. (2006), but the concentration of MSA was generally at or below the detection limit (0.021 $\mu g/m^3$ as determined by multiplying by 3 the standard deviation when the AMS was sampling through a filter). Based on this detection limit, the MSA concentration was 5% or less of the total organic and sulfate mass concentration during the two measured growth events, GE3 and GE6.

In addition to the measurements of the bulk aerosol composition shown in Figure 3, the dependence of the composition on the particle size is shown in Figure 8. The PToF data revealed that the smallest particles sampled by the AMS (between 50 and 80 nm in diameter) during the two different growth events were enriched in organics, with little to no sulphate. Between 80 and 1000 nm, the measured aerosol composition changes depending on the particle size and the larger aerosol particles contain a greater fraction of sulphate. The higher concentration of sulphate in the larger particles is most likely explained by the presence of a distinct accumulation mode having a history and source different from the Aitken mode aerosols.

To further evaluate the organic aerosol composition only, two important fragments in the measured mass spectra of the organic aerosol, m/z 43 and 44, are plotted in Figure 8e and Figure 8f. For organic aerosol, m/z 44 corresponds to the concentration of carboxylic acids, whereas m/z 43 correlates with other oxygen containing functional groups in the particle phase (e.g. alcohols). The size-resolved measurements of these fragments show that the organic composition varied with particle size. The smallest particles were less oxidized, with the fraction of carboxylic acids increasing with the particle diameter between 80 and 400 nm. While this relative trend was observed for both growth events, the absolute ratios of m/z 43 to m/z 44 were different, which indicates some variation in the amount of organic aerosol oxidation during growth events.

To complement the analysis of the organic aerosol composition shown in Figure 8, the fractions of the total organic mass measured at m/z 43 and at m/z 44 (abbreviated as f_{43} and f_{44}) are plotted against each other in Figure 9, in which the data are colored as a function of time. For reference, the size-resolved f_{43} and f_{44} are also shown in Figure S12. Lambe et al. (2011) demonstrated in a series of laboratory studies that secondary organic aerosol (SOA) formed from a variety of different precursors, both anthropogenic and biogenic, falls within a well-defined space in the f_{44} versus f_{43} plot, shown as the black triangle in Figure 9. The organic aerosols measured at the PEARL RidgeLab have f_{44} and f_{43} ratios that are consistent with the previous work of Lambe et al. and others (Ng et al. 2011). Furthermore, the mean f_{44} and f_{43} for the seven hours at the beginning and end of GE3 and GE6 are included in Figure 9 in order to evaluate the overall change in SOA composition. For GE 3, there was a clear trend during the evolution of the growth event wherein both f_{44} and f_{43} increase, which is consistent with an increase in the relative concentration of carboxylic acids and non-acid oxygenates in the organic aerosol. For GE 6, a change in organic composition is not apparent. The f_{44} may have increased, but the trend with time is more ambiguous than for GE 3. In comparison, the size-resolved composition measurements shown in Figure 8, show smaller particles have a higher fraction of m/z 43 and larger particles formed later during the growth events have a higher fraction of m/z 44 suggesting that aerosol growth led to an increase in the amount of oxidation due to, in part, the production of carboxylic acids. However, we emphasize that our results are for a very limited data set and further analysis of SOA composition during additional growth events using f_{44} and f_{43} would be necessary to confirm our observations.

In summary, the concentration and evolution of oxygenated organics as well as the presence of small organic particles measured by the AMS together suggest that SOA formation contributes to particle growth measured at the PEARL RidgeLab. While the origin of the SOA precursors is unknown, it can be concluded that the organic composition is inconsistent with SOA formation from MSA alone. Recently published work has suggested that marine microbial processes

may be an important source of these VOCs (Collins et al. 2017). Abiotic heterogeneous processes in the marine boundary layer may also be a source of oxidized VOCs as indicated in several laboratory studies (Bruggemann et al. 2017; Chiu et al. 2017). Consistent with this previous research, the first growth event observed at the PEARL RidgeLab in 2016, coincided approximately with the melting of the sea ice in the Slidre Fjord and the Eureka Sound located to the south and west of the PEARL RidgeLab. Observations of the sea ice taken from the PEARL RidgeLab are shown in Figure S13. The pictures show, for summer 2016, the sea ice during the first (25 June 2016) and last (10 September 2016) growth events. Also shown are two additional images. One is of the first time that open water was observed (14 July 2016), and the other is the last available image of Eureka Sound and Slidre Fjord for 2016 (28 September 2016) before polar sunset made it too dark for photographs. On 25 June, it is not possible to see regions of open water during the first growth event. However, open water was observed 300 km to the south of Eureka on the same day in NASA Worldview images. (Figure S9). Moreover, the NASA Worldview images show open water on 7 July in Eureka Sound and Slidre Fjord. It should also be noted that the first growth event occurred much later than polar sunrise on 21 February 2016. During the last observed growth event (10 September 2016), there was very little or no sea ice, and open water was persistently observed until the end of September. This is consistent with measurements of DMS and MSA at Alert which show relatively high concentrations persisting into September (Sharma et al. 2012; Leaitch et al. 2013). Given these observations, there is a possible relationship between the onset of the growth events and the melting of the sea ice in the region around Eureka. This would be consistent with back-trajectory analyses showing that newly formed particles measured during summertime cruises in the Arctic Ocean are associated with air that has experienced more open water or melting sea ice regions (Heintzenberg et al. 2015; Dall'Osto et al. 2017). In contrast, the decrease in the number of events in September was more likely due to the lack of solar radiation, as shown in Figure S14 and previous measurements at Alert (Sharma et al. 2012), which limits photochemistry. This finding supports the recent suggestion that photochemical processing of emissions from the ocean may be a source of ultrafine particles in the Arctic (Collins et al. 2017).

4. Conclusions

In this study, particle growth events were characterized during the summers of 2015 and 2016 at the PEARL RidgeLab (in Eureka, Nunavut, Canada) as well as at Alert, Canada. Both sites are located on Ellesmere Island separated by a distance of 480 km providing an opportunity to evaluate the growth events on a regional scale for the complete 2016 summer season as well as for a portion of the 2015 summer season. During both years, frequent growth events occurred and these events were correlated between the sites. In addition to the concomitant events, the particle concentrations measured at Alert and the PEARL RidgeLab were similar, with the 10^{th}, 25^{th}, 50^{th}, 75^{th} and 90^{th} percentiles not varying by more than a factor of 1.67 suggesting the growth events were not isolated local events. Additionally, the mean particle growth rate from a subset of events at the PEARL RidgeLab and at Alert was 0.5 ± 0.3 nm hr^{-1}. In total, the measurements of the particle number size distribution support the conclusion that particle nucleation and growth events can occur over spatial scales of at least 500 km in the Canadian Arctic Archipelago. Previous work in the summer time Arctic found that particles smaller than

50 nm could be contributing to cloud droplet activation (Leaitch et al. 2016). The growth of small particles to diameters larger than 60 nm observed in our study could therefore make them an important contributor to CCN, ultimately impacting the radiation balance and hydrologic cycle.

Moreover, in this study AMS measurements showed that particles between 50 and 80 nm in diameter during two observed growth events were predominately organic. This result is in contrast to previous indirect measurements of aerosol composition using a volatility tandem differential mobility analyzer system installed near Ny-Ålesund, Svalbard (Giamarelou et al. 2016), which suggested that 12 nm particles were predominately ammonium sulphate, although it was not possible in that study to conclusively distinguish ammonium sulphate from organics with similar volatility. The amount of oxidation of the organic fraction also changed with particle size, with the ratio of m/z 43 to m/z 44 increasing for smaller particles sizes, which is consistent with a greater fraction of non-acid oxygenates relative to carboxylic acids. Overall, our limited AMS measurements support the conclusion that condensation of organic vapors contributed to particle growth.

It has been recently suggested that secondary organic aerosols formed from VOCs emitted by marine sources may be an important source of ultrafine particles in the Arctic during summertime. The results of the research presented here are consistent with this possibility. In addition to the SMPS and AMS measurements discussed above, the growth events were most likely observed at the PEARL RidgeLab when the inversion was non-existent or weak, allowing the site's instruments to sample the boundary layer which had a low aerosol condensation sink as well as presumably fresh marine emissions. Finally, the onset of the growth events in 2016 coincided more with the opening of the sea ice near the PEARL RidgeLab, rather than polar sunrise. However, future work should focus on the incorporation of more sea ice data as well as further gas phase measurements to understand the timing and chemical processes driving particle nucleation and growth in the Arctic.

Acknowledgements

This work was partially supported by the Université de Montréal and the Natural Science and Engineering Research Council of Canada (Discovery Grant RGPIN-05002-2014, Discovery Grant RGPIN-05173-2014 and Climate Change and Atmospheric Research (CCAR) Program funding awarded to the Probing the Atmosphere of the High Arctic (PAHA) project led by PI James R. Drummond). Support from Environment and Climate Change Canada (ECCC) for the Arctic field work performed at both Eureka and Alert is also acknowledged. The authors also acknowledge the Canadian Network for the Detection of Atmospheric Change (CANDAC) staff for maintaining the infrastructure at the PEARL site, Canadian Forces Station Alert for the maintenance of Alert base, and the use of the FLEXPART Lagrangian dispersion model (https://www.flexpart.eu/wiki/FpDownloads) and the Pflexible Python module (https://bitbucket.org/jfburkhart/pflexible) developed by John F. Burkhart, which were modified here to plot the FLEXPART sensitivities in this paper. The NCEP CFS data used are listed in the references. Radiation measurements have received support from ECCC, CANDAC and the Arctic Research Program of the NOAA Climate Program Office. Finally, the authors are indebted to James Sloan, Asan Bacak,

Thomas Kuhn and Richard Damoah for their early efforts in installing and maintaining the AMS at PEARL and to James Drummond for his continued dedication in support of PEARL.

References

Allan, J. D., Williams, P. I., Najera, J., Whitehead, J. D., Flynn, M. J., Taylor, J. W., Liu, D., Darbyshire, E., Carpenter, L. J., Chance, R., Andrews, S. J., Hackenberg, S. C., and McFiggans, G.: Iodine observed in new particle formation events in the Arctic atmosphere during ACCACIA, Atmospheric Chemistry and Physics, 15, 5599-5609, 2015.

Allen, M. R., Stott, P. A., Mitchell, J. F. B., Schnur, R., and Delworth, T. L.: Quantifying the uncertainty in forecasts of anthropogenic climate change, Nature, 407, 617-620, 2000.

Almeida, J., Schobesberger, S., Kurten, A., Ortega, I. K., Kupiainen-Maatta, O., Praplan, A. P., Adamov, A., Amorim, A., Bianchi, F., Breitenlechner, M., David, A., Dommen, J., Donahue, N. M., Downard, A., Dunne, E., Duplissy, J., Ehrhart, S., Flagan, R. C., Franchin, A., Guida, R., Hakala, J., Hansel, A., Heinritzi, M., Henschel, H., Jokinen, T., Junninen, H., Kajos, M., Kangasluoma, J., Keskinen, H., Kupc, A., Kurten, T., Kvashin, A. N., Laaksonen, A., Lehtipalo, K., Leiminger, M., Leppa, J., Loukonen, V., Makhmutov, V., Mathot, S., McGrath, M. J., Nieminen, T., Olenius, T., Onnela, A., Petaja, T., Riccobono, F., Riipinen, I., Rissanen, M., Rondo, L., Ruuskanen, T., Santos, F. D., Sarnela, N., Schallhart, S., Schnitzhofer, R., Seinfeld, J. H., Simon, M., Sipila, M., Stozhkov, Y., Stratmann, F., Tome, A., Trostl, J., Tsagkogeorgas, G., Vaattovaara, P., Viisanen, Y., Virtanen, A., Vrtala, A., Wagner, P. E., Weingartner, E., Wex, H., Williamson, C., Wimmer, D., Ye, P. L., Yli-Juuti, T., Carslaw, K. S., Kulmala, M., Curtius, J., Baltensperger, U., Worsnop, D. R., Vehkamaki, H., and Kirkby, J.: Molecular understanding of sulphuric acid-amine particle nucleation in the atmosphere, Nature, 502, 359-369, 2013.

Bey, I., Jacob, D. J., Yantosca, R. M., Logan, J. A., Field, B. D., Fiore, A. M., Li, Q. B., Liu, H. G. Y., Mickley, L. J., and Schultz, M. G.: Global modeling of tropospheric chemistry with assimilated meteorology: Model description and evaluation, Journal of Geophysical Research-Atmospheres, 106, 23073-23095, 2001.

Browse, J., Carslaw, K. S., Mann, G. W., Birch, C. E., Arnold, S. R., and Leck, C.: The complex response of Arctic aerosol to sea-ice retreat, Atmospheric Chemistry and Physics, 14, 7543-7557, 2014.

Bruggemann, M., Hayeck, N., Bonnineau, C., Pesce, S., Alpert, P. A., Perrier, S., Zuth, C., Hoffmann, T., Chen, J. M., and George, C.: Interfacial photochemistry of biogenic surfactants: a major source of abiotic volatile organic compounds, Faraday Discussions, 200, 59-74, 2017.

Burkart, J., Hodshire, A. L., Mungall, E. L., Pierce J., R., Collins, D. B., Ladino, L. A., Lee, A. K. Y., Irish, V., Wentzell, J. J. B., Liggio, J., Papakyriakou, T., Murphy, J., and Abbatt, J.: Organic Condensation and Particle Growth to CCN Sizes in the Summertime Marine Arctic Is Driven by Materials More Semivolatile Than at Continental Sites, Geophysical Research Letters, 44, 10725-10734, 2017.

Canagaratna, M. R., Jayne, J. T., Jimenez, J. L., Allan, J. D., Alfarra, M. R., Zhang, Q., Onasch, T. B., Drewnick, F., Coe, H., Middlebrook, A., Delia, A., Williams, L. R., Trimborn, A. M., Northway, M. J., DeCarlo, P. F., Kolb, C. E., Davidovits, P., and Worsnop, D. R.: Chemical and microphysical characterization of ambient aerosols with the aerodyne aerosol mass spectrometer, Mass Spectrometry Reviews, 26, 185-222, 2007.

Chang, R. Y. W., Sjostedt, S. J., Pierce, J. R., Papakyriakou, T. N., Scarratt, M. G., Michaud, S., Levasseur, M., Leaitch, W. R., and Abbatt, J. P. D.: Relating atmospheric and oceanic DMS levels to particle nucleation events in the Canadian Arctic, Journal of Geophysical Research-Atmospheres, 116, D00s03, 2011.

Charlson, R. J., Schwartz, S. E., Hales, J. M., Cess, R. D., Coakley, J. A., Hansen, J. E., and Hofmann, D. J.: Climate forcing by anthropogenic aerosols, Science, 255, 423-430, 1992.

Chiu, R., Tinel, L., Gonzalez, L., Ciuraru, R., Bernard, F., George, C., and Volkamer, R.: UV photochemistry of carboxylic acids at the air-sea boundary: A relevant source of glyoxal and other oxygenated VOC in the marine atmosphere, Geophysical Research Letters, 44, 1079-1087, 2017.

Christian, K. E., Brune, W. H., and Mao, J. Q.: Global sensitivity analysis of the GEOS-Chem chemical transport model: ozone and hydrogen oxides during ARCTAS (2008), Atmospheric Chemistry and Physics, 17, 3769-3784, 2017.

Clarke, A. D., Davis, D., Kapustin, V. N., Eisele, F., Chen, G., Paluch, I., Lenschow, D., Bandy, A. R., Thornton, D., Moore, K., Mauldin, L., Tanner, D., Litchy, M., Carroll, M. A., Collins, J., and Albercook, C.: Particle nucleation in the tropical boundary layer and its coupling to marine sulfur sources, Science, 282, 89-92, 1998.

Clarke, A. D., Owens, S. R., and Zhou, J. C.: An ultrafine sea-salt flux from breaking waves: Implications for cloud condensation nuclei in the remote marine atmosphere, Journal of Geophysical Research-Atmospheres, 111, D06202, 2006.

Collins, D. B., Burkart, J., Chang, R. Y. W., Lizotte, M., Boivin-Rioux, A., Blais, M., Mungall, E. L., Boyer, M., Irish, V. E., Massé, G., Kunkel, D., Tremblay, J. É, Papakyriakou, T., Bertram, A. K., Bozem, H., Gosselin, M., Levasseur, M., and Abbatt, J. P. D.: Frequent Ultrafine Particle Formation and growth in the Canadian Arctic marine and coastal environment, Atmospheric Chemistry and Physics, 17, 13119-13138, 2017.

Crippa, P., and Pryor, S. C.: Spatial and temporal scales of new particle formation events in eastern North America, Atmospheric Environment, 75, 257-264, 2013.

Croft, B., Martin, R. V., Leaitch, W. R., Tunved, P., Breider, T. J., D'Andrea, S. D., and Pierce, J. R.: Processes controlling the annual cycle of Arctic aerosol number and size distributions, Atmospheric Chemistry and Physics, 16, 3665-3682, 2016a.

Croft, B., Wentworth, G. R., Martin, R. V., Leaitch, W. R., Murphy, J. G., Murphy, B. N., Kodros, J. K., Abbatt, J. P. D., and Pierce, J. R.: Contribution of Arctic seabird-colony ammonia to atmospheric particles and cloud-albedo radiative effect, Nature Communications, 7, 13444, 2016b.

Dall'Osto, M., Beddows, D. C. S., Tunved, P., Krejci, R., Strom, J., Hansson, H. C., Yoon, Y. J., Park, K. T., Becagli, S., Udisti, R., Onasch, T., O'Dowd, C. D., Simo, R., and Harrison, R. M.: Arctic sea ice melt leads to atmospheric new particle formation, Scientific Reports, 7, 2017.

DeCarlo, P. F., Slowik, J. G., Worsnop, D. R., Davidovits, P., and Jimenez, J. L.: Particle morphology and density characterization by combined mobility and aerodynamic diameter measurements. Part 1: Theory, Aerosol Science and Technology, 38, 1185-1205, 2004.

Engvall, A. C., Krejci, R., Strom, J., Treffeisen, R., Scheele, R., Hermansen, O., and Paatero, J.: Changes in aerosol properties during spring-summer period in the Arctic troposphere, Atmospheric Chemistry and Physics, 8, 445-462, 2008.

Fogal, P. F., LeBlanc, L. M., and Drummond, J. R.: The Polar Environment Atmospheric Research Laboratory (PEARL): Sounding the Atmosphere at 80 degrees North, Arctic, 66, 377-386, 2013.

Freud, E., Krejci, R., Tunved, P., Leaitch, R., Nguyen, Q. T., Massling, A., Skov, H., and Barrie, L.: Pan-Arctic aerosol number size distributions: seasonality and transport patterns, Atmospheric Chemistry and Physics, 17, 8101-8128, 2017.

Fu, P. Q., Kawamura, K., Chen, J., Charriere, B., and Sempere, R.: Organic molecular composition of marine aerosols over the Arctic Ocean in summer: contributions of primary emission and secondary aerosol formation, Biogeosciences, 10, 653-667, 2013.

Giamarelou, M., Eleftheriadis, K., Nyeki, S., Tunved, P., Torseth, K., and Biskos, G.: Indirect evidence of the composition of nucleation mode atmospheric particles in the high Arctic, Journal of Geophysical Research-Atmospheres, 121, 965-975, 2016.

Heintzenberg, J., Leck, C., and Tunved, P.: Potential source regions and processes of aerosol in the summer Arctic, Atmospheric Chemistry and Physics, 15, 6487-6502, 2015.

Hoppel, W. A., Frick, G. M., and Larson, R. E.: Effect of nonprecipitating clouds on the aerosol size distribution in the marine boundary-layer, Geophysical Research Letters, 13, 125-128, 1986.

Hussein, T., Dal Maso, M., Petaja, T., Koponen, I. K., Paatero, P., Aalto, P. P., Hameri, K., and Kulmala, M.: Evaluation of an automatic algorithm for fitting the particle number size distributions, Boreal Environment Research, 10, 337-355, 2005.

Jeong, C. H., Evans, G. J., McGuire, M. L., Chang, R. Y. W., Abbatt, J. P. D., Zeromskiene, K., Mozurkewich, M., Li, S. M., and Leaitch, A. R.: Particle formation and growth at five rural and urban sites, Atmospheric Chemistry and Physics, 10, 7979-7995, 2010.

Kirkby, J., Curtius, J., Almeida, J., Dunne, E., Duplissy, J., Ehrhart, S., Franchin, A., Gagne, S., Ickes, L., Kurten, A., Kupc, A., Metzger, A., Riccobono, F., Rondo, L., Schobesberger, S., Tsagkogeorgas, G., Wimmer, D., Amorim, A., Bianchi, F., Breitenlechner, M., David, A., Dommen, J., Downard, A., Ehn, M., Flagan, R. C., Haider, S., Hansel, A., Hauser, D., Jud, W., Junninen, H., Kreissl, F., Kvashin, A., Laaksonen, A., Lehtipalo, K., Lima, J., Lovejoy, E. R., Makhmutov, V., Mathot, S., Mikkila, J., Minginette, P., Mogo, S., Nieminen, T., Onnela, A., Pereira, P., Petaja, T., Schnitzhofer, R., Seinfeld, J. H., Sipila, M., Stozhkov, Y., Stratmann, F., Tome, A., Vanhanen, J., Viisanen, Y., Vrtala, A., Wagner, P. E., Walther, H., Weingartner, E., Wex, H., Winkler, P. M., Carslaw, K. S., Worsnop, D. R., Baltensperger, U., and Kulmala, M.: Role of sulphuric acid, ammonia and galactic cosmic rays in atmospheric aerosol nucleation, Nature, 476, 429-U477, 2011.

Kirkby, J., Duplissy, J., Sengupta, K., Frege, C., Gordon, H., Williamson, C., Heinritzi, M., Simon, M., Yan, C., Almeida, J., Trostl, J., Nieminen, T., Ortega, I. K., Wagner, R., Adamov, A., Amorim, A., Bernhammer, A. K., Bianchi, F., Breitenlechner, M., Brilke, S., Chen, X. M., Craven, J., Dias, A., Ehrhart, S., Flagan, R. C., Franchin, A., Fuchs, C., Guida, R., Hakala, J., Hoyle, C. R., Jokinen, T., Junninen, H., Kangasluoma, J., Kim, J., Krapf, M., Kurten, A., Laaksonen, A., Lehtipalo, K., Makhmutov, V., Mathot, S., Molteni, U., Onnela, A., Perakyla, O., Piel, F., Petaja, T., Praplan, A. P., Pringle, K., Rap, A., Richards, N. A. D., Riipinen, I., Rissanen, M. P., Rondo, L., Sarnela, N., Schobesberger, S., Scott, C. E., Seinfeld, J. H., Sipila, M., Steiner, G., Stozhkov, Y., Stratmann, F., Tome, A., Virtanen, A., Vogel, A. L., Wagner, A. C., Wagner, P. E., Weingartner, E., Wimmer, D., Winkler, P. M., Ye, P. L., Zhang, X., Hansel, A., Dommen, J., Donahue, N. M., Worsnop, D. R., Baltensperger, U., Kulmala, M., Carslaw, K. S., and Curtius, J.: Ion-induced nucleation of pure biogenic particles, Nature, 533, 521-526, 2016.

Korhonen, H., Carslaw, K. S., Spracklen, D. V., Ridley, D. A., and Strom, J.: A global model study of processes controlling aerosol size distributions in the Arctic spring and summer, Journal of Geophysical Research-Atmospheres, 113, D08211, 2008.

Kulmala, M., Vehkamaki, H., Petaja, T., Dal Maso, M., Lauri, A., Kerminen, V. M., Birmili, W., and McMurry, P. H.: Formation and growth rates of ultrafine atmospheric particles: a review of observations, Journal of Aerosol Science, 35, 143-176, 2004.

Lambe, A. T., Onasch, T. B., Massoli, P., Croasdale, D. R., Wright, J. P., Ahern, A. T., Williams, L. R., Worsnop, D. R., Brune, W. H., and Davidovits, P.: Laboratory studies of the chemical composition and cloud condensation nuclei (CCN) activity of secondary organic aerosol (SOA) and oxidized primary organic aerosol (OPOA), Atmospheric Chemistry and Physics, 11, 8913-8928, 2011.

Leaitch, W. R., Korolev, A., Aliabadi, A. A., Burkart, J., Willis, M. D., Abbatt, J. P. D., Bozem, H., Hoor, P., Kollnr, F., Schneider, J., Herber, A., Konrad, C., and Brauner, R.: Effects of 20-100nm particles on liquid clouds in the clean summertime Arctic, Atmospheric Chemistry and Physics, 16, 11107-11124, 2016.

Leaitch, W. R., Russell, L. M., Liu, J., Kolonjari, F., Toom, D., Huang, L., Sharma, S., Chivulescu, A., Veber, D., and Zhang, W.: Organic Functional Groups in the Submicron Aerosol at 82.5° N from 2012 to 2014, Atmospheric Chemistry and Physics, 18, 3269-3287, 2018.

Leaitch, W. R., Sharma, S., L., Huang, Toom-Sauntry, D., Chivulescu, A., Macdonald, A. M., von Salzen, K., Pierce J., R., Bertram, A. K., Schroder, J. C., Shantz, N. C., Chang, R. Y.-W., and A.-L., Norman: Dimethyl sulfide control of the clean summertime Arctic aerosol and cloud. Elem Sci Anth., Elementa Science of the Antropocene, 1, 17, 2013.

Leck, C., and Bigg, E. K.: Biogenic particles in the surface microlayer and overlaying atmosphere in the central Arctic Ocean during summer, Tellus Series B-Chemical and Physical Meteorology, 57, 305-316, 2005a.

Leck, C., and Bigg, E. K.: Source and evolution of the marine aerosol - A new perspective, Geophysical Research Letters, 32, 2005b.

Lohmann, U., and Feichter, J.: Global indirect aerosol effects: a review, Atmospheric Chemistry and Physics, 5, 715-737, 2005.

Mahajan, A. S., Shaw, M., Oetjen, H., Hornsby, K. E., Carpenter, L. J., Kaleschke, L., Tian-Kunze, X., Lee, J. D., Moller, S. J., Edwards, P., Commane, R., Ingham, T., Heard, D. E., and Plane, J. M. C.: Evidence of reactive iodine chemistry in the Arctic boundary layer, Journal of Geophysical Research-Atmospheres, 115, 2010.

Middlebrook, A. M., Bahreini, R., Jimenez, J. L., and Canagaratna, M. R.: Evaluation of Composition-Dependent Collection Efficiencies for the Aerodyne Aerosol Mass Spectrometer using Field Data, Aerosol Science and Technology, 46, 258-271, 2012.

Mungall, E. L., Abbatt, J. P. D., Wentzell, J. J. B., Lee, A. K. Y., Thomas, J. L., Blais, M., Gosselin, M., Miller, L. A., Papakyriakou, T., Willis, M. D., and Liggio, J.: Microlayer source of oxygenated volatile organic compounds in the summertime marine Arctic boundary layer, Proceedings of the National Academy of Sciences of the United States of America, 114, 6203-6208, 2017.

Napari, I., Noppel, M., Vehkamaki, H., and Kulmala, M.: Parametrization of ternary nucleation rates for H(2)SO(4)-NH(3)-H(2)O vapors, Journal of Geophysical Research-Atmospheres, 107, 4381, 2002.

Ng, N. L., Canagaratna, M. R., Jimenez, J. L., Chhabra, P. S., Seinfeld, J. H., and Worsnop, D. R.: Changes in organic aerosol composition with aging inferred from aerosol mass spectra, Atmospheric Chemistry and Physics, 11, 6465-6474, 2011.

Nguyen, Q. T., Glasius, M., Sorensen, L. L., Jensen, B., Skov, H., Birmili, W., Wiedensohler, A., Kristensson, A., Nojgaard, J. K., and Massling, A.: Seasonal variation of atmospheric particle number concentrations, new particle formation and atmospheric oxidation capacity at the high Arctic site Villum Research Station, Station Nord, Atmospheric Chemistry and Physics, 16, 11319-11336, 2016.

Nieminen, T., Kerminen, V. M., Petäjä, T., Aalto, P. P., Arshinov, M., Asmi, E., Baltensperger, U., Beddows, D. C. S., Beukes, J. P., Collins, D., Ding, A., Harrison, R. M., Henzing, B., Hooda, R., Hu, M., Hõrrak, U., Kivekäs, N., Komsaare, K., Krejci, R., Kristensson, A., Laakso, L., Laaksonen, A., Leaitch, W. R., Lihavainen, H., Mihalopoulos, N., Németh, Z., Nie, W., O'Dowd, C., Salma, I., Sellegri, K., Svenningsson, B., Swietlicki, E., Tunved, P., Ulevicius, V., Vakkari, V., Vana, M., Wiedensohler, A., Wu, Z., Virtanen, A., and Kulmala, M.: Global analysis of continental boundary layer new particle formation based on long-term measurements, Atmospheric Chemistry and Physics Discussion, 2018, 1-34, 2018.

Park, K. T., Jang, S., Lee, K., Yoon, Y. J., Kim, M. S., Park, K., Cho, H. J., Kang, J. H., Udisti, R., Lee, B. Y., and Shin, K. H.: Observational evidence for the formation of DMS-derived aerosols during Arctic phytoplankton blooms, Atmospheric Chemistry and Physics, 17, 9665-9675, 2017.

Phinney, L., Leaitch, W. R., Lohmann, U., Boudries, H., Worsnop, D. R., Jayne, J. T., Toom-Sauntry, D., Wadleigh, M., Sharma, S., and Shantz, N.: Characterization of the aerosol over the sub-arctic north east Pacific Ocean, Deep-Sea Research Part II - Topical Studies in Oceanography, 53, 2410-2433, 2006.

Pierce, J. R., Leaitch, W. R., Liggio, J., Westervelt, D. M., Wainwright, C. D., Abbatt, J. P. D., Ahlm, L., Al-Basheer, W., Cziczo, D. J., Hayden, K. L., Lee, A. K. Y., Li, S. M., Russell, L. M., Sjostedt, S. J., Strawbridge, K. B., Travis, M., Vlasenko, A., Wentzell, J. J. B., Wiebe, H. A., Wong, J. P. S., and Macdonald, A. M.: Nucleation and condensational growth to CCN sizes during a sustained pristine biogenic SOA event in a forested mountain valley, Atmospheric Chemistry and Physics, 12, 3147-3163, 2012.

Quinn, P. K., Shaw, G., Andrews, E., Dutton, E. G., Ruoho-Airola, T., and Gong, S. L.: Arctic haze: current trends and knowledge gaps, Tellus Series B-Chemical and Physical Meteorology, 59, 99-114, 2007.

Raso, A. R. W., Custard, K. D., May, N. W., Tanner, D., Newburn, M. K., Walker, L., Moore, R. J., Huey, L. G., Alexander, L., Shepson, P. B., and Pratt, K. A.: Active molecular iodine photochemistry in the Arctic, Proceedings of the National Academy of Sciences of the United States of America, 114, 10053-10058, 2017.

Riipinen, I., Yli-Juuti, T., Pierce, J. R., Petaja, T., Worsnop, D. R., Kulmala, M., and Donahue, N. M.: The contribution of organics to atmospheric nanoparticle growth, Nature Geoscience, 5, 453-458, 2012.

Saha, Suranjana, Moorthi, Shrinivas, Wu, Xingren, Wang, Jiande, Nadiga, Sudhir, Tripp, Patrick, Behringer, David, Hou, Yu-Tai, Chuang, Hui-ya, Iredell, Mark, Ek, Michael, Meng, Jesse, Yang, Rongqian, Mendez, Malaquias Pena, Dool, Huug van den, Zhang, Qin, Wang, Wanqiu, Chen, Mingyue, and Becker, Emily: The NCEP Climate Forecast System Version 2, Journal of Climate, 27, 2185-2208, 2014.

Salma, I., Borsos, T., Weidinger, T., Aalto, P., Hussein, T., Dal Maso, M., and Kulmala, M.: Production, growth and properties of ultrafine atmospheric aerosol particles in an urban environment, Atmospheric Chemistry and Physics, 11, 1339-1353, 2011.

Sharma, S., Chan, E., Ishizawa, M., Toom-Sauntry, D., Gong, S. L., Li, S. M., Tarasick, D. W., Leaitch, W. R., Norman, A., Quinn, P. K., Bates, T. S., Levasseur, M., Barrie, L. A., and Maenhaut, W.: Influence of transport and ocean ice extent on biogenic aerosol sulfur in the Arctic atmosphere, Journal of Geophysical Research-Atmospheres, 117, D12209, 2012.

Sharma, S., Ishizawa, M., Chan, D., Lavoue, D., Andrews, E., Eleftheriadis, K., and Maksyutov, S.: 16-year simulation of Arctic black carbon: Transport, source contribution, and sensitivity analysis on deposition, Journal of Geophysical Research-Atmospheres, 118, 943-964, 2013.

Sharma, S., Lavoue, D., Cachier, H., Barrie, L. A., and Gong, S. L.: Long-term trends of the black carbon concentrations in the Canadian Arctic, Journal of Geophysical Research-Atmospheres, 109, D15203, 2004.

Stohl, A.: Characteristics of atmospheric transport into the Arctic troposphere, Journal of Geophysical Research-Atmospheres, 111, D11306, 2006.

Stohl, A., Forster, C., Frank, A., Seibert, P., and Wotawa, G.: Technical note: The Lagrangian particle dispersion model FLEXPART version 6.2, Atmospheric Chemistry and Physics, 5, 2461-2474, 2005.

Trostl, J., Chuang, W. K., Gordon, H., Heinritzi, M., Yan, C., Molteni, U., Ahlm, L., Frege, C., Bianchi, F., Wagner, R., Simon, M., Lehtipalo, K., Williamson, C., Craven, J. S., Duplissy, J., Adamov, A., Almeida, J., Bernhammer, A. K., Breitenlechner, M., Brilke, S., Dias, A., Ehrhart, S., Flagan, R. C., Franchin, A., Fuchs, C., Guida, R., Gysel, M., Hansel, A., Hoyle, C. R., Jokinen, T., Junninen, H., Kangasluoma, J., Keskinen, H., Kim, J., Krapf, M., Kurten, A., Laaksonen, A., Lawler, M., Leiminger, M., Mathot, S., Mohler, O., Nieminen, T., Onnela, A., Petaja, T., Piel, F. M., Miettinen, P., Rissanen, M. P., Rondo, L., Sarnela, N., Schobesberger, S., Sengupta, K., Sipila, M., Smith, J. N., Steiner, G., Tome, A., Virtanen, A., Wagner, A. C., Weingartner, E., Wimmer, D., Winkler, P. M., Ye, P. L., Carslaw, K. S., Curtius, J., Dommen, J., Kirkby, J., Kulmala, M., Riipinen, I., Worsnop, D. R., Donahue, N. M., and Baltensperger, U.: The role of low-volatility organic compounds in initial particle growth in the atmosphere, Nature, 533, 527-546, 2016.

Tunved, P., Strom, J., and Krejci, R.: Arctic aerosol life cycle: linking aerosol size distributions observed between 2000 and 2010 with air mass transport and precipitation at Zeppelin station, Ny-Alesund, Svalbard, Atmospheric Chemistry and Physics, 13, 3643-3660, 2013.

Twomey, S.: The Influence of Pollution on the Shortwave Albedo of Clouds, Journal of the Atmospheric Sciences, 34, 1149-1152, 1977.

Wild, O., and Prather, M. J.: Global tropospheric ozone modeling: Quantifying errors due to grid resolution, Journal of Geophysical Research-Atmospheres, 111, D11305, 2006.

Willis, M. D., Burkart, J., Thomas, J. L., Kollner, F., Schneider, J., Bozem, H., Hoor, P. M., Aliabadi, A. A., Schulz, H., Herber, A. B., Leaitch, W. R., and Abbatt, J. P. D.: Growth of nucleation mode particles in the summertime Arctic: a case study, Atmospheric Chemistry and Physics, 16, 7663-7679, 2016.

Zhang, R. Y., Wang, L., Khalizov, A. F., Zhao, J., Zheng, J., McGraw, R. L., and Molina, L. T.: Formation of nanoparticles of blue haze enhanced by anthropogenic pollution, Proceedings of the National Academy of Sciences of the United States of America, 106, 17650-17654, 2009.

Ziemba, L. D., Dibb, J. E., Griffin, R. J., Huey, L. G., and Beckman, P.: Observations of particle growth at a remote, Arctic site, Atmospheric Environment, 44, 1649-1657, 2010.

Table 1. Particle growth rates for five growth events during the summers of 2015 and 2016.

Growth Event Number	Time period (UTC)		Growth rate (nm/h)
	Start	End	
GE 3 (Eureka)	2015-07-29 05:00	2015-07-30 11:00	0.420 ± 0.004
GE 3 (Alert)	2015-07-29 03:00	2015-07-30 12:00	0.50 ± 0.02
GE 6 (Eureka)	2015-08-02 04:00	2015-08-03 05:00	0.12 ± 0.08
GE 30 (Eureka)	2016-06-25 20:00	2016-06-27 14:00	1.01 ± 0.08
GE 32 (Eureka)	2016-07-05 01:00	2016-07-08 09:00	0.44 ± 0.01
GE 38 (Eureka)	2016-07-21 19:00	2016-07-25 17:00	0.352 ± 0.004

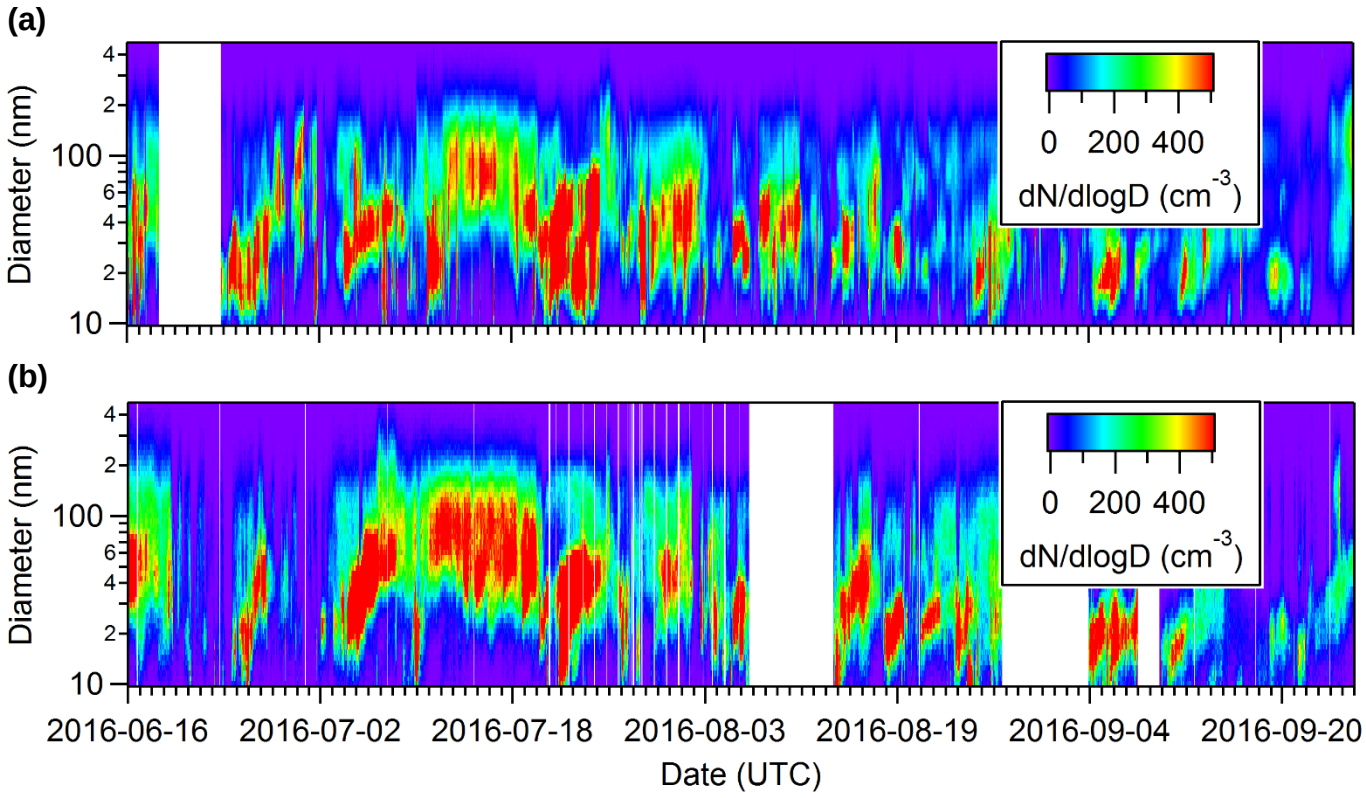

Figure 1. The size resolved particle concentration measured by SMPS instruments during summer 2016 in Alert **(a)** and at the PEARL RidgeLab **(b)** in the Canadian Arctic Archipelago. The sizes are mobility diameters measured by an SMPS, which are equal to the physical diameters under the assumption that the particles were spherical and contained no voids.

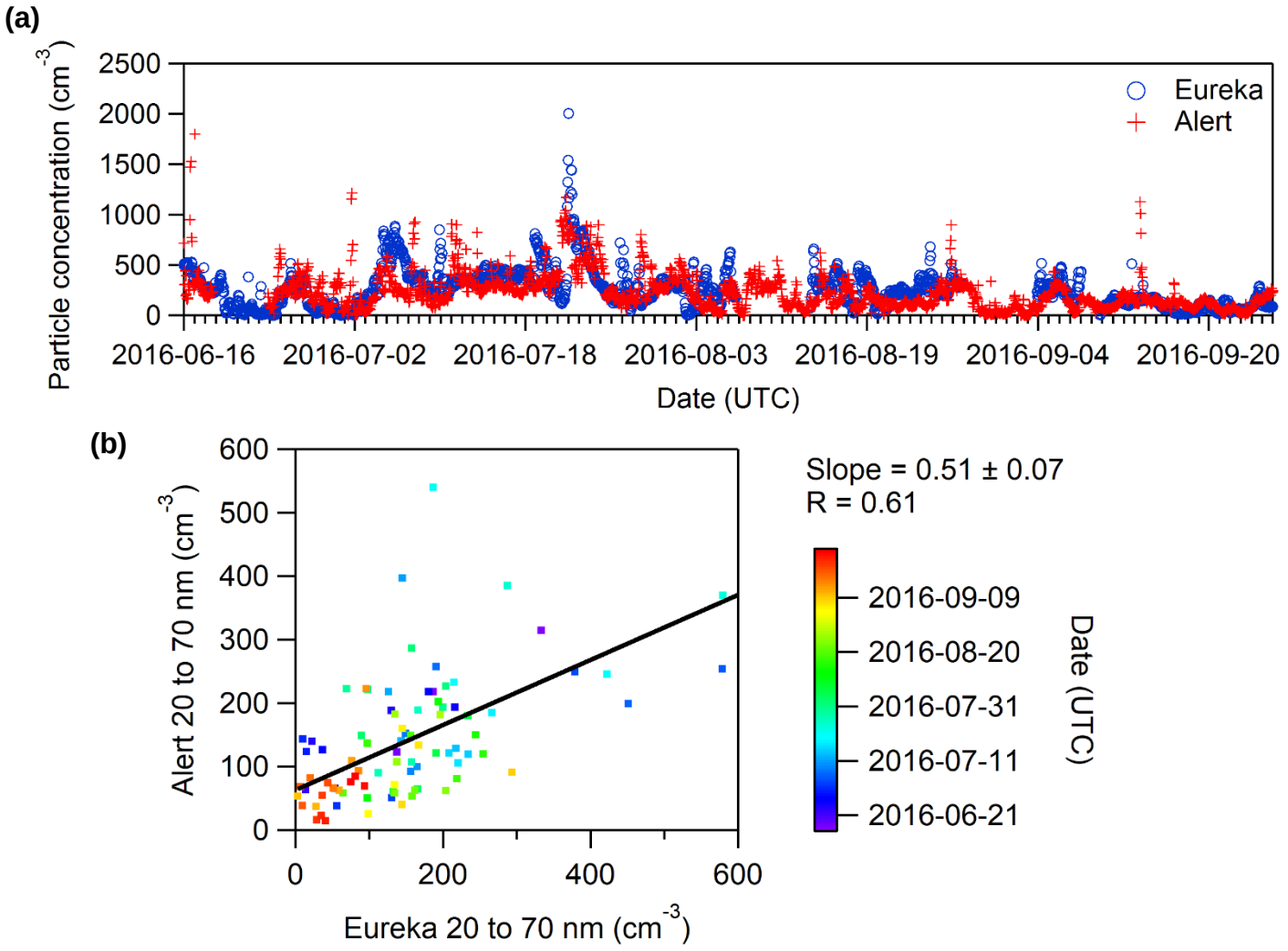

Figure 2. Total hourly particle number concentrations measured at the PEARL RidgeLab near Eureka and in Alert during summer 2016 for sizes between 10 – 487 nm **(a)**. Scatter plot showing the correlation of the particle number concentrations measured in Alert and near Eureka **(b)**. Note that the data in the scatter plot correspond to daily averages of particles with diameters between 20 and 70 nm.

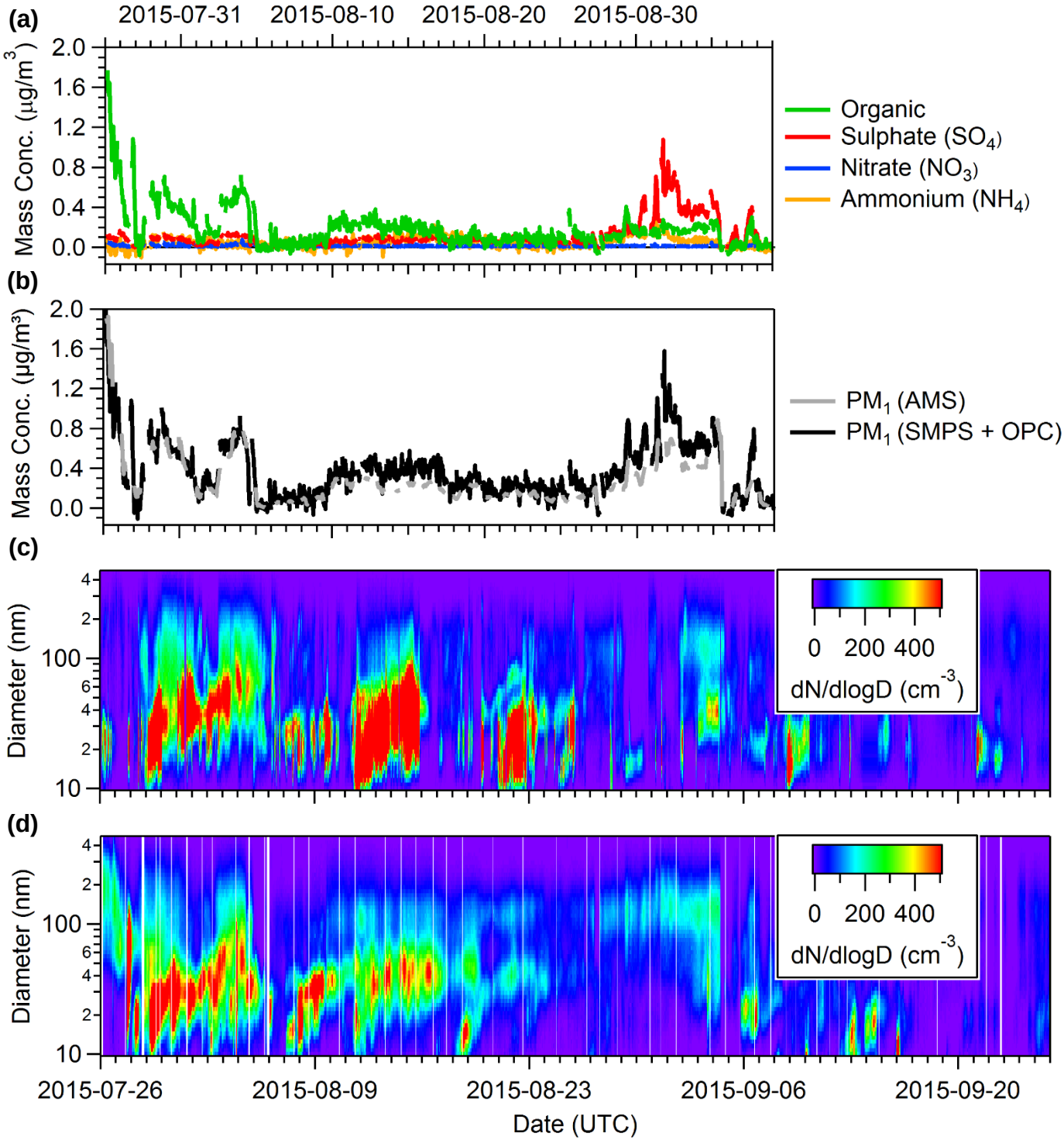

Figure 3. Aerosol mass spectrometry measurements of aerosol composition taken at the PEARL RidgeLab near Eureka **(a)**. The total concentration of non-refractory PM_1 aerosol measured by the mass spectrometer is also compared against the total PM_1 concentration measured by the SMPS and OPC, and exhibits good agreement with a linear regression analysis yielding a slope of 1.16 and a correlation coefficient of 0.89 **(b)**. In addition, the size resolved particle concentration measured by SMPS instruments during summer 2015 in Alert **(c)** and at the PEARL RidgeLab **(d)** are shown in the bottom two panels. The sizes are mobility diameters measured by an SMPS, which are equal to the physical diameters under the assumption that the particles were spherical and contained no voids. All data are plotted on the same time scale.

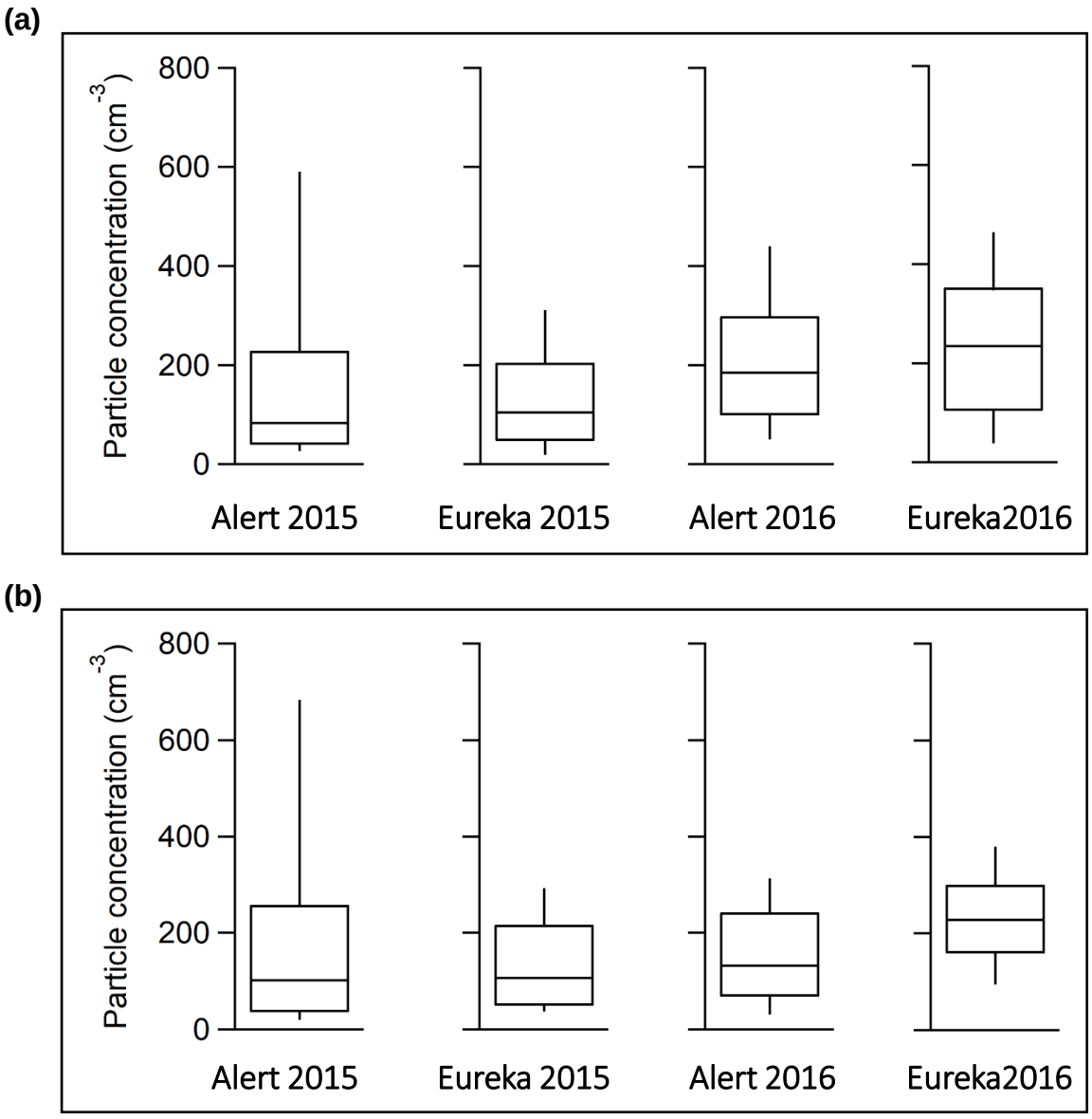

Figure 4. Box and whiskers plots of hourly particle number concentrations for diameters between **(a)** 10 – 487 nm, and **(b)** 10 – 100 nm measured during 27 Jul to 9 Sep 2015 and 2016 in Alert and at the PEARL RidgeLab near Eureka. The plots indicate the 10^{th}, 25^{th}, 50^{th}, 75^{th} and 90^{th} percentiles.

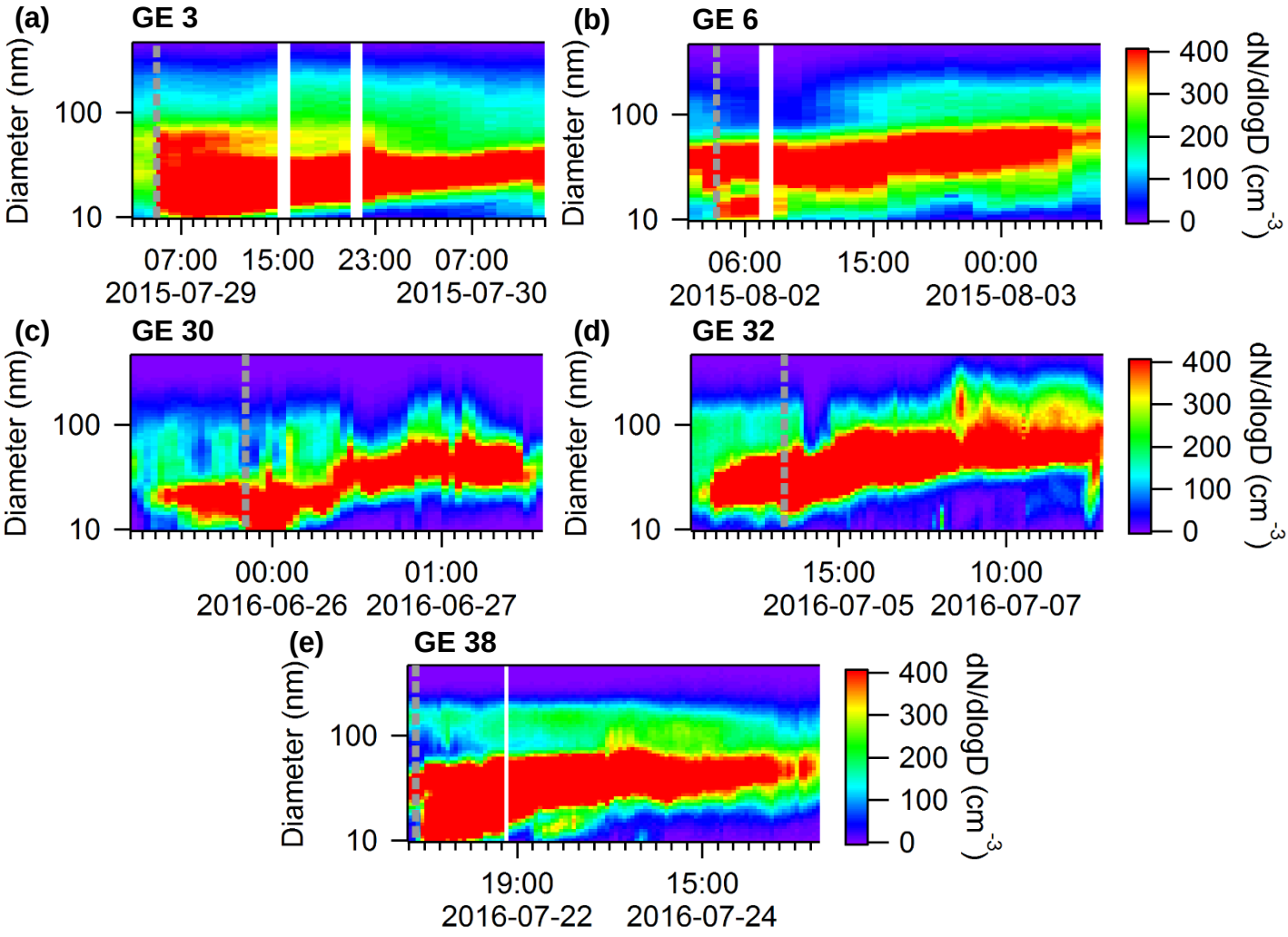

Figure 5. Five selected growth events near Eureka during the summers of 2015 and 2016. The grey dashed line indicates the start of each growth event. The sizes are mobility diameters measured by an SMPS, which are equal to the physical diameters under the assumption that the particles were spherical and contained no voids.

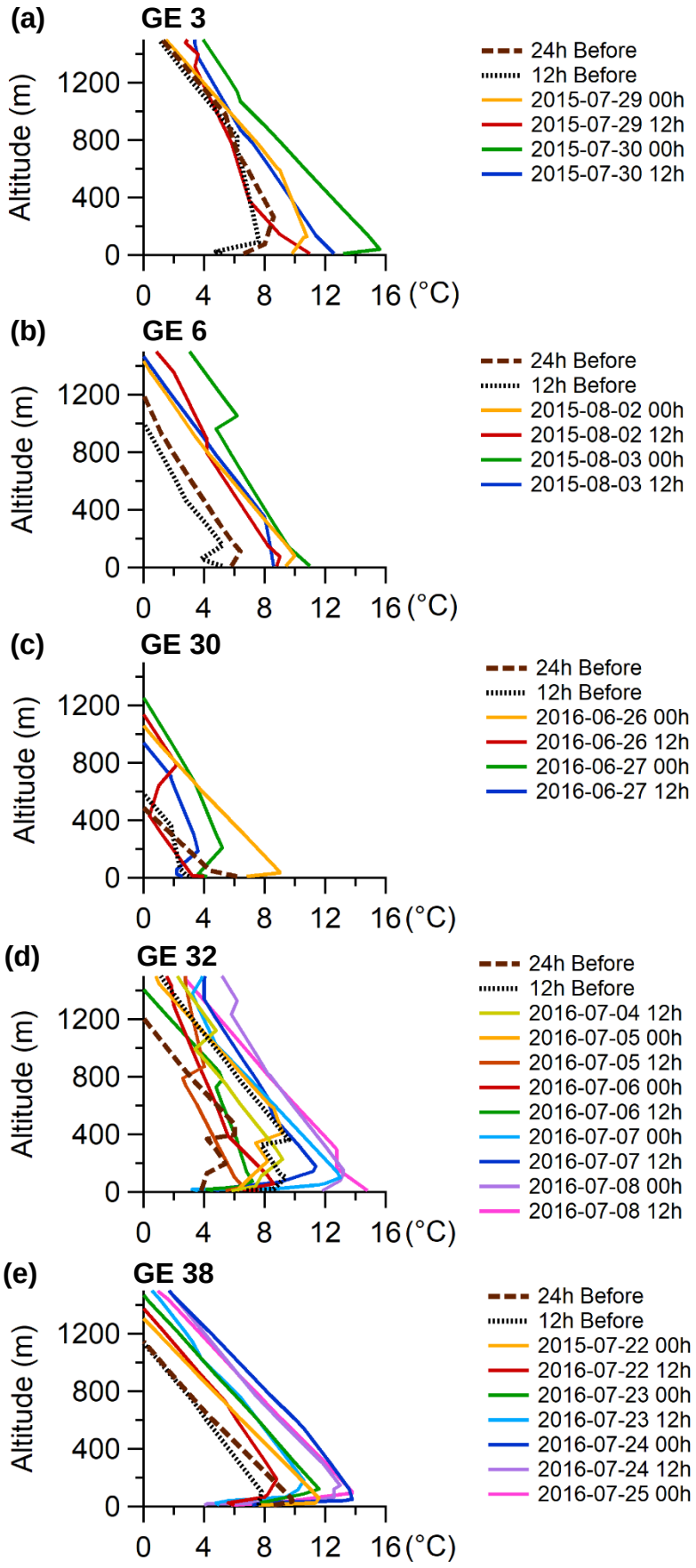

Figure 6. Vertical temperature profiles every 12 h during the 5 selected growth events that are shown in the previous figure. Data includes 24 h and 12 h prior to the start of the growth event.

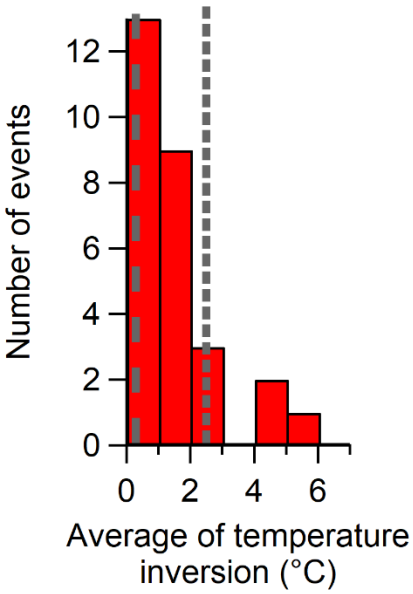

Figure 7. Histogram of the number of growth events near Eureka, binned by the average change in the temperature from 10 to 600 m above sea level. The average temperature change of each event is provided in Table S1, and was calculated from radiosonde measurements during 2015 and 2016, as shown in Figure 6. The dashed line indicates the average change in temperature during periods of low particle concentrations as shown in Table S2 and Figure S5 (0.3 ± 0.2 °C), and the dotted line indicates the average change in temperature during periods with a persistent accumulation mode as shown in Table S2 and Figure S6 (2.5 ± 1.2 °C). The values in parenthesis are the averages and their standard deviations.

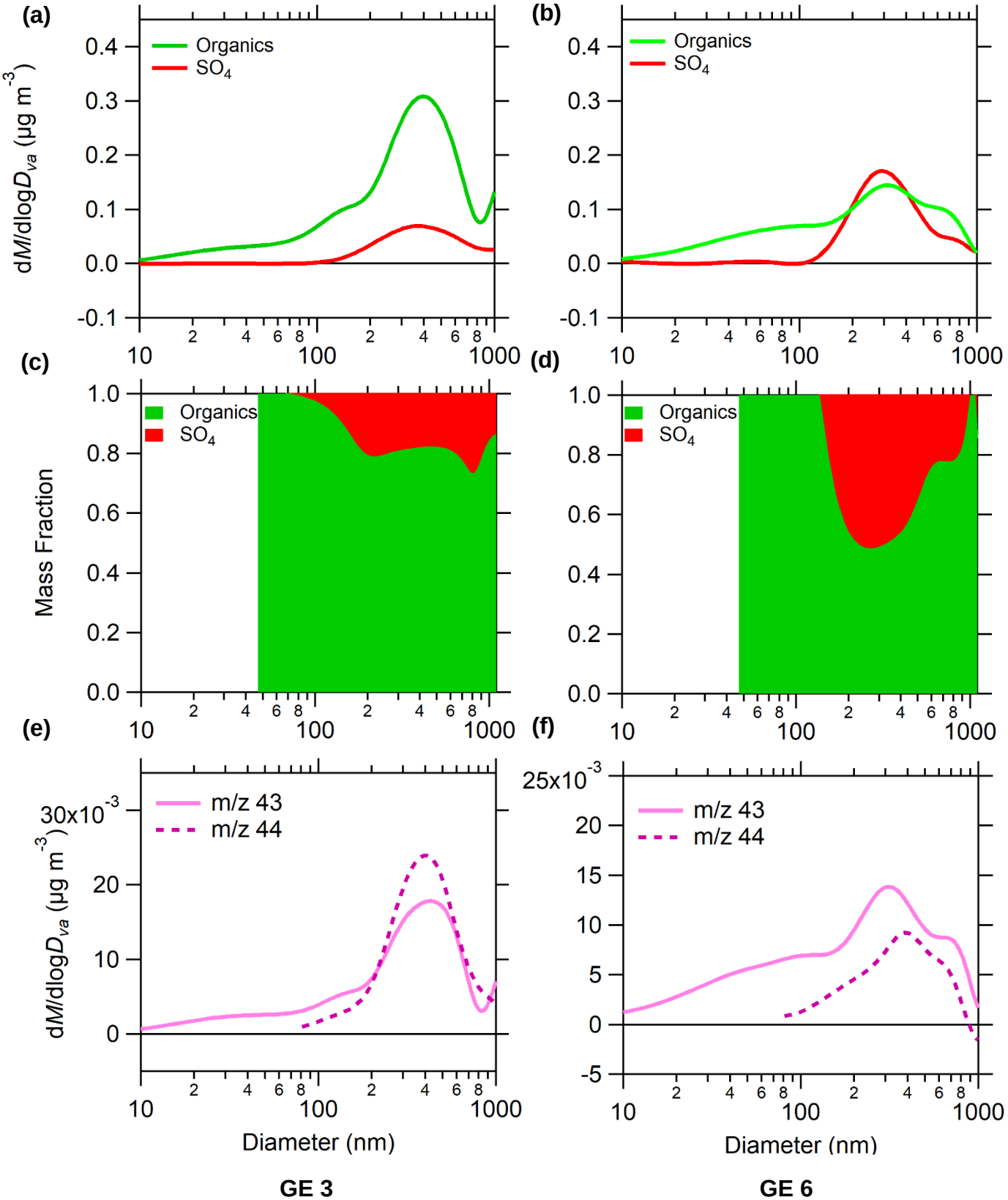

Figure 8. Size-resolved aerosol chemical composition for GE 3 **(a, c, e)** and GE 6 **(b, d, f)** measured near Eureka and averaged over the periods indicated in Table 1. The absolute organic and sulfate aerosol mass concentration **(a, b)**, the corresponding mass fractions **(c, d)**, and the nitrate-equivalent mass concentration of the m/z 43 and 44 fragments **(e, f)** are shown for each growth event. The data for m/z 44 is not shown below 80 nm due interference from gaseous CO_2. The uncertainties of a, b, e and f are 30 % and for c and d are 5 %.

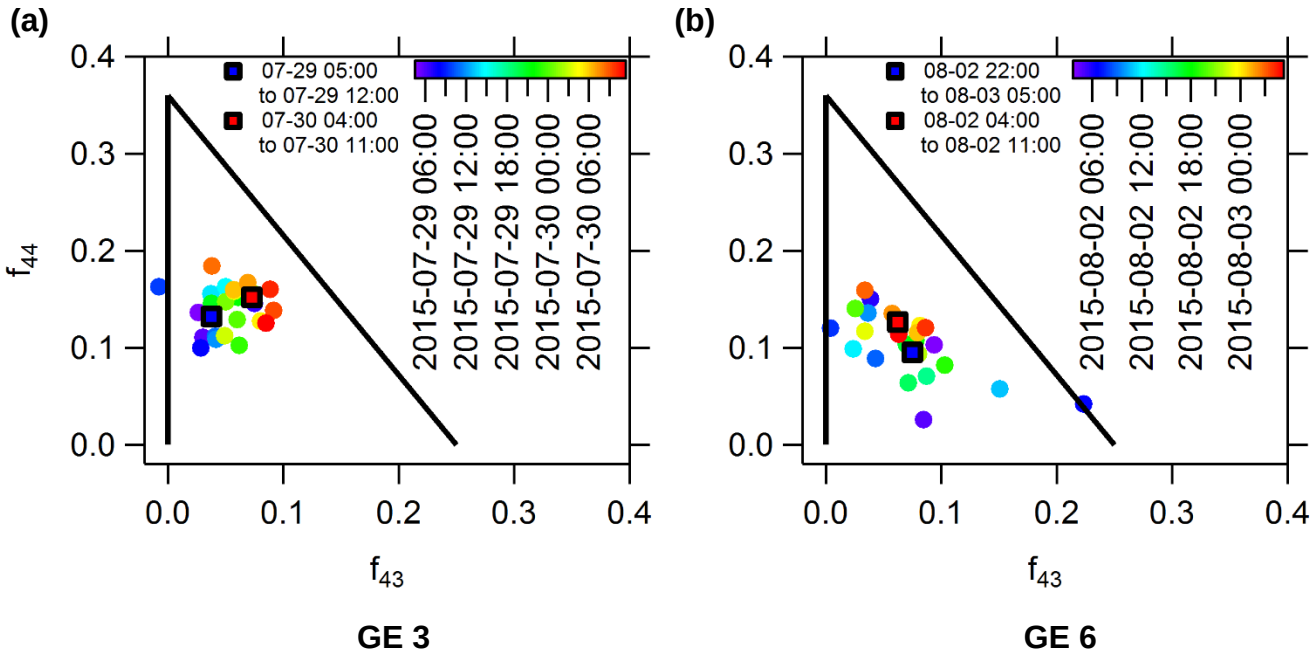

Figure 9. Scatter plot of the organic aerosol fraction measured at m/z 43 versus that measured at m/z 44 during GE 3 **(a)** and GE 6 **(b)** near Eureka. Also shown are the average values corresponding to the first seven and final seven hours of the growth event.

Supporting Information for:

Characterization of aerosol growth events over Ellesmere Island during the summers of 2015 and 2016

Samantha Tremblay,[1] Jean-Christophe Picard,[1] Jill O. Bachelder[1], Erik Lutsch,[2] Kimberly Strong,[2] Pierre Fogal,[2] W. Richard Leaitch,[3] Sangeeta Sharma,[3] Felicia Kolonjari,[3] Christopher J. Cox,[4] Rachel Y.-W. Chang,[5] Patrick L. Hayes[1]

(1) Department of Chemistry, Université de Montréal, Montréal, Québec, Canada

(2) Department of Physics, University of Toronto, Toronto, Ontario, Canada

(3) Climate Research Division, Environment and Climate Change Canada, Toronto, Ontario, Canada

(4) Cooperative Institute for Research in Environmental Sciences (CIRES), Boulder, CO, USA and NOAA Physical Sciences Division, Boulder, CO, USA

(5) Department of Physics and Atmospheric Science, Dalhousie University, Halifax, Nova Scotia, Canada

Correspondence to: Patrick L. Hayes (patrick.hayes@umontreal.ca), Rachel Chang (rachel.chang@dal.ca)

Supplementary RidgeLab aerosol inlet description

At the PEARL RidgeLab, the instruments sampled year-round through a common aerosol inlet, made of 6 m of stainless steel tubing with a 25.4 mm outer diameter (OD) and an inner diameter (ID) of 22 mm, sampling 2 m above the roof of the laboratory with a total flow rate of 11 L/min, as previously described by Kuhn et al. (2010). The SMPS flow passed first through 0.5 m of 25.4 mm OD and 22 mm ID stainless steel tubing connected to the common aerosol inlet; this flow then entered a 9.53 mm OD stainless steel tube with a length of 0.45 m and finally passed through a 6.35 mm OD and 4.72 mm ID copper tube that was 1.05 m long. For the OPC, the flow passed from the common aerosol inlet into a 12.7 mm OD copper tube with an ID of 9.40 mm and a length of 0.8 m, and then into a 6.35 mm OD copper tube with an ID of 4.72 mm and a length of 0.58 m, which was connected to the OPC by 6.35 mm OD conductive rubber tubing with an ID of 3.18 mm and a length of 0.04 m. Particle transmission efficiency to the SMPS has been calculated and the resulting transmission curve is shown in Figure S1 (von der Weiden et al. 2009). From the common aerosol inlet, the AMS flow passed first through 0.5 m of 25.4 mm OD and 22 mm ID stainless steel tubing and then through a 9.53 mm OD stainless steel tube with a length of 0.45 m before entering the AMS.

References

Kuhn, T., Damoah, R., Bacak, A., and Sloan, J. J.: Characterising aerosol transport into the Canadian High Arctic using aerosol mass spectrometry and Lagrangian modelling, Atmospheric Chemistry and Physics, 10, 10489-10502, 2010.

von der Weiden, S. L., Drewnick, F., and Borrmann, S.: Particle Loss Calculator - a new software tool for the assessment of the performance of aerosol inlet systems, Atmospheric Measurement Techniques, 2, 479-494, 2009.

Table S1. List of all growth events observed near Eureka during the summers of 2015 and 2016 .

Event Number	Date and Time (UTC)		Average temp. change from 10 to 600 m (°C)
	Start	End	
GE 1	2015-07-27 18:00	2015-07-28 03:00	2.00
GE 3	2015-07-29 05:00	2015-07-30 11:00	1.10
GE 6	2015-08-02 04:00	2015-08-03 05:00	0.20
GE 9	2015-08-07 03:00	2015-08-08 05:00	0.00
GE 10	2015-08-07 21:00	2015-08-09 02:00	1.23
GE 15	2015-08-18 12:00	2015-08-19 04:00	1.28
GE 27	2016-06-15 00:00	2016-06-17 18:00	1.20
GE 28	2016-06-17 00:00	2016-06-18 13:00	2.25
GE 30	2016-06-25 20:00	2016-06-27 14:00	1.30
GE 32	2016-07-05 01:00	2016-07-08 09:00	2.91
GE 33	2016-07-08 07:00	2016-07-09 01:00	0.00
GE 34	2016-07-09 20:00	2016-07-13 18:00	4.89
GE 37	2016-07-20 18:00	2016-07-22 03:00	1.80
GE 38	2016-07-21 19:00	2016-07-25 17:00	5.77
GE 39	2016-07-27 02:00	2016-07-27 17:00	0.47
GE 43	2016-08-03 18:00	2016-08-04 14:00	0.07
GE 45	2016-08-05 03:00	2016-08-05 23:00	0.00
GE 46	2016-08-05 21:00	2016-08-06 17:00	0.00
GE 47	2016-08-13 19:00	2016-08-17 12:00	0.46
GE 48	2016-08-17 23:00	2016-08-19 20:00	0.00
GE 49	2016-08-20 23:00	2016-08-22 15:00	0.00
GE 51	2016-08-23 19:00	2016-08-25 15:00	0.18
GE 53	2016-08-26 19:00	2016-08-27 20:00	2.27
GE 54	2016-09-04 01:00	2016-09-05 09:00	1.45
GE 55	2016-09-05 09:00	2016-09-06 01:00	4.30
GE 56	2016-09-05 15:00	2016-09-08 01:00	0.56
GE 58	2016-09-10 12:00	2016-09-12 16:00	1.28
GE 59	2016-09-19 00:00	2016-09-20 06:00	0.15

Table S2. List of selected periods of low and high particle concentrations observed near Eureka during the summers of 2015 and 2016 . The periods of high concentrations do not exhibit particle growth and are therefore distinct from the growth events. The SMPS measurements for the periods of low and high concentrations are shown in Figure S5 and S6, respectively.

Non-Event (NE)	Time period (UTC)				Average temp. change from 10 to 600 m (°C)
	Start		End		
NEA (low)	2015-08-06	06:00	2015-08-07	02:00	0.00
NEB (low)	2015-08-24	11:00	2015-08-26	12:00	0.36
NEC (low)	2015-09-04	12:00	2015-09-05	18:00	0.60
NED (low)	2016-06-23	08:00	2016-06-24	15:00	0.13
NEE (low)	2016-06-30	12:00	2016-07-01	15:00	0.07
NEF (low)	2016-08-02	00:00	2016-08-02	12:00	0.50
NEG (high)	2015-08-10	07:00	2015-08-11	10:00	3.60
NEH (high)	2015-08-19	22:00	2015-08-24	10:00	1.98
NEI (high)	2015-08-29	07:00	2015-09-04	12:00	0.76
NEJ (high)	2016-07-13	19:00	2016-07-19	12:00	3.78
NEK (high)	2016-07-25	18:00	2016-07-26	03:00	2.90
NEL (high)	2016-07-30	00:00	2016-08-02	00:00	1.71

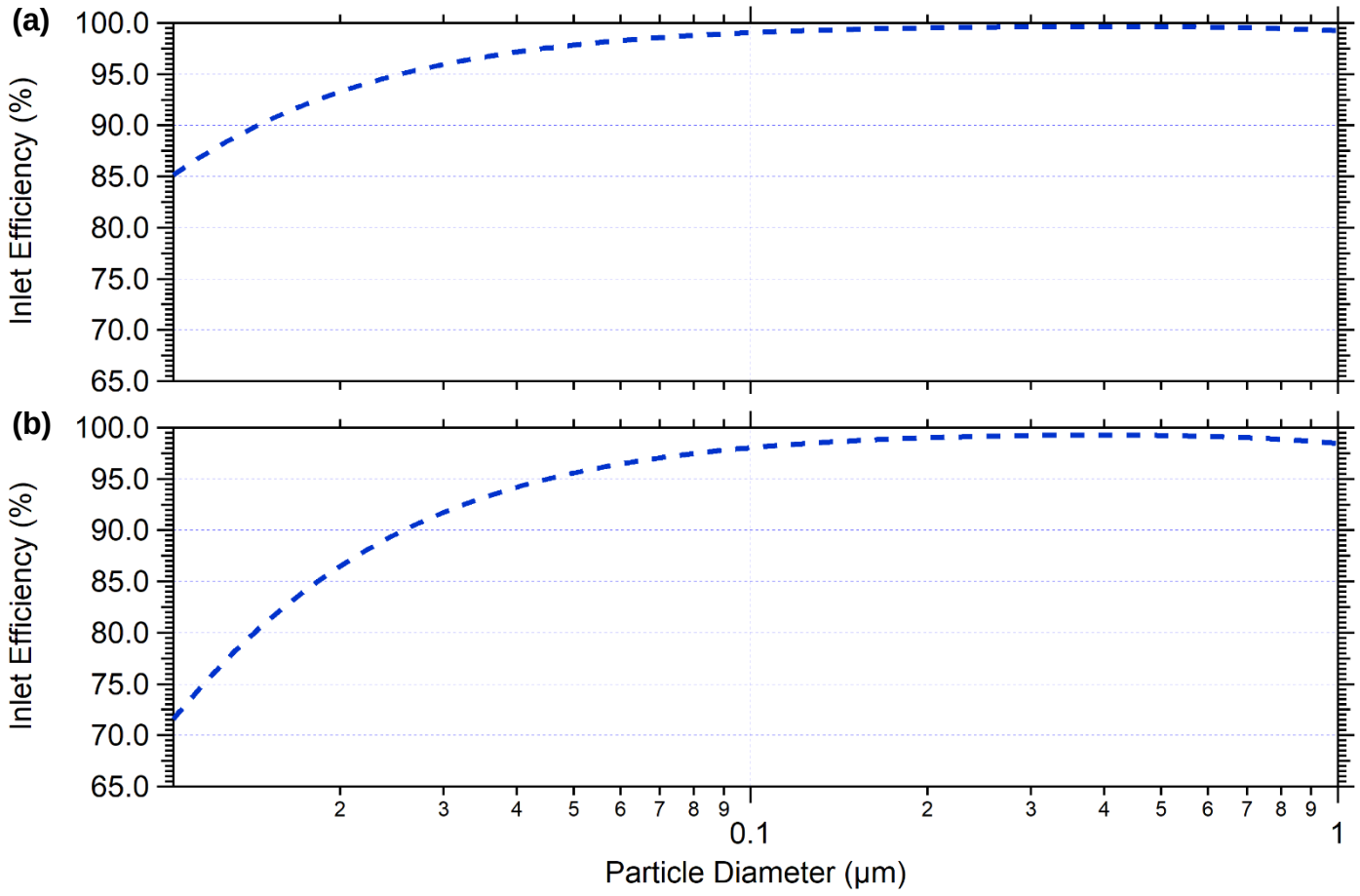

Figure S1. Inlet particle transmission efficiency for the AMS (a) and SMPS (b) at the PEARL RigdeLab. Note that the curves do not include the instrument transmission efficiencies for the AMS (Jayne et al. *Aerosol Sci. Technol.* **2000,** *33,* 49-70) or for the SMPS (Wiedensohler et al. *Atmos. Meas. Tech.* **2012,** *5,* 657-685).

(a)

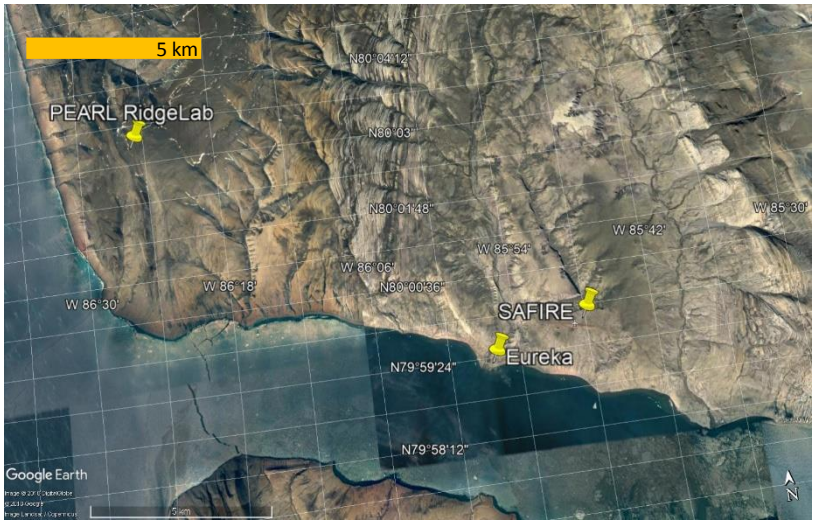

(b)

Figure S2. Local map of PEARL RidgeLab, SAFIRE and Eureka weather station (a) and zoomed-out map of Alert and Eureka (b).

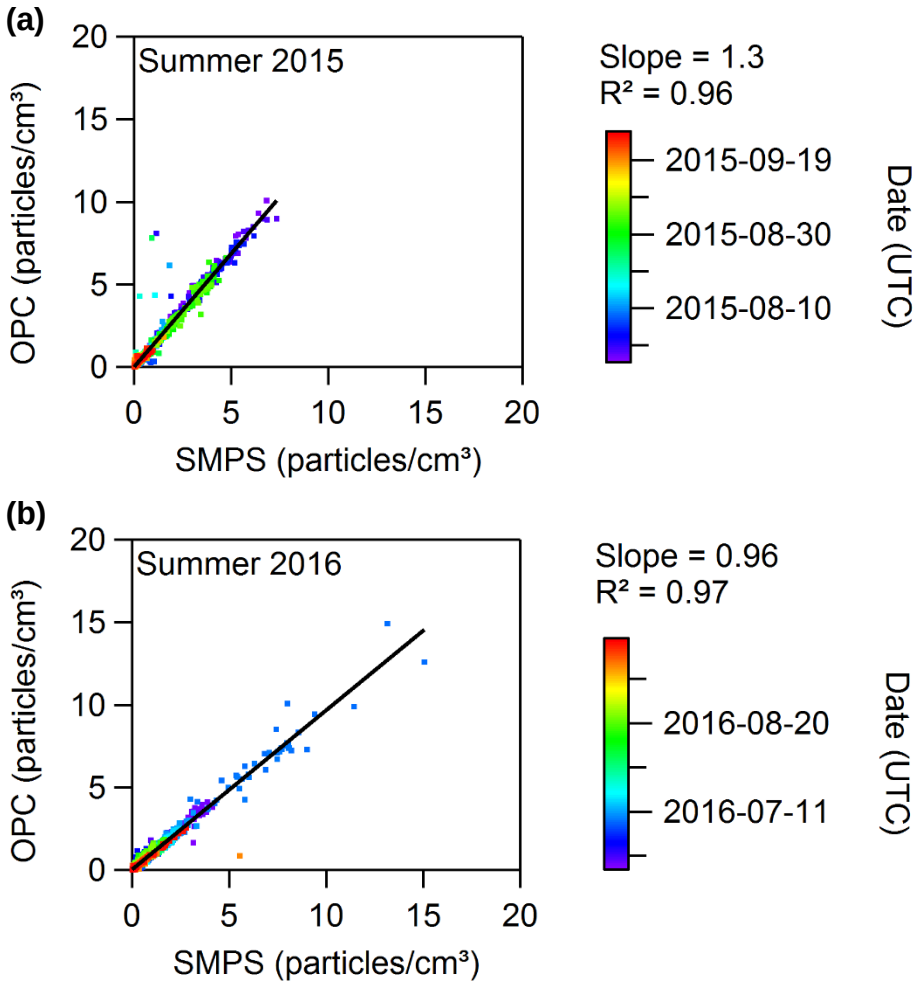

Figure S3. Scatter plots of the hourly particle number concentrations measured by the SMPS (300 – 487 nm) and the OPC (300 – 500 nm) near Eureka for the summers of 2015 (26 July to 26 September 2015) **(a)** and 2016 (16 June to 26 September 2016) **(b)**.

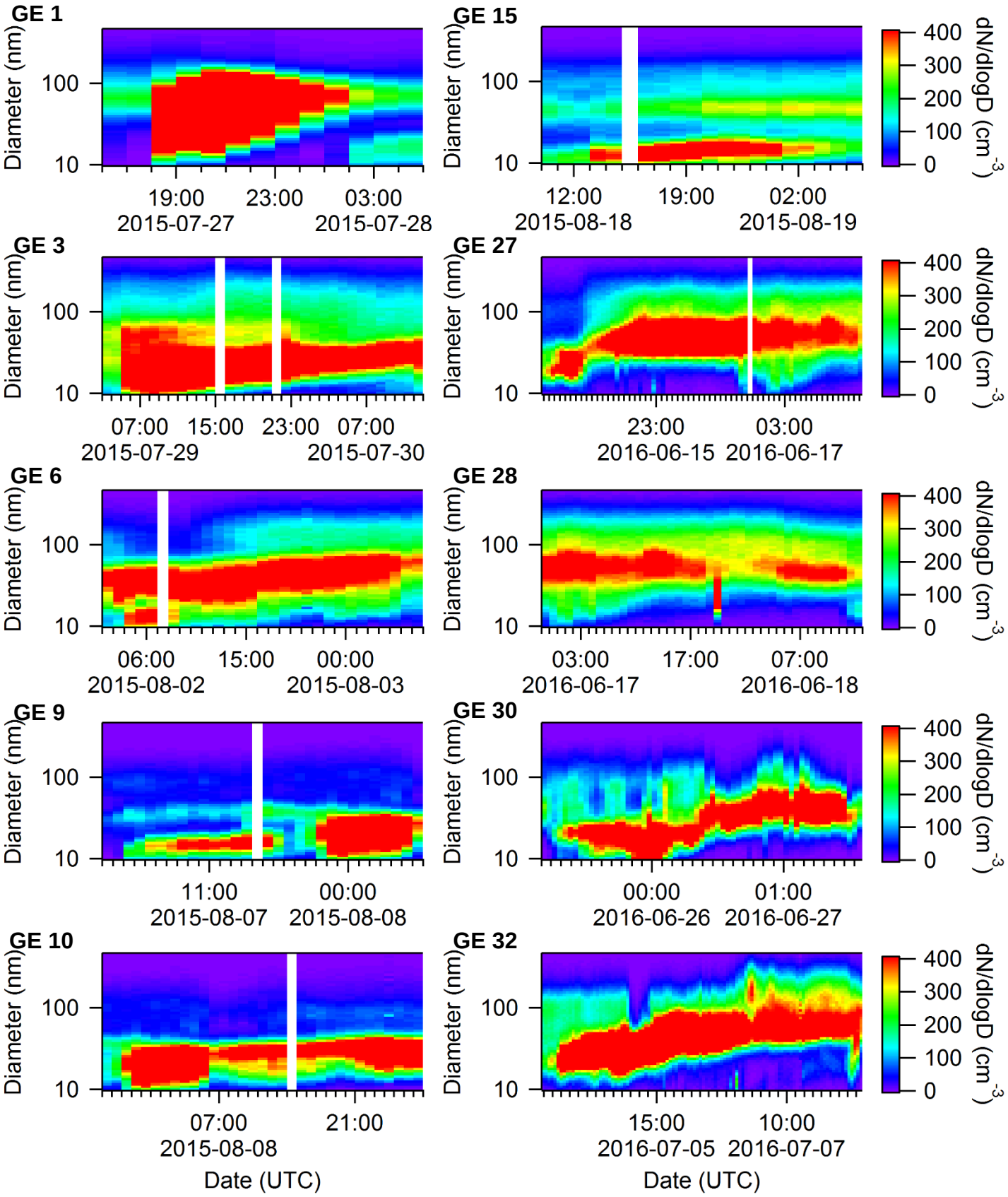

Figure S4. SMPS measurements of each growth event observed near Eureka during the summers of 2015 and 2016 as summarized in Table S1. The sizes are mobility diameters measured by an SMPS, which are equal to the physical diameters under the assumption that the particles were spherical and contained no voids.

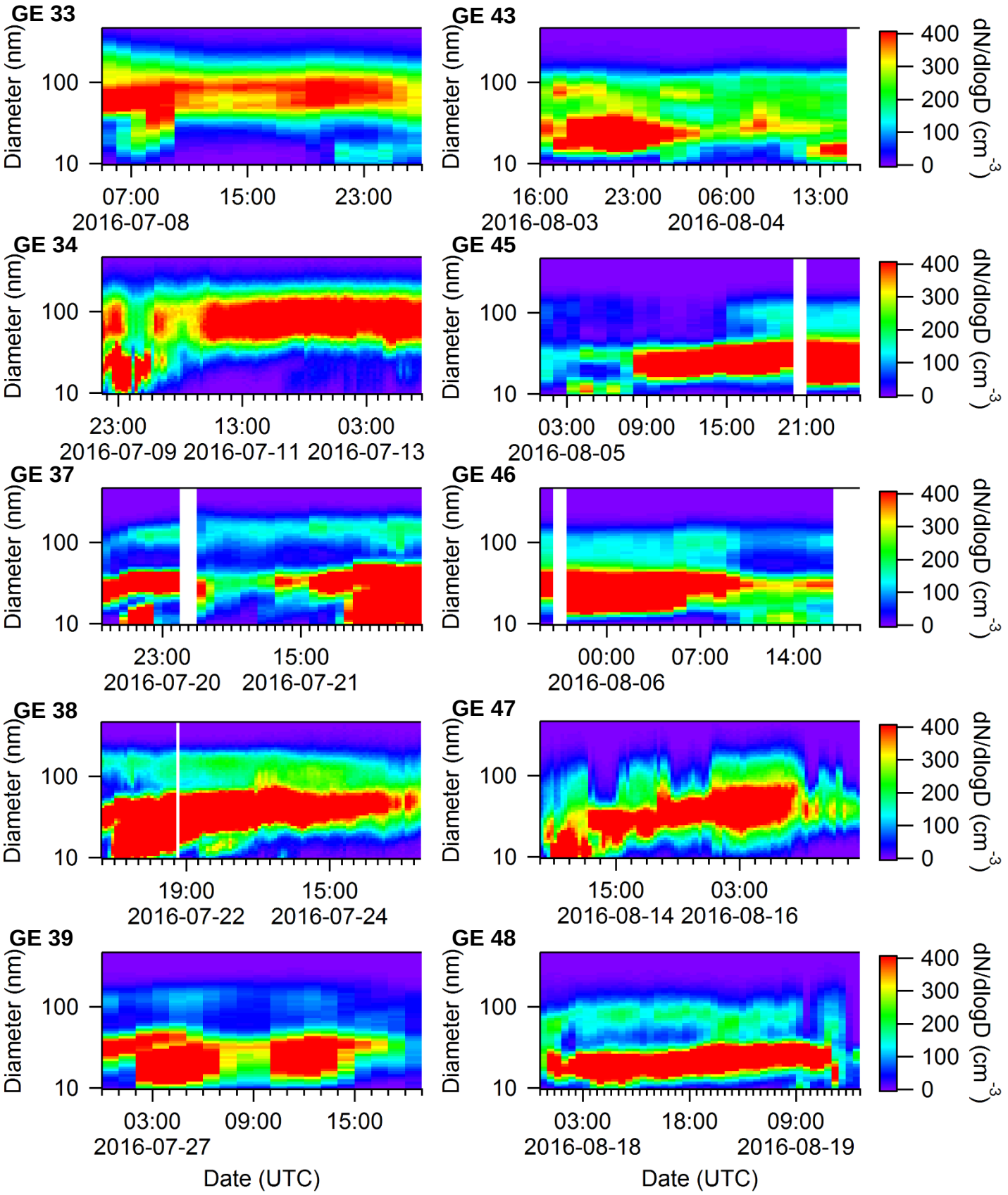

Figure S4. SMPS measurements of each growth event observed near Eureka during the summers of 2015 and 2016 as summarized in Table S1 (continued). The sizes are mobility diameters measured by an SMPS, which are equal to the physical diameters under the assumption that the particles were spherical and contained no voids.

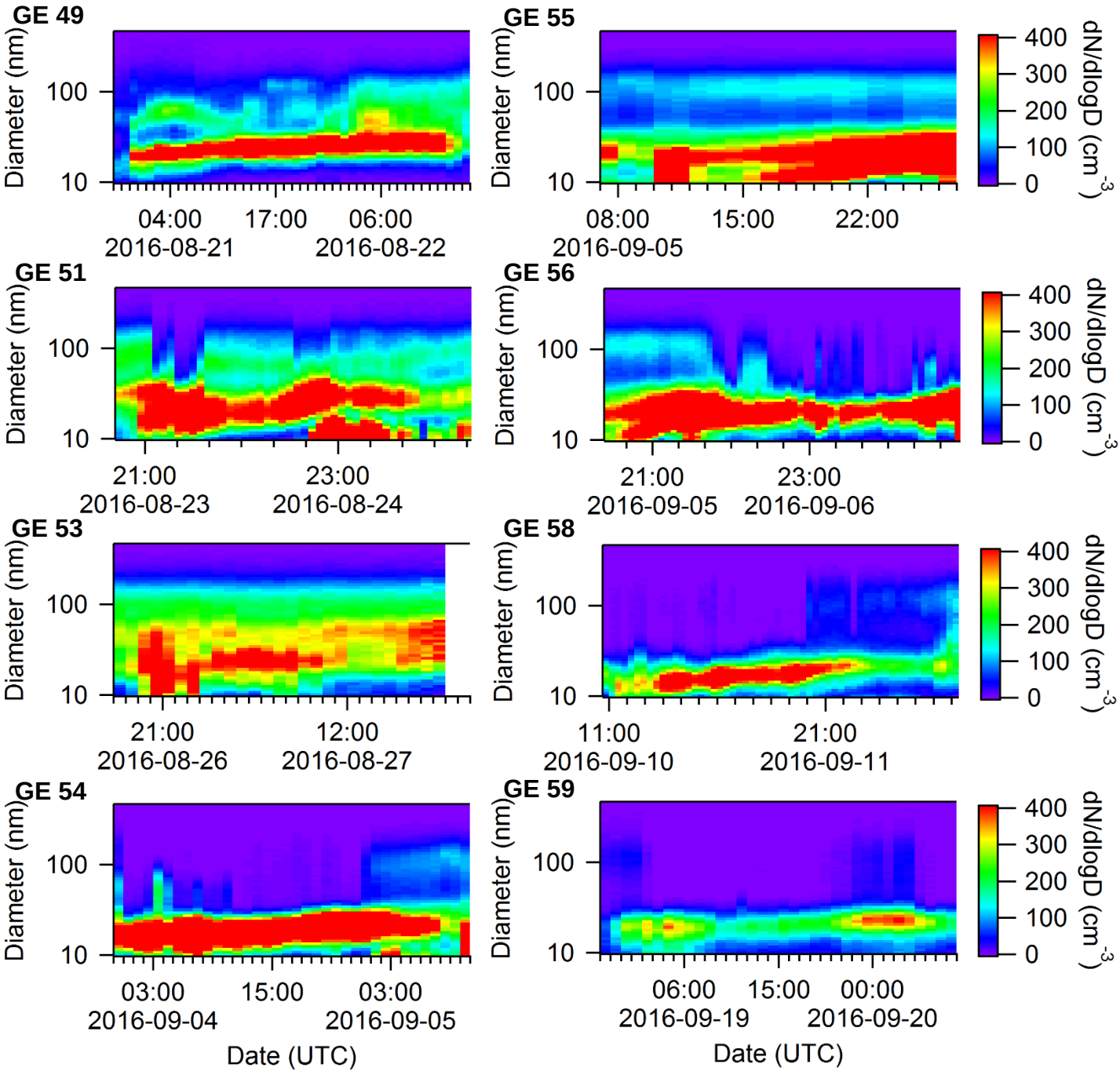

Figure S4. SMPS measurements of each growth event observed near Eureka during the summers of 2015 and 2016 as summarized in Table S1 (continued). The sizes are mobility diameters measured by an SMPS, which are equal to the physical diameters under the assumption that the particles were spherical and contained no voids.

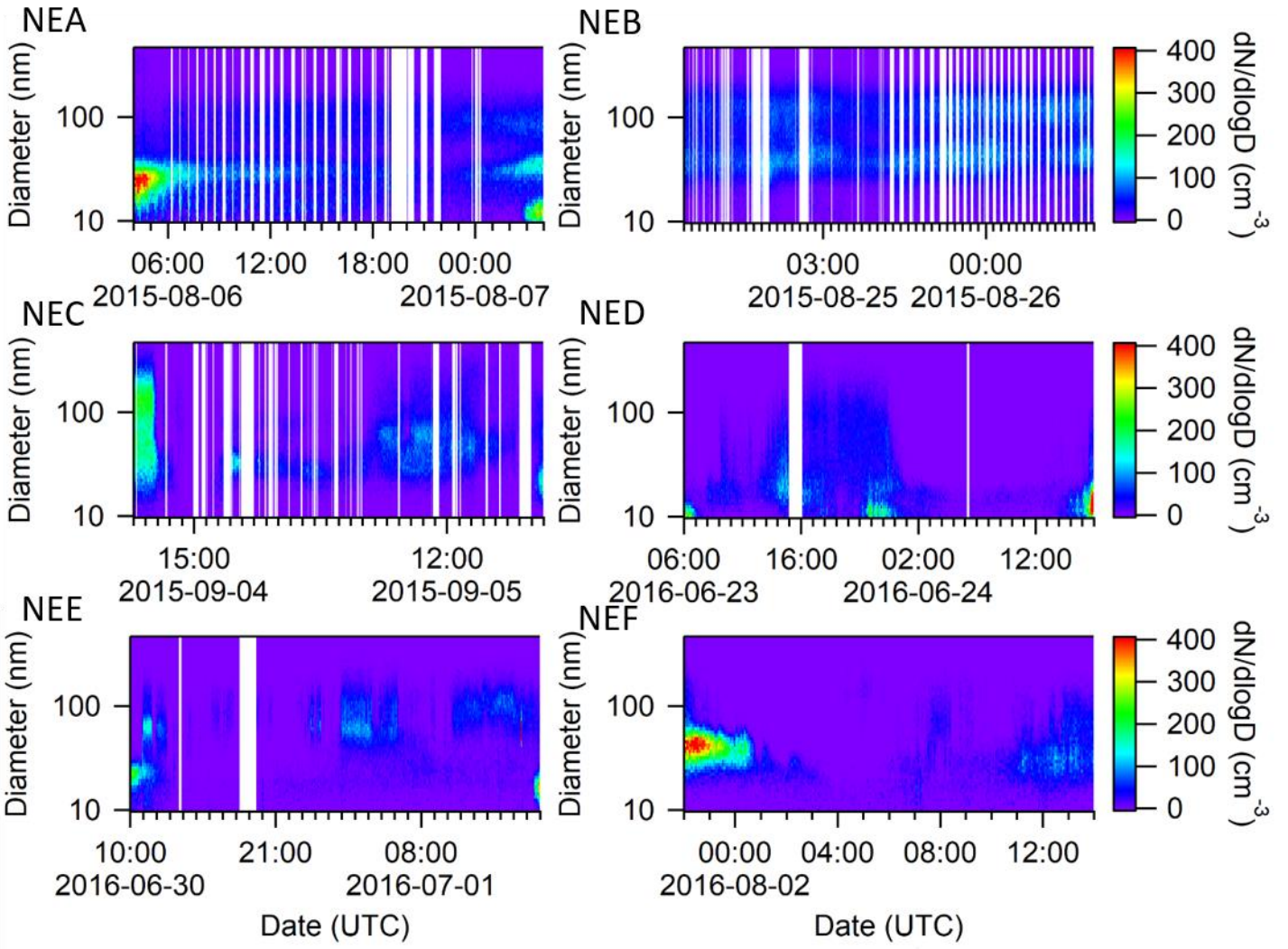

Figure S5. SMPS measurements of selected periods with low particle concentrations observed near Eureka during the summers of 2015 and 2016 as summarized in Table S2. Note that the figures display an additional 2 hours before and after the analyzed period. The sizes are mobility diameters measured by an SMPS, which are equal to the physical diameters under the assumption that the particles were spherical and contained no voids.

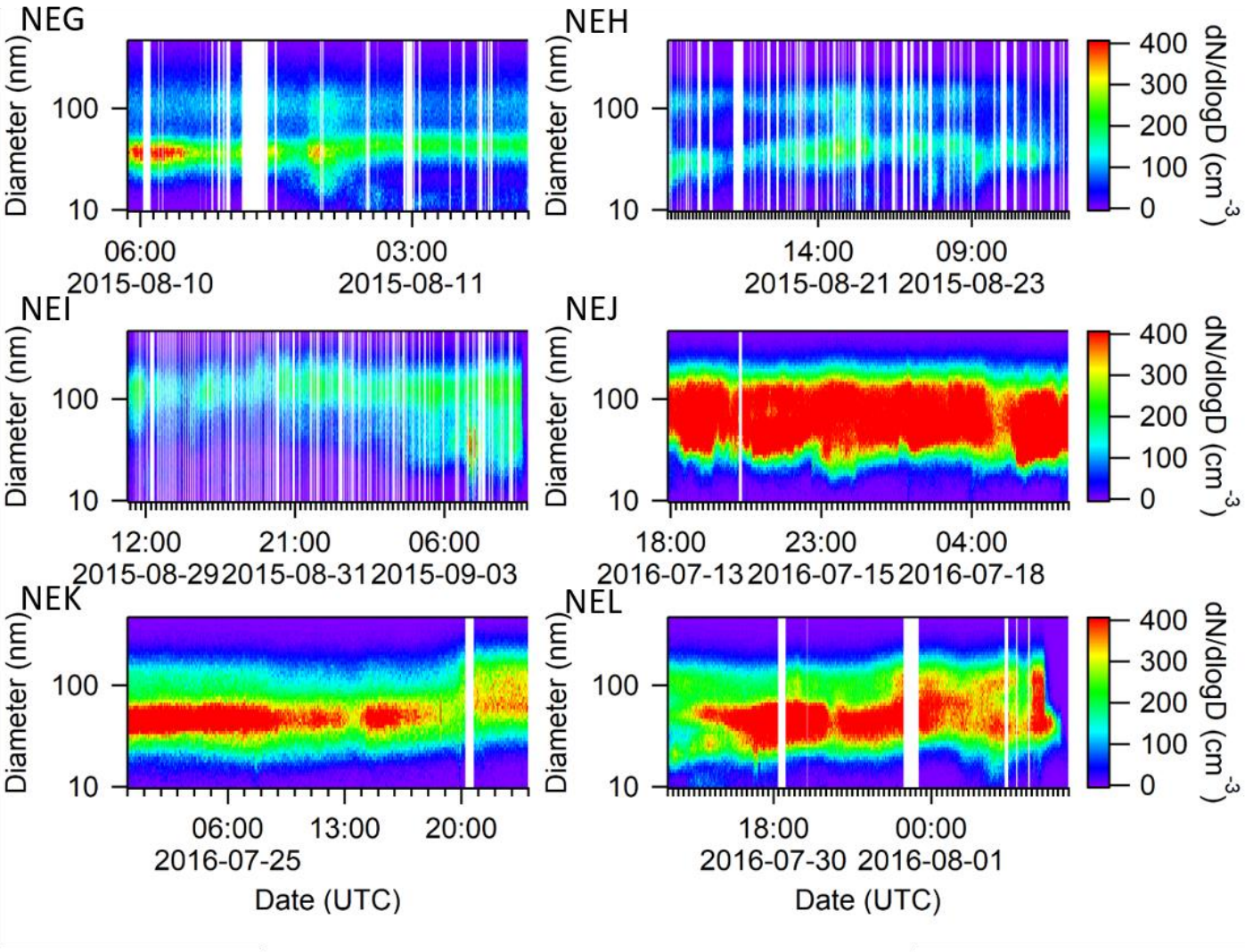

Figure S6. SMPS measurements of selected periods with high particle concentrations and without growth observed near Eureka during the summers of 2015 and 2016 as summarized in Table S2. Note that the figures display an additional 2 hours before and after the analyzed period. The sizes are mobility diameters measured by an SMPS, which are equal to the physical diameters under the assumption that the particles were spherical and contained no voids.

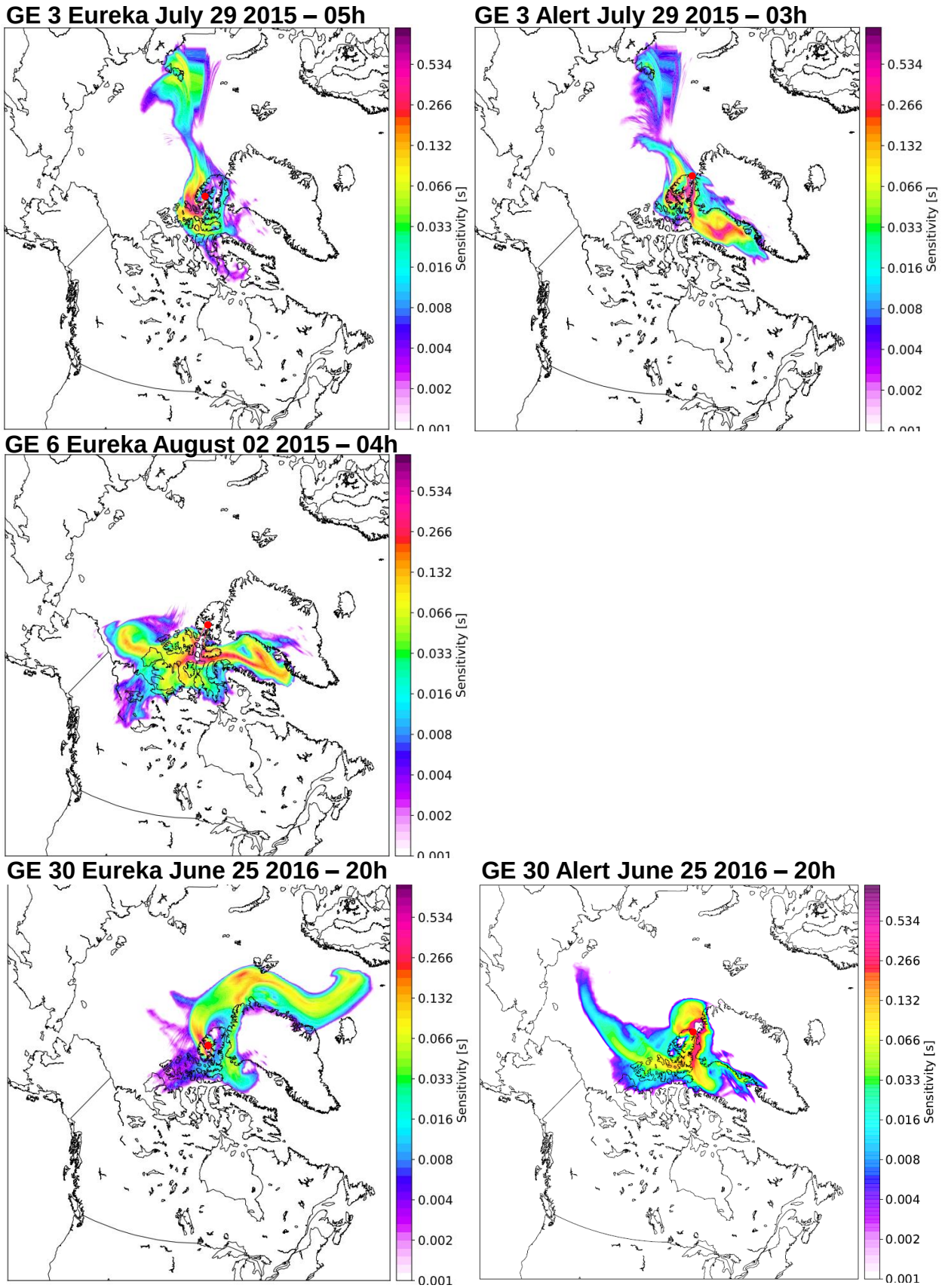

Figure S7. Evaluation of the air mass history during the five selected growth events summarized in Table 1 and shown in Figure 5 of the main text. The back-trajectory and potential emissions sensitivity were calculated using FLEXPART. The left column corresponds to air masses arriving at Eureka and the right column corresponds to those arriving at Alert.

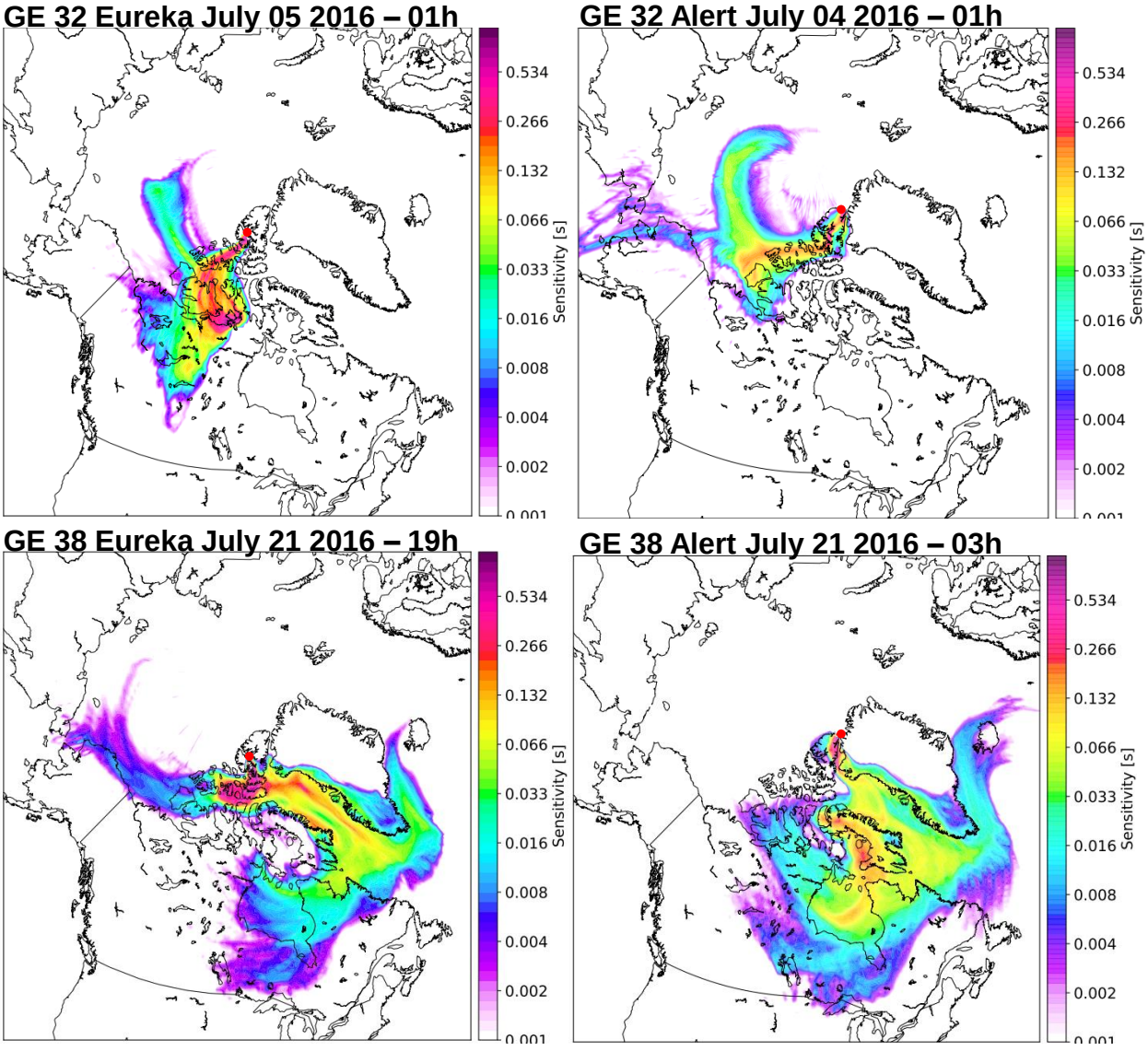

Figure S7. Evaluation of the air mass history during the five selected growth events summarized in Table 1 and shown in Figure 5 of the main text. The back-trajectory and potential emissions sensitivity were calculated using FLEXPART. The left column corresponds to air masses arriving at Eureka and the right column corresponds to those arriving at Alert (continued).

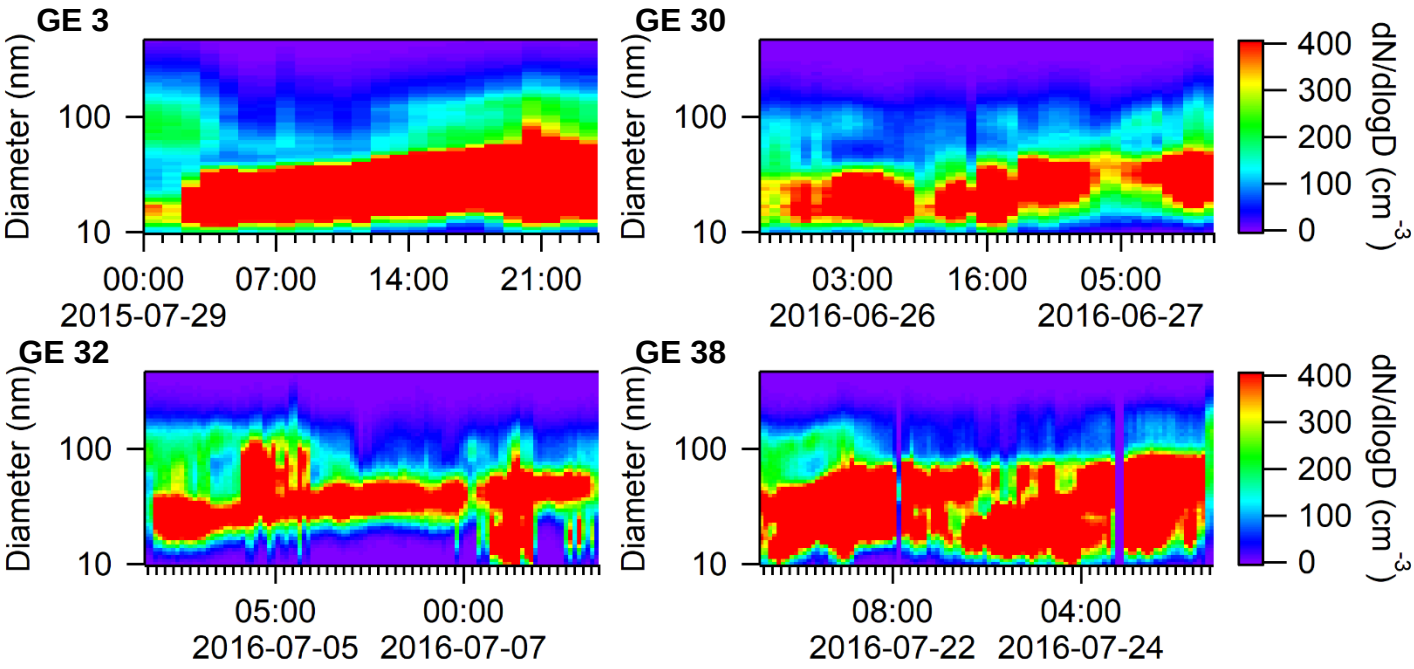

Figure S8. SMPS measurements of 4 growth events at Alert during the summers of 2015 and 2016 corresponding to the periods summarized in Table 1. The sizes are mobility diameters measured by an SMPS, which are equal to the physical diameters under the assumption that the particles were spherical and contained no voids.

(a)

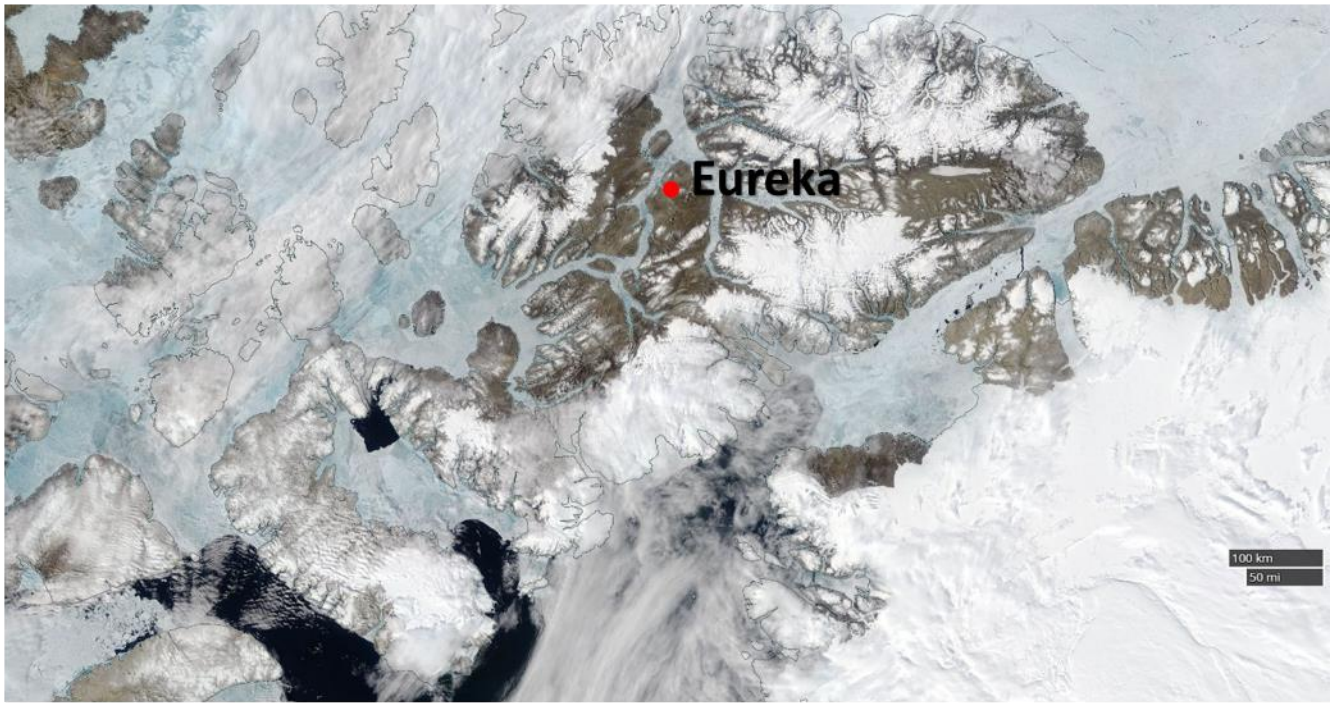

(b)

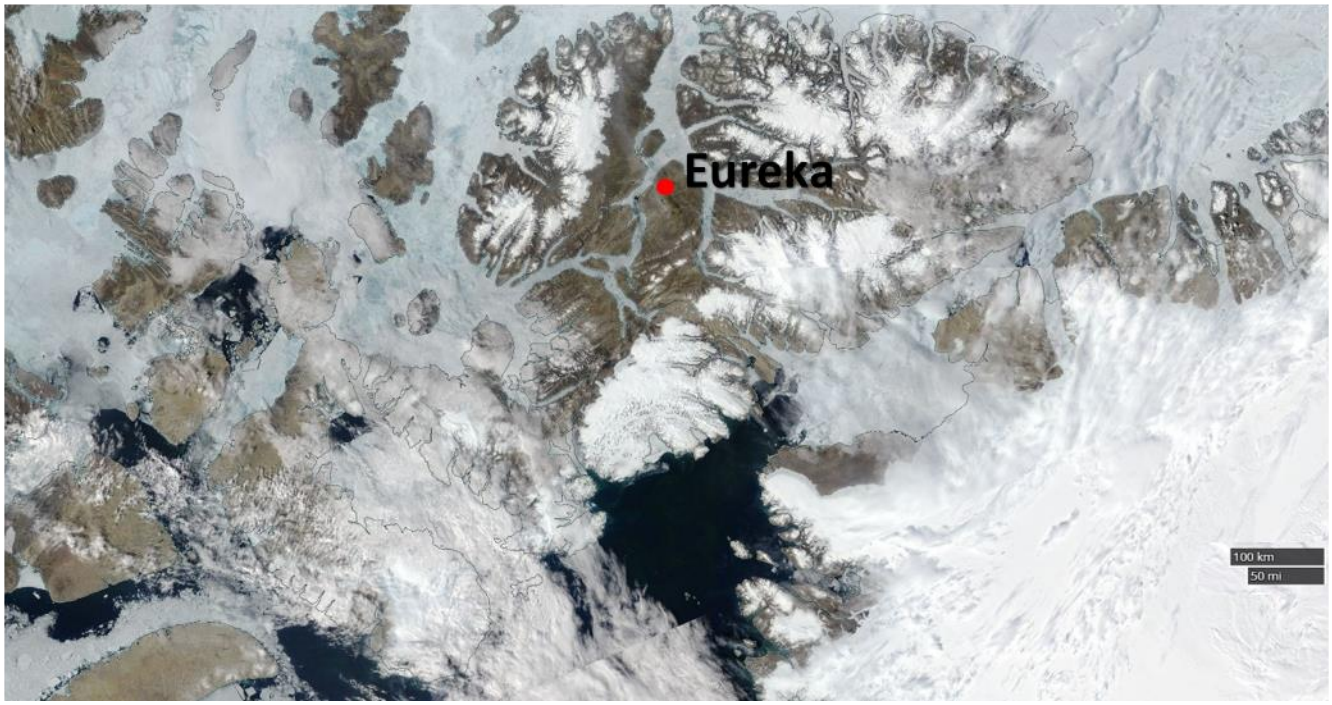

Figure S9. Image of the ice coverage around Eureka during 25 June 2016 (a) and during 7 July 2016 (b) given by NASA Worldview.

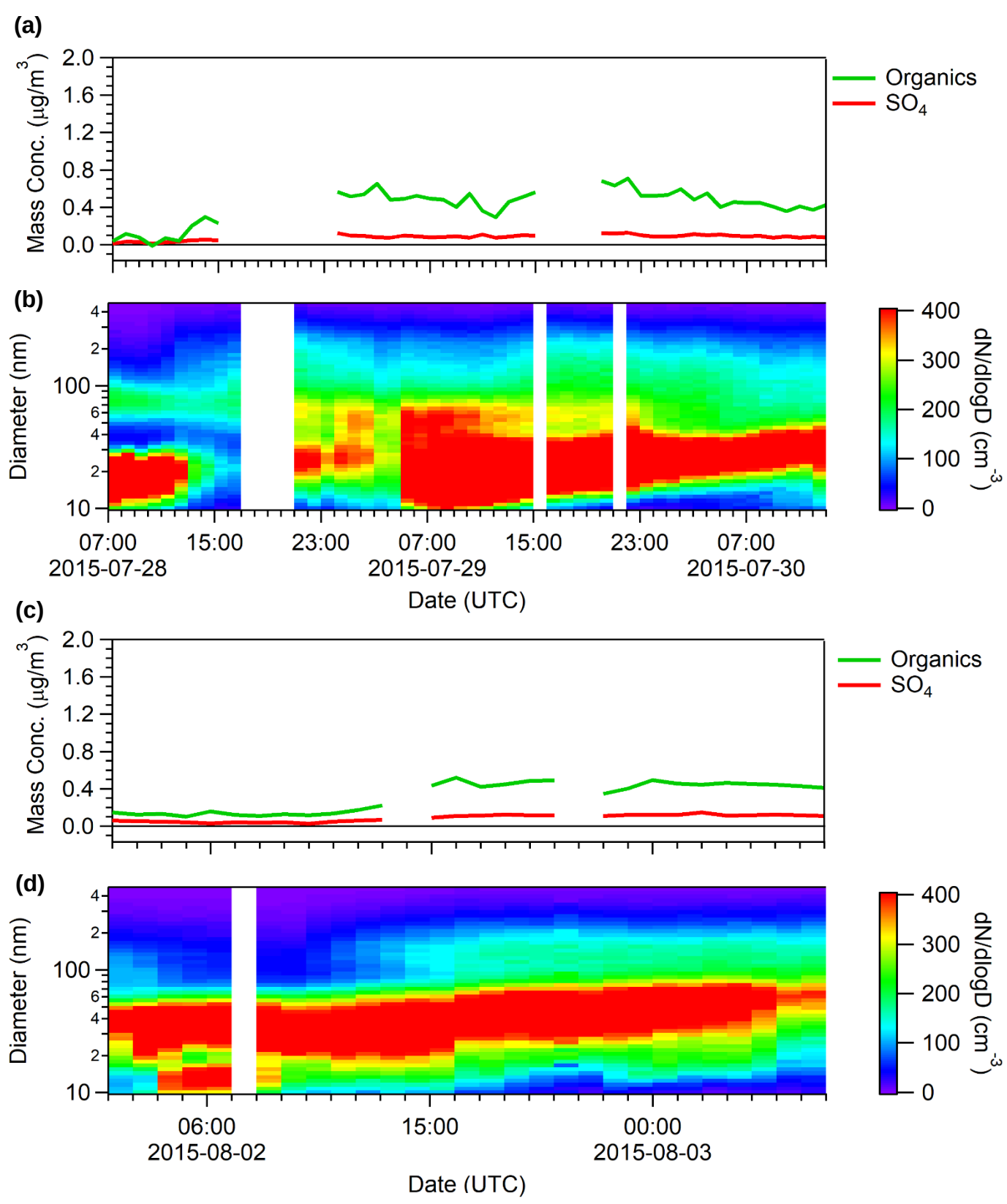

Figure S10. Aerosol mass spectrometry measurements of aerosol composition taken at the PEARL RidgeLab near Eureka showing only the organic and sulphate (SO_4) composition for GE3 **(a)** and GE6 **(c)** and the corresponding SMPS data for GE3 **(b)** and GE6 **(d)**. The sizes are mobility diameters measured by an SMPS, which are equal to the physical diameters under the assumption that the particles were spherical and contained no voids.

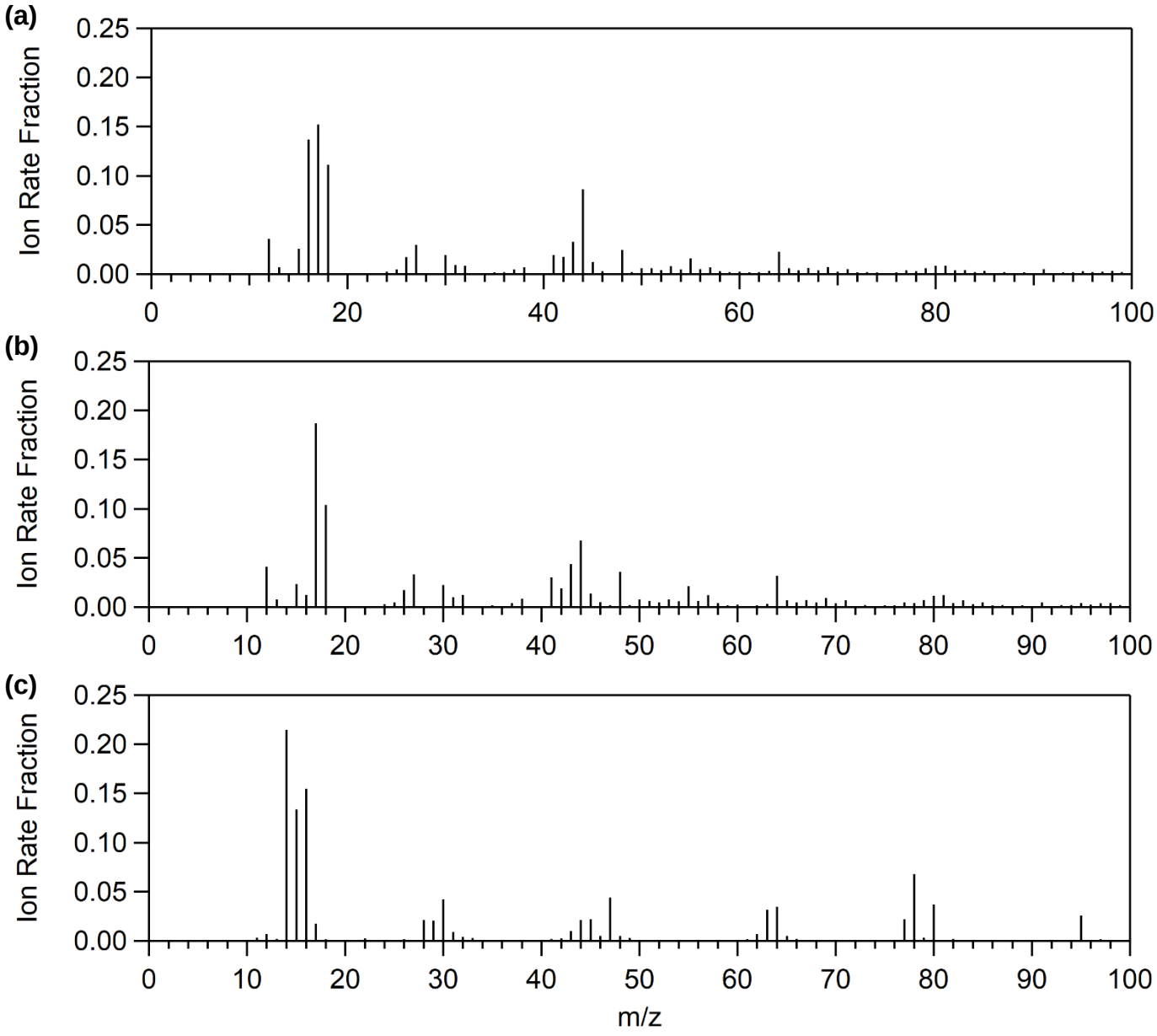

Figure S11. AMS average ambient aerosol mass spectrum of GE 3 (a) and GE 6 (b) compared with the mass spectrum of MSA (c). The Ion Rate Fraction is the normalized Ion Rate (in Hz).

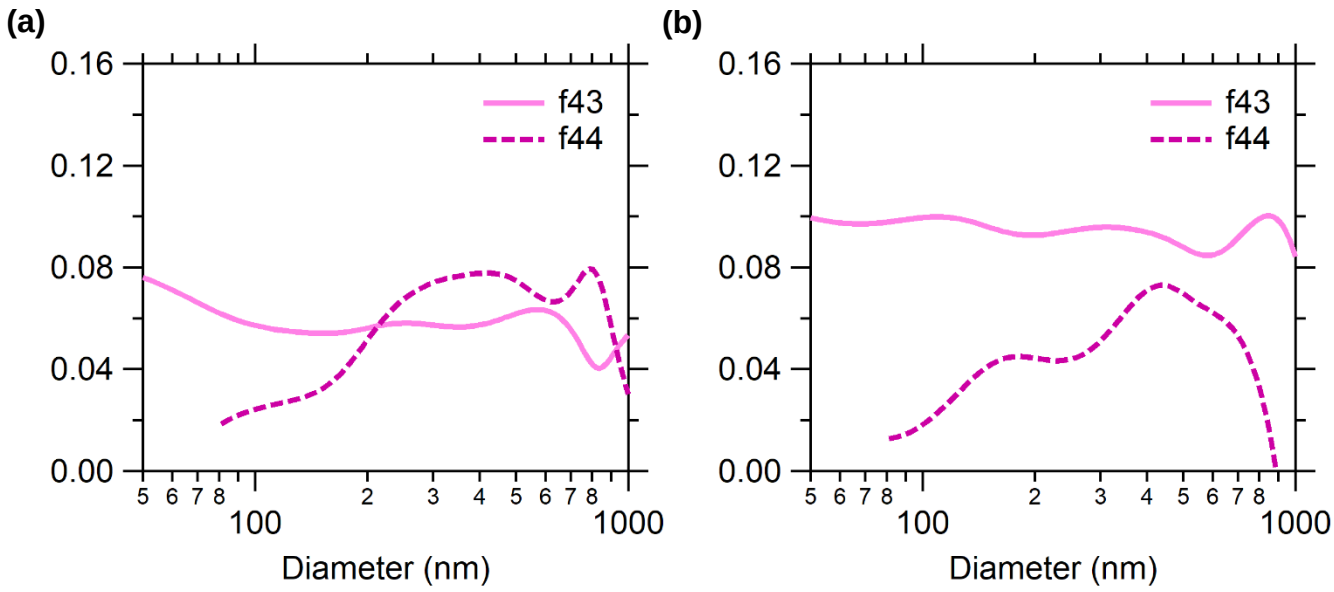

Figure S12. Organic aerosol fraction measured at m/z 43 and m/z 44 during GE 3 (a) and GE 6 (b) near Eureka.

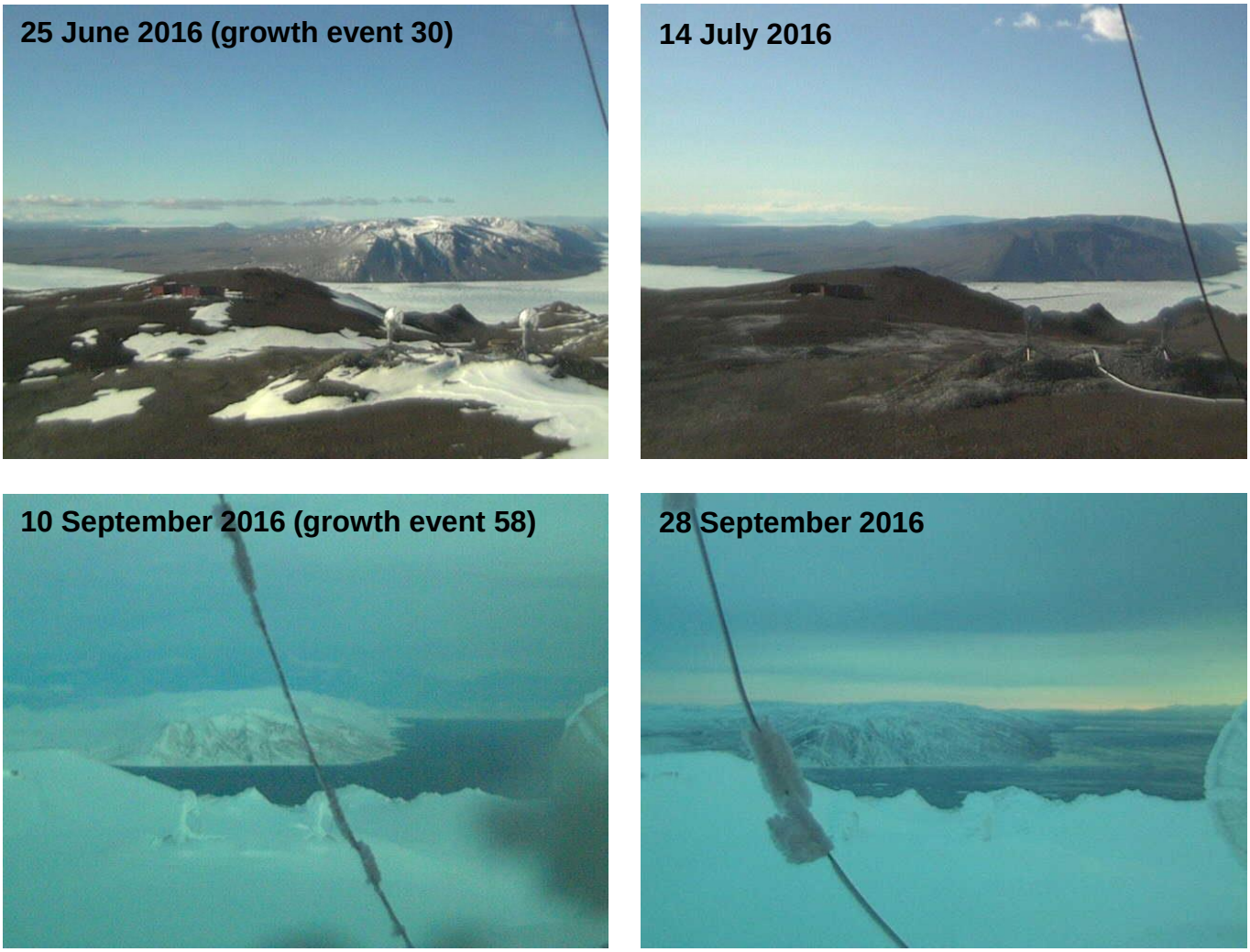

Figure S13. Photos from the PEARL RidgeLab, at 610 m above sea level. The images correspond to: the first observed growth event for 2016 **(25 June)**, the first time open water is observed **(14 July)**, the last observed growth event for 2016 **(10 September)**, and the last image available for the year **(28 September)** due to poor visibility related to meteorological conditions as well as polar sunset.

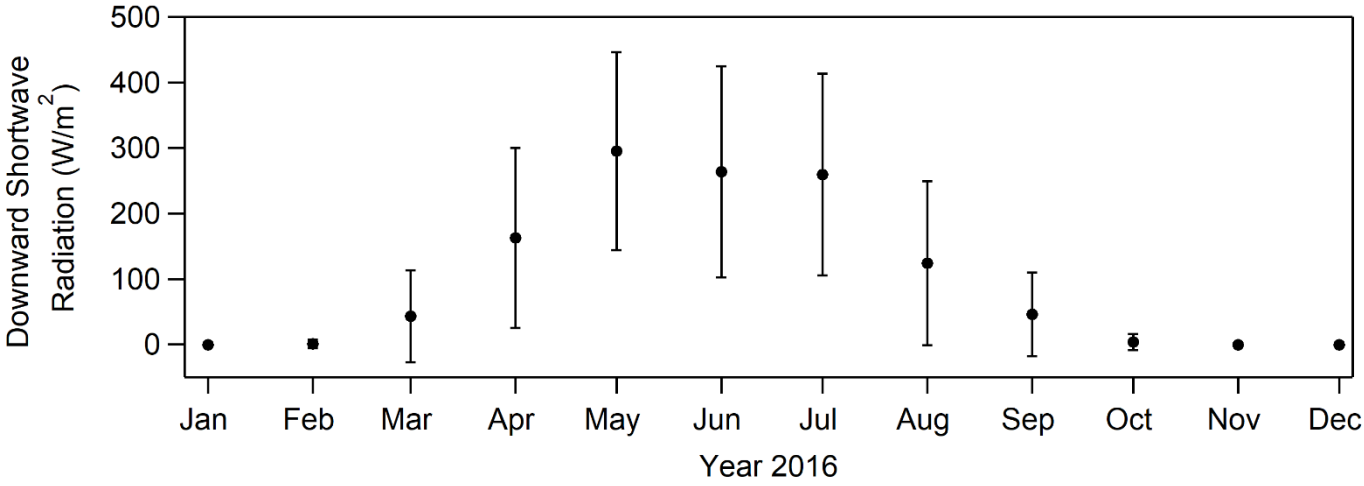

Figure S14. Average by month of the downwelling shortwave radiation for the year 2016 at Eureka, as measured at the SAFIRE facility at 85 m above sea level. The standard deviation of the one-minute average fluxes for each month is indicated along with the average.